

Phylogeographic diversification of the *Mesalina olivieri* species complex (Squamata: Lacertidae) with the description of a new species and a new subspecies endemic from North West Africa

Cristian Pizzigalli^{1,2}  | Pierre-André Crochet³  | Philippe Geniez⁴ |
Fernando Martínez-Freiría¹  | Guillermo Velo-Antón¹  | José Carlos Brito^{1,2} 

¹CIBIO/InBIO, Centro de Investigação em Biodiversidade e Recursos Genéticos da Universidade do Porto, Vairão, Portugal

²Departamento de Biologia da Faculdade de Ciências da Universidade do Porto, Porto, Portugal

³CEFE, CNRS, Univ Montpellier, EPHE, IRD, Univ Paul Valéry Montpellier 3, Montpellier, France

⁴CEFE, Univ Montpellier, CNRS, EPHE-PSL University, IRD, Univ Paul Valéry Montpellier 3, Biogéographie et Ecologie des Vertébrés, Montpellier, France

Correspondence

Cristian Pizzigalli, CIBIO/InBIO, Centro de Investigação em Biodiversidade e Recursos Genéticos da Universidade do Porto, Vairão, Portugal.

Email: pizzigalli.cristian@cibio.up.pt

Funding information

AGRIGEN-NORTE, Grant/Award Number: 01-0145-FEDER-000007; National Geographic Society, Grant/Award Number: CRE 7629-04 and CRE 8412-08; Operational Programme for Competitiveness Factors - COMPETE, Grant/Award Number: FCOMP-01-0124-FEDER-008917/028276; Fundação para a Ciência e a Tecnologia, Grant/Award Number: PTDC/BIA-BEC/099934/2008 and PTDC/BIA-BIC/2903/2012; Municipality of Martinengo, Grant/Award Number: Determinazione del 16-11-2020 Settore IV – Ser; Mohamed bin Zayed Species Conservation Fund, Grant/Award Number: 11052709, 11052707 and 11052499

Abstract

Numerous molecular studies emphasized how past climatic oscillations in the Sahara-Sahel have left strong imprints on current biodiversity patterns and identified the Atlantic coast and the Northwest African Mountains as refugia and speciation hot-spots. Yet, the biodiversity inventory in the region is still far from complete. We use an integrative taxonomy framework to revise the systematics of the *Mesalina olivieri* species complex; integrating molecular, morphological, and environmental data, we evaluated levels of genetic and phenotypic differentiation among species/lineages and revised the species distribution limits of the *M. olivieri* complex, refining the distribution of *Mesalina simoni*, and *Mesalina pasteuri*. Our study confirmed one previously unidentified speciation event, leading to the description of *Mesalina adrarensis* sp. nov. Together with this new species, we also describe the south-western Moroccan populations of *M. olivieri* as *Mesalina simoni saharae* ssp. nov. *Mesalina adrarensis* sp. nov. is sympatric with *M. pasteuri* and parapatric with *M. simoni saharae* ssp. nov. in Mauritania and southern Morocco. Based on our revised taxonomy, *M. simoni* now includes most populations of the *M. olivieri* complex in Morocco, *M. olivieri* being restricted in Morocco to the east and southeast of the country. We also build on these results to provide further insight on the biogeography of North Africa. Our results point to a diversification of the complex during the late Miocene, that led to the formation of the four species *M. simoni*, *M. olivieri*, *M. pasteuri*, and *M. adrarensis* sp. nov. After these four speciation events, high intraspecific diversification processes occurred since the beginning of the Plio-Pleistocene transition, in parallel with the beginning of the humid and arid cycles. Through our phylogenetic analysis, we highlight the existence of high levels of undescribed intraspecific diversity in *M. olivieri* and *M. pasteuri* that will need to be addressed in future studies. Moreover, we uncover

Contributing authors: Pierre-André Crochet (pierre-andre.crochet@cefe.cnrs.fr), Philippe Geniez (philippe.geniez@cefe.cnrs.fr), Fernando Martínez-Freiría (fmartinez-freiria@cibio.up.pt), Guillermo Velo-Antón (guillermo.velo@gmail.com), José Carlos Brito (jcbrito@cibio.up.pt)

Zoobank Links: LSID: <http://zoobank.org/NomenclaturalActs/dc6c167b-8138-4017-82a4-513d8244072a>

Online ISSN: 1439-0469

LSID: <http://zoobank.org/NomenclaturalActs/30f33118-ec56-48a6-87b9-1d811dac016e>

instances of cytonuclear discordances, stressing the need of considering both mitochondrial and nuclear DNA for integrative taxonomic studies to explore biodiversity.

KEY WORDS

Adrar Atar, Atlantic Sahara, cytonuclear discordance, integrative taxonomy, Maghreb

Sommario

Molteplici studi molecolari enfatizzano come le passate oscillazioni climatiche nel Sahara-Sahel abbiano avuto un forte impatto sulla distribuzione della biodiversità North Africa, ed identificano la costa Atlantica e le montagne del Nordovest Africano come rifugi e hotspot di speciazione. Tuttavia, la catalogazione della biodiversità in quest'area è, ad oggi, ancora lontana dall'essere completa. Attraverso l'approccio multidisciplinare della tassonomia integrativa, è stata revisionata la sistematica del complesso di specie "*Mesalina olivieri*". Integrando dati molecolari, morfologici e ambientali, sono stati valutati livelli di differenziazione genetica e fenotipica tra specie/linee evolutive e rivisti i limiti di distribuzione del complesso di specie *M. olivieri*, rifinendo la distribuzione di *Mesalina simoni* e *M. pasteurii*. Questo studio mette in luce un precedente evento di speciazione, ad oggi non ancora confermato, che ha condotto alla descrizione di *Mesalina adrarensis* sp. nov.. Inoltre, insieme a questa nuova specie, sono descritte le popolazioni di *M. olivieri* del sud-ovest del Marocco come *Mesalina simoni saharae* ssp. nov.. *Mesalina adrarensis* sp. nov è simpatrica con *Mesalina pasteurii* e parapatrica con *M. simoni saharae* ssp. nov. in Mauritania e Sud Marocco. In base alla nostra tassonomia revisionata, *M. simoni* ora include la maggior parte delle popolazioni del complesso *M. olivieri* in Marocco, e la distribuzione di *M. olivieri* è ora ristretta all'est e sud-est del paese. Ci si è basati su questi risultati per fornire ulteriori conoscenze sulla biogeografia del Nord Africa. I risultati evidenziano una diversificazione del complesso durante il tardo Miocene, il quale ha condotto alla formazione delle quattro specie *M. simoni*, *M. olivieri*, *M. pasteurii* e *M. adrarensis* sp. nov.. Successivamente a questi quattro eventi di speciazione, processi di alta diversificazione intraspecifica si sono verificati dall'inizio della transizione Plio-Pleistocenica, in parallelo con l'inizio delle passate oscillazioni climatiche nel Sahara-Sahel. Attraverso analisi filogenetiche è stata evidenziata l'esistenza di alti livelli di diversità intraspecifica ancora non descritta in *M. olivieri* e *M. pasteurii*, la quale necessita ulteriori approfondimenti futuri. Inoltre, questo studio rivela molteplici esempi di discordanza cito-nucleare, sottolineando la necessità di considerare sia il DNA mitocondriale che nucleare per gli studi di tassonomia integrativa.

1 | INTRODUCTION

Past climatic oscillations have left strong imprints on current biodiversity patterns worldwide (Bryson et al., 2012) and the Sahara Desert and the neighboring Sahel are no exceptions (Brito et al., 2014). In these ecoregions, dry-humid cycles lead to series of contraction/expansion events in species ranges, with recurrent isolation of populations that promoted diversification and sometimes speciation processes see Brito et al. (2014, for a review). In this context, recent studies unveiled the key role of topographic features

(e.g., mountains, valleys) and particular regions (i.e., coastal areas) as major refugia and/or as corridors for many species, facilitating gene flow during favorable climatic conditions (e.g., Gonçalves, Martínez-Freiría, et al., 2018; Gonçalves, Pereira, et al., 2018; Velo-Antón et al., 2018). However, large portions of central Sahara and most Saharan mountains are still widely under-sampled due to their remoteness and long-term regional instability (Brito et al., 2014, 2018). Consequently, knowledge on the biodiversity of the Sahara-Sahel is still relatively scant compared with other biomes (Brito & Pleguezuelos, 2019). The region is heavily affected by the seven

types of shortfalls that limit knowledge on biodiversity of the globe (reviewed by Hortal et al., 2015). Indeed, a large fraction of cryptic (and not-cryptic) diversity in North Africa and the Sahara Desert remains undescribed (Brito et al., 2014, 2018), and these regions must be prioritized to reduce biodiversity shortfalls. The genus *Mesalina* (Lacertidae, Eremiadiinae; Gray, 1838) provides an appealing case study to address the influence of geological events and past climatic oscillations on diversification events across the Sahara-Sahel. This genus comprises diurnal, xeric-adapted small lacertids widely distributed from the Atlantic Sahara through North Africa, the Middle East, and the Arabian Peninsula to Pakistan (Sindaco et al., 2008). These fast-moving lizards occur in different habitats (Trape et al., 2012): rocky and mountain areas, sandy habitats or xeric shrublands and mesic regions on the transition between the Sahara and the Mediterranean and Atlantic coasts. Previous studies have addressed the phylogeny, systematics, and biogeography of the genus (Arnold, 1986; Kapli et al., 2015; Simó-Riudalbas et al., 2019; Sindaco et al., 2018; Šmid et al., 2017) using both molecular and morphological data. The genus currently comprises 19 recognized species (Uetz et al., 2020), subdivided into seven species complexes: (a) *Mesalina watsonana* (Stoliczka, 1872), (b) *Mesalina martini* (Boulenger, 1897), (c) the *Mesalina olivieri* group, (d) *Mesalina rubropunctata* (Lichtenstein, 1823), (e) the *Mesalina adramitana* group, (f) the *Mesalina brevirostris* group, and (g) the *Mesalina guttulata* group (Simó-Riudalbas et al., 2019).

The ancestor of the *M. olivieri* complex colonized North Africa and started its diversification around 8 Mya (Kapli et al., 2015) into two well-supported clades: (a) one restricted to Morocco (including the Atlantic Sahara) and Mauritania, and (b) another ranging from Israel to Mauritania. There are currently three recognized species within this species complex: (a) *Mesalina simoni* (Boettger, 1881),

endemic to Morocco (north and west of the Atlas Mountains), (b) *Mesalina olivieri* (Audouin, 1829), distributed from the Atlantic coast to Iraq and Saudi Arabia, and (c) *Mesalina pasteuri* (Bons, 1960), scattered distributed across the Sahara in Mauritania, southern Morocco, southern Algeria, Niger, Mali, and western Egypt. This current taxonomy needs to be revised as several mitochondrial DNA (mtDNA) lineages identified by Kapli et al. (2015) render *M. olivieri* and *M. pasteuri* paraphyletic. These include (a) one “*olivieri*” mtDNA lineage from the Atlantic Sahara (AS hereafter) and (b) one “*olivieri*” lineage distributed from the south of the High Atlas Mountains to the Saharan Atlas and the eastern Anti-Atlas in Morocco (AM) (that both group with the Moroccan endemic species *M. simoni*); (c) one “*olivieri*” lineage from Mauritania (ADR) (sister to a clade composed by *M. simoni* and AS and AM) and (d) a *pasteuri*-like specimen from the Tagant region in Mauritania embedded in the “*olivieri*” lineage of the same region (TAG); (e) one “*olivieri*” lineage from Algeria (ALG1) (clustering with specimens of *M. pasteuri* from Mauritania). In addition to the mtDNA paraphyly, previous studies (Arnold et al., 2007; Kapli et al., 2008, 2015; Simó-Riudalbas et al., 2019) stressed that the wide distribution and morphological variation (mostly in the scales number and coloration; Hosseini Yousefkhan et al., 2015; Trape et al., 2012) of the *M. olivieri* complex could hide several undescribed species. Yet, despite the efforts in gathering information about the morphological diversity in the *Mesalina* genus, there is no comprehensive revision on the dichotomous characters for the *M. olivieri* species complex.

In this integrative study, we re-evaluate phylogenetic relationships within the *M. olivieri* species complex and provide insight on the historical and evolutionary processes that generated its diversity in the Maghreb region. More precisely, we (a) combine mtDNA data with independent nuclear markers to recover the evolution of the

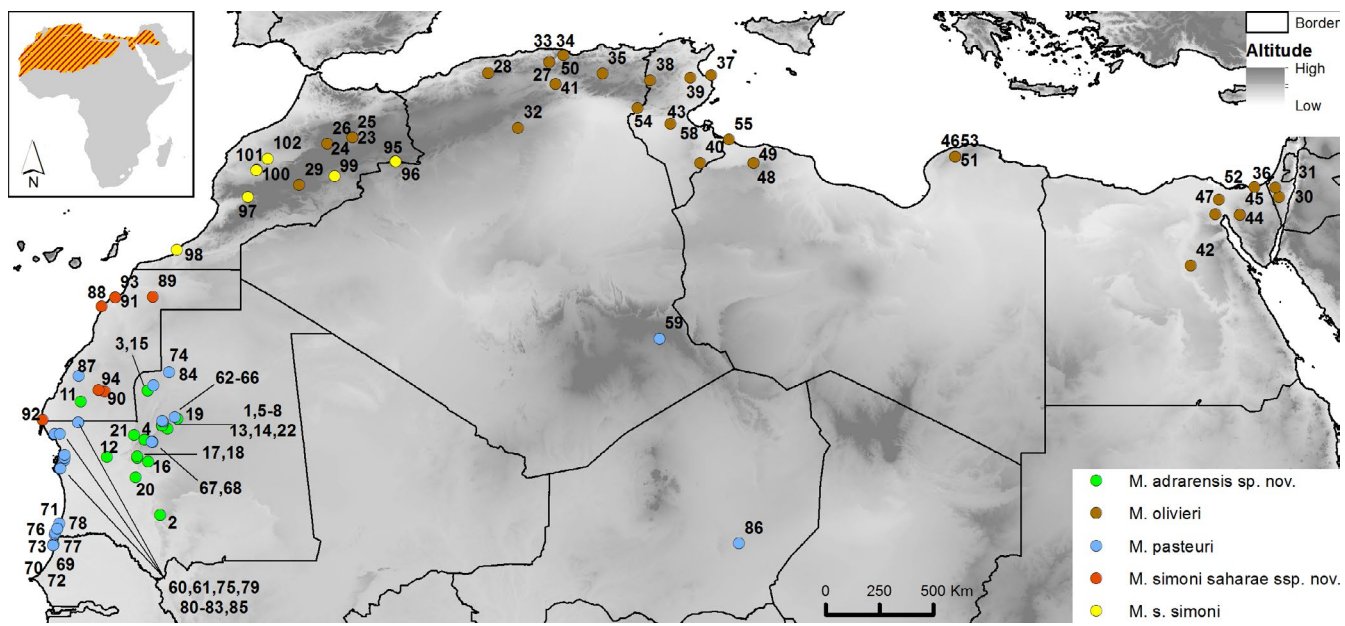


FIGURE 1 Localities of the *Mesalina olivieri* species complex samples included in this study for the genetic analyses. Dots numbers correspond to the samples in Table 1 and Table S1. The distribution of the complex is shown in the upper right corner of the map

TABLE 1 Samples codes, localities, and clades correspondences for the nuclear, mitochondrial, and concatenated (Concat.) trees (Figures 2a,b and 3, respectively)

No.	Sample code	Country	Latitude	Longitude	Nuc. clades	Mit. clades	Concat. clades
<i>Mesalina adrarensis</i> sp. nov.							
1	BEV.10457	Mauritania	21.0150	-11.7180	ADR	ADR	ADR
2	BEV.10823	Mauritania	17.3982	-12.0305	TAG	TAG	TAG
3	BEV.14800	Mauritania	22.6086	-12.5569	-	ADR	ADR
4	BEV.15060	Mauritania	20.5537	-12.6916	ADR	ADR	ADR
5	BEV.15061	Mauritania	21.1596	-11.9362	ADR	ADR	ADR
6	BEV.15062	Mauritania	21.1596	-11.9362	ADR	ADR	ADR
7	BEV.15063	Mauritania	21.1596	-11.9362	ADR	ADR	ADR
8	BEV.15064	Mauritania	21.1596	-11.9362	ADR	ADR	-
9	BEV.15163	Mauritania	20.5537	-12.6916	ADR	ADR	ADR
10	BEV.T661	Mauritania	20.7485	-13.1276	ADR	ADR	ADR
11	CIBIO11440	Morocco	22.1557	-15.3468	ADR	ADR	ADR
12	CIBIO11973	Mauritania	19.8265	-14.2555	ADR	ADR	ADR
13	CIBIO12011	Mauritania	21.1596	-11.9362	ADR	ADR	ADR
14	CIBIO12018	Mauritania	21.1502	-11.9623	-	ADR	-
15	CIBIO13640	Mauritania	22.6086	-12.5569	ADR	ADR	ADR
16	CIBIO13814	Mauritania	19.6289	-12.5344	ADR	ADR	ADR
17	CIBIO1861	Mauritania	19.7972	-12.9980	ADR	ADR	ADR
18	CIBIO1862	Mauritania	19.8632	-12.9909	-	ADR	ADR
19	CIBIO2902	Mauritania	21.4282	-11.3139	ADR	ADR	ADR
20	CIBIO2952	Mauritania	18.9849	-13.0647	ADR	ADR	ADR
21	CIBIO5865	Mauritania	20.5537	-12.6916	-	ADR	-
22	CIBIO5905	Mauritania	21.1521	-11.9470	ADR	ADR	ADR
<i>Mesalina olivieri</i>							
23	BEV.10013	Morocco	33.1860	-3.9900	-	MOR2	-
24	BEV.10014	Morocco	33.1860	-3.9900	-	MOR2	-
25	BEV.10015	Morocco	33.1860	-3.9900	MOR2	MOR2	MOR2
26	BEV.11948	Morocco	32.9297	-5.0465	MOR3	MOR3	MOR3
27	BEV.13322	Algeria	36.6245	4.8517	ALG3	ALG2/ALG3	ALG2/ALG3
28	BEV.13621	Algeria	35.8802	1.6841	ALG2	ALG2/ALG3	ALG2/ALG3
29	BEV.6402	Morocco	31.1940	-6.2100	-	MOR1	-
30	BEV.8796	Israel	30.7077	34.7845	-	ISR	-
31	BEV.8830	Israel	31.0858	34.6310	ISR	ISR	ISR
32	BEV.9225	Algeria	33.5914	2.9508	ALG1	ALG1	ALG1
33	BEV.T3036	Algeria	36.3413	4.2509	ALG3	ALG2/ALG3	ALG2/ALG3
34	BEV.T3037	Algeria	36.3413	4.2509	ALG3	ALG2/ALG3	ALG2/ALG3
35	BEV.T3038	Algeria	35.8585	6.4908	ALG1	ALG1	ALG1
36	BEV.T395	Egypt	31.1200	33.7600	-	EGY1	EGY1
37	BEV.T6678	Tunisia	35.8006	11.0361	TUN2	TUN1/TUN2/TUN3	TUN1/TUN2/TUN3
38	CIBIO308	Tunisia	35.5822	8.4826	TUN1	TUN1/TUN2/TUN3	TUN1/TUN2/TUN3
39	NHMC80.3.119.29	Tunisia	35.6895	10.1501	-	TUN1/TUN2/TUN3	-
40	NHMC80.3.119.10	Tunisia	32.1287	10.5638	-	TUN1/TUN2/TUN3	-
41	NHMC80.3.119.108	Algeria	35.4151	4.5190	-	ALG2/ALG3	-
42	NHMC80.3.119.109	Egypt	27.8300	31.1068	-	LYB1	-

(Continues)

TABLE 1 (Continued)

No.	Sample code	Country	Latitude	Longitude	Nuc. clades	Mit. clades	Concat. clades
43	NHMC80.3.119.14	Tunisia	33.7531	9.3350	-	TUN1/TUN2/TUN3	-
44	NHMC80.3.119.16	Egypt	29.9651	33.1606	-	EGY2	-
45	NHMC80.3.119.19	Egypt	29.9651	33.1606	-	EGY2	-
46	NHMC80.3.119.2	Libya	32.3912	21.2404	-	LYB1	-
47	NHMC80.3.119.20	Egypt	29.9797	32.1187	-	EGY1	-
48	NHMC80.3.119.21	Libya	32.1247	12.8068	-	LYB2	-
49	NHMC80.3.119.22	Libya	32.1247	12.8068	-	LYB2	-
50	NHMC80.3.119.23	Algeria	35.4151	4.5190	-	ALG2/ALG3	-
51	NHMC80.3.119.3	Libya	32.3912	21.2404	-	LYB1	-
52	NHMC80.3.119.40	Egypt	30.5965	32.2715	-	EGY1	-
53	NHMC80.3.119.5	Libya	32.3912	21.2404	-	LYB1	-
54	NHMC80.3.119.9	Tunisia	34.4076	7.9448	-	TUN1/TUN2/TUN3	-
55	NHMC80.3.164.19	Libya	33.0956	11.7626	-	TUN1/TUN2/TUN3	-
56	SPM002917	Egypt	-	-	-	EGY1	-
57	SPM002920	Egypt	-	-	-	EGY1	-
58	CIBIO319	Tunisia	32.9974	10.6080	TUN3	TUN1/TUN2/TUN3	TUN1/TUN2/TUN3
<i>Mesalina pastouri</i>							
59	BEV.10179	Algeria	24.7839	8.8719	MAU3 + ALG	MAU3 + ALG/ MAU4 + NIG	MAU3 + ALG
60	BEV.10454	Mauritania	21.2777	-15.4703	MAU2 + MOR	MAU3 + ALG/ MAU4 + NIG	MAU4 + NIG
61	BEV.10455	Mauritania	21.2777	-15.4703	MAU2 + MOR	MAU3 + ALG/ MAU4 + NIG	MAU4 + NIG
62	BEV.14803	Mauritania	21.4866	-11.4139	MAU3 + ALG	MAU1/MAU2 + MOR	MAU2 + MOR
63	BEV.14804	Mauritania	21.2970	-11.9199	MAU2 + MOR	MAU1/MAU2 + MOR	MAU2 + MOR
64	BEV.14805	Mauritania	21.2970	-11.9199	MAU2 + MOR	MAU1/MAU2 + MOR	MAU2 + MOR
65	BEV.9177	Mauritania	21.3321	-11.9512	MAU4 + NIG	MAU1/MAU2 + MOR	MAU2 + MOR
66	BEV.9380	Mauritania	20.4600	-12.3560	MAU4 + NIG	MAU1/MAU2 + MOR	MAU2 + MOR
67	BEV.T662	Mauritania	20.4563	-12.3602	-	MAU4	-
68	BEV.T663	Mauritania	20.4641	-12.3790	MAU1	MAU1/MAU2 + MOR	MAU1
69	CIBIO10706	Mauritania	16.2051	-16.5034	MAU4 + NIG	MAU3 + ALG/ MAU4 + NIG	MAU4 + NIG
70	CIBIO11653	Mauritania	16.6072	-16.4418	MAU4 + NIG	MAU3 + ALG/ MAU4 + NIG	MAU4 + NIG
71	CIBIO11656	Mauritania	16.6554	-16.4242	MAU4 + NIG	MAU3 + ALG/ MAU4 + NIG	MAU4 + NIG
72	CIBIO12821	Mauritania	16.1307	-16.5112	MAU4 + NIG	MAU3 + ALG/ MAU4 + NIG	MAU4 + NIG
73	CIBIO12822	Mauritania	16.1307	-16.5112	MAU4 + NIG	MAU3 + ALG/ MAU4 + NIG	MAU4 + NIG
74	CIBIO13770	Mauritania	23.3699	-11.6696	-	MAU1/MAU2 + MOR	-
75	CIBIO2765	Mauritania	20.8061	-16.4561	MAU1	MAU3 + ALG/ MAU4 + NIG	MAU3 + ALG
76	CIBIO4449	Mauritania	17.0674	-16.2555	MAU4 + NIG	MAU3 + ALG/ MAU4 + NIG	MAU4 + NIG
77	CIBIO4467	Mauritania	16.8484	-16.3503	MAU4 + NIG	MAU3 + ALG/ MAU4 + NIG	MAU4 + NIG

(Continues)

TABLE 1 (Continued)

No.	Sample code	Country	Latitude	Longitude	Nuc. clades	Mit. clades	Concat. clades
78	CIBIO4468	Mauritania	16.8484	-16.3503	-	MAU3 + ALG/ MAU4 + NIG	-
79	CIBIO5061	Mauritania	19.6851	-16.0641	MAU3 + ALG	MAU3 + ALG/ MAU4 + NIG	MAU3 + ALG
80	CIBIO5077	Mauritania	19.7795	-16.0390	MAU2 + MOR	MAU3 + ALG/ MAU4 + NIG	MAU4 + NIG
81	CIBIO5100	Mauritania	19.9197	-16.0280	MAU2 + MOR	MAU3 + ALG/ MAU4 + NIG	MAU4 + NIG
82	CIBIO526	Mauritania	21.2777	-15.4703	-	MAU3 + ALG/ MAU4 + NIG	-
83	CIBIO5299	Mauritania	20.7972	-16.2221	MAU3 + ALG	MAU3 + ALG/ MAU4 + NIG	MAU3 + ALG
84	CIBIO5822	Mauritania	22.8350	-12.3292	MAU1	MAU1/MAU2 + MOR	MAU1
85	CIBIO6279	Mauritania	19.3514	-16.2004	MAU3 + ALG	MAU3 + ALG/ MAU4 + NIG	MAU3 + ALG
86	CIBIO6692	Niger	16.2178	12.1985	MAU4 + NIG	MAU3 + ALG/ MAU4 + NIG	MAU4 + NIG
87	CIBIO7333	Morocco	23.2185	-15.4468	MAU2 + MOR	MAU1/MAU2 + MOR	MAU2 + MOR
<i>Mesalina simoni saharae</i> ssp. nov.							
88	BEV.10453	Morocco	26.1256	-14.4799	-	AS	-
89	BEV.10849	Morocco	26.5298	-12.3364	AM	AS	AS
90	BEV.10850	Morocco	22.5709	-14.3544	AS	AS	AS
91	BEV.9114	Morocco	26.4925	-13.9198	AS	AS	AS
92	BEV.T1242	Morocco	21.3963	-16.9579	AS	AS	AS
93	BEV.T1256	Morocco	26.4925	-13.9198	AS	AS	AS
94	CIBIO9163	Morocco	22.6215	-14.6044	AS	AS	AS
<i>Mesalina simoni</i> ssp.							
95	BEV.8508	Morocco	32.1900	-2.2037	AM	AM	AM
96	BEV.8509	Morocco	32.1750	-2.1650	AM	AM	AM
97	BEV.9429	Morocco	30.7076	-8.3577	SOUSS	SOUSS	SOUSS
98	BEV.T12122	Morocco	28.4876	-11.3366	SOUSS	-	SOUSS
99	BEV.T353	Morocco	31.5740	-4.7380	AM	AM	AM
<i>Mesalina simoni simoni</i>							
100	BEV.9430	Morocco	31.8301	-7.9829	SIM	SIM	SIM
101	BEV.9431	Morocco	31.8129	-8.0138	SIM	SIM	SIM
102	BEV.T6301/E259	Morocco	32.3011	-7.5307	SIM	SIM	SIM

Note: The acronym "BEV" and "BEV.T" indicate vouchers and tissue samples deposited at the Biogéographie et Ecologie des Vertébrés-CEFE (Montpellier, France); the acronym "CIBIO" indicates vouchers and tissue samples deposited at CIBIO/InBIO, Centro de Investigação em Biodiversidade e Recursos Genéticos da Universidade do Porto (Vairão, Portugal); the acronym "NHMC" incates vouchers and tissue samples deposited at the Natural History Museum of Crete. The samples SPM002917 and SPM002920 have been obtained from Simó-Riudalbas et al. (2019).

M. olivieri species group; (b) identify the role of speciation in generating its current biodiversity, and (c) identify the spatiotemporal drivers of diversification in the context of what is known on the history of the Sahara-Sahel. To do so, we assembled (a) a mtDNA dataset of 378 specimens including all the 19-different species of *Mesalina* recognized to date; (b) a nuclear concatenated dataset of 84 specimens; and (c) a combined dataset including one mitochondrial and four

nuclear genes for 102 specimens of the *M. olivieri* species complex. We used our datasets to test the monophyly of the lineages AS, AM, ADR, TAG, and ALG1 and addressed their phylogenetic relationships, genetic divergence, and potential reproductive isolation. To assess the species status of the new putative species from Mauritania (ADR and TAG lineages), we examined patterns of allele sharing for the nuclear markers in sympatry or narrow parapatry to evaluate their

level of reproductive isolation. We also explored the interspecific morphological difference between this lineage and the other species of the complex and analyzed spatial data to model the distribution of this potential new species and its habitat requirements.

2 | MATERIALS AND METHODS

2.1 | Sampling and study area

This study focuses on the status of the *M. olivieri* species complex populations in North West Africa. For comparative purpose, we added representative samples from each major mitochondrial lineage of the *M. olivieri* complex identified outside our study area by Kapli et al. (2015) and Simó-Riudalbas et al. (2019). A total of 79 samples from *M. olivieri* (including seven and four samples from the AS and AM lineages, and 21 from the ADR), 39 from *M. pasteurii* (including one sample from the TAG lineage), and three from *M. simoni* were amplified and successfully sequenced for this work (samples and species distributions are shown in Figure 1). The complete list of all the new specimens sequenced plus the sequences downloaded from GenBank are provided in Table 1 and Table S1. The distribution and source of the samples are shown in Figure S1.

2.2 | Genetic analysis

2.2.1 | DNA extraction and amplification

Total genomic DNA was extracted from ethanol-preserved tissue using a proteinase K (10 mg/ml) digestion followed by a standard salt-extraction protocol. Amplifications were performed in 5 µl of 2x MyTaq Mix and 0.4 µM of each primer. The PCR conditions adopted for every primer pair are specified in Table 2. Some samples required minor adjustments to the temperature and time of annealing from the reported conditions. We amplified one fragment from the mitochondrial cytochrome *b* gene (Cyt-*b*, 400 bp, Kapli et al., 2015) and four nuclear DNA (nucDNA) gene fragments from the *beta fibrinogen intron 7* (β -fib7, 600 bp), *melanocortin receptor one gene* (MC1R, 630 bp), *ornithine decarboxylase gene* (OD, 467 bp), and *phosphogluconase dehydrogenase intron 7* (PgD7, 414 bp). These markers were selected because they were found to be informative in previous studies (Kapli et al., 2015; Simó-Riudalbas et al., 2019; Sindaco et al., 2018) or during our preliminary analyses. PCR products were cleaned using ExoSAP. Purification, and sequencing were outsourced to GENEWIZ, Leipzig, Germany. Amplified fragments were sequenced for the forward strand only (primers sequences are listed in Table 2). Obtained DNA sequences were checked for errors using Codon-Code Aligner (v. 2.0.6, Codon-Code Corporation). Heterozygote positions of nuclear sequences were coded using IUPAC ambiguity codes. The absence of stop codons was checked with MEGAX (Kumar et al., 2018). DNA sequences were aligned using MAFFT v.7 (Katoh et al., 2019) applying the default parameters (Auto strategy,

Gap opening penalty: 1.53, Offset value: 0.0). Homozygous indels were coded with dashes to maintain the overall alignment. The length of each indel was reduced to the minimum to maintain the number of variable positions. All sequences that were newly produced for the present study were deposited in GenBank (Accession numbers from MZ223473 to MZ223857; Table S1).

A total of 80, 72, 74, 71, and 68 new samples were successfully sequenced for Cyt-*b* (Alignment S1), β -fib7 (Alignment S2), MC1R (Alignment S3), PgD7 (Alignment S4), and OD (Alignment S5), respectively (Table S1). Three datasets were produced: (a) Dataset S1: a mitochondrial dataset (Cyt-*b*; 285 bp), including outgroup (listed below) and all sequences available from the most recent publications (Kapli et al., 2015; Simó-Riudalbas et al., 2019; Sindaco et al., 2018; Šmid et al., 2017) for a total of 378 sequences; (b) Dataset S2: a concatenated multilocus nuclear dataset (1700 bp) with a total of 78 sequences (including only samples with at least three genes) of the *M. olivieri* species complex, a few representative specimens of the other species of the genus and one specimen of *Acanthodactylus erythrurus* as outgroup; (c) Dataset S3: a concatenated mt + nucDNA dataset with a total of 86 concatenated sequences (1986 bp) of the *M. olivieri* species complex (including only samples with at least three genes) plus four species used as outgroup: *Gallotia atlantica*, *Psammodromus algirus*, *Podarcis pityusensis*, and *Podarcis lilfordi*, this dataset was used to calculate the phylogeny of the species complex and the time of divergence. Specific details of each database, as well as their implementations, are resumed in Table S2.

2.2.2 | Phylogenetic analyses

For all datasets, Bayesian inferences (BI) were performed with BEAST 1.10.4 (Suchard et al., 2018). The best-fitting model of nucleotide substitutions for each gene was determined with PartitionFinder v.1.1.1 (Lanfear et al., 2012). The program was set as follows: branch lengths unlinked, only models available in BEAST were evaluated, BIC model selection criterion applied, and all partition schemes analyzed. Each gene was tested independently. The partition scheme and models of sequence evolution selected were β -fib7: HKY+G; MC1R: HKY+I; OD: HKY; PgD7: K80+G; and Cyt-*b*: HKY+G+I. No partition by codon position was selected for any of the genes.

To test whether the genes studied evolve in a clock-like manner (strict clock) a preliminary BI analyses was run in BEAST 1.10.4 (Suchard et al., 2018) using a relaxed clock for all the markers. The results of this preliminary run were verified using TRACER 1.6. (<http://tree.bio.ed.ac.uk/software/tracer>). The strict-clock model was rejected when the standard deviation of the uncorrelated log-normal relaxed clock parameter (ucl.stdev) and the coefficient of variation were greater than one. We used a Speciation Yule Process model assuming a constant lineage birth rate for each branch in the tree. Three independent MCMC runs of 100 million generations were implemented for each analysis for each dataset, sampling

TABLE 2 Data on the primers used in this study (with their orientation, sequences, references, and PCR conditions)

Gene	Ampli con length	Alignment size	Primers	Reference	Sequence 5'-3'	PCR cycling
Cyt-b	400 bp	303 bp	Mes_cytb_F Mes_cytb_R	Kapli et al. (2015)	CGWAAAACAAACACCCVATCCT GATATTGGTCCTCADGGHA	95° (5:00); [95° (0:30); 50 to 53° (0:45)-72° (1:00)] for 45 cycles; 60° (10:00)
β -fib7	600 bp	384 bp	BFXF BF8	Sequeira et al. (2006) Pinho et al. (2008)	CAGGGAGAGCTACTTTGATTAGAC CACCAACCGCTCTTTGGAAACACTG	95° (10:00); [95° (0:30); 52° (0:30)-72° (1:00)] for 38 cycles; 60° (10:00)
MC1R	630 bp	582 bp	MC1RF MC1RR	Pinho et al. (2009)	GGCNGCCATYGTCAAGAACCGGAACC CTCCGRAAGGCRTAAATGATGGGGTCCAC	95° (5:00); [94° (0:30); 58° (1:30)-72° (1:00)] for 40 cycles; 72° (7:00)
OD	467 bp	425 bp	OD1ez F OD1ez R	Friesen et al. (1999)	GCTTACACTAAAAAACCGACAG CCACCAATATCAAGCAGGTAC	95° (5:00); [94° (0:30); 56 to 58° (1:30)-72° (1:00)] for 40 to 42 cycles; 72° (7:00)
PgD7	414 bp	309 bp	PgDP8F PgDP7R	Pinho et al. (2008)	GACATGCAGCTGATCTGTGAGGCC GAGTCCAGCTCAGTCTTATTCCAC	95° (5:00); [94° (0:30); 58° (1:30)-72° (1:00)] for 40 cycles; 72° (7:00)

every 10,000 generations, and 10% of the trees were discarded as burn-in.

To root and calibrate the mt + nucDNA tree, four species were used as outgroup: *G. atlantica*, *P. algirus*, *P. pityusensis*, and *P. lilfordi*. The calibration points (in millions of years ago) and priors applied to the divergence time estimation correspond to those used Simó-Riuibalbas et al. (2019): (a) the split between *G. atlantica* and *P. algirus* (age of the Canary Islands Fuerteventura and Lanzarote; normal distribution, mean 18, SD 2); (b) the split between *P. pityusensis* and *P. lilfordi* (end of the Messinian Salinity Crisis; normal distribution, mean 5.32, SD 0.05).

2.2.3 | Haplotype networks reconstruction and genetic distances

Haplotype networks were reconstructed for each nuclear marker. Nuclear sequences were initially phased per lineage using the PHASE algorithm, implemented in DNAsP 5.10.01 (Librado & Rozas, 2009). The algorithm was run five times, for 10,000 iterations, with a burn-in of 1000. The most probable reconstructed haplotypes were used to create the haplotype networks. Haplotype networks were then reconstructed in TCS (Clement et al., 2000) with a 95% parsimony threshold for the nuclear genes: β -fib7 (186 sequences), MC1R (152 sequences), OD (120 sequences), and PgD7 (124 sequences), and then displayed in tcsBU (Múrias dos Santos et al., 2016).

Computation of sequence divergence (uncorrected *p*-distances) for the Cyt-b fragment was performed in MEGAX (Kumar et al., 2018) to provide an overview of the genetic divergence among taxa. The grouping referred to the topology of the Cyt-b tree built using a database containing the sequences from this study and those published by Kapli et al. (2015).

2.3 | Additional analyses for the species description

2.3.1 | Morphological analyses

For the morphological data, we examined voucher specimens housed in the collection of the Biogeography and Ecology of Vertebrates (BEV) in the CEFE lab in Montpellier. A total of 32 morphological variables were measured in 252 specimens: 138 of *M. olivieri* (including eleven specimens from the AS/AM lineages and 18 from the ADR lineage), 37 of *M. pastouri* (including the TAG lineage) and 21 of *M. simoni* (samples localities are given in Table 1 and Table S1). Variables were selected according to their relevance as diagnostic characters of the genus *Mesalina* in previous sources (e.g., Hosseiniyan Yousefkhani et al., 2015; Trape et al., 2012) or based on our own examination of specimens of the various lineages. We scored each individual for: (a) five quantitative biometric variables; (b) 11 quantitative pholidotic variables; (c) 10 semi-quantitative (ordinal) chromatic variables; (d) four semi-quantitative (ordinal) variables describing morphological

states (Table 3). Scale nomenclature, scale counts, and measurements follow Bons and Geniez (1995). All morphological data were obtained by the same observer (CP).

To identify diagnostic characters and to quantify the amount of morphological differentiation between the ADR and TAG lineages and the other species of the *olivieri* complex, we conducted multivariate analyses over three morphological datasets: biometry (Table S3), pholidosis (Table S4), and coloration (Table S5). Multivariate analyses were restricted to adult specimens to reduce variation due to the strong ontogenetic modifications in color patterns in the genus *Mesalina*. Both sexes were treated separately, as preliminary analyses revealed significant sexual dimorphism for many variables in every clade (results not shown). Due to the small sample size, statistical tests were not conducted. An exploratory investigation was first performed with Excel using a heating map to facilitate an

immediate visualization of the most relevant interspecific differences. Then, Principal Component Analyses (PCAs) were run on each database for a pairwise comparison of the potential new species with the other species of the complex. The data were normalized to zero mean and unit variance prior to PCAs. All analyses were run on PAST 3.24 Software (Hammer et al., 2001).

2.3.2 | Distribution modeling and habitat comparison

An ecological niche model was performed to assess the potential distribution and characterize the realized ecological niche of the ADR and TAG lineages. For this analysis, we aimed to include all the known localities of these two lineages. To do so, we considered

TABLE 3 Morphological variables measured for this study

Type	Acronym	Extended name
Biometry (Quantitative)	SVL	Snout-vent length (mm)
	TL	Tail length (mm)
	HL	Head length (mm)
	HW	Head width (mm)
	HH	Head height (mm)
Pholidotic (Quantitative)	D	No. of longitudinal rows of dorsal scales counted around midbody
	V	No. of transvers rows of ventral plates
	G	No. of gular scales in one straight line from the collar to the infralabials (collar included)
	Pf (Dx and Sx)	No. of femoral pores on the right and left sides
	Lam	No. of lamellae beneath the fourth toe
	NTS	No. of rows of temporal granulae (average of left and right side)
	TR	No. of scales around the tail at the 10th scale ring
	SL	No. of supralabials in contact with the subocular on the right and left sides
	IL (Dx and Sx)	No. of infralabials on the right and left sides
	Col	No. of enlarged scales forming a collar
	EL	No. of enlarged scales on the lower eyelid (forming the palpebral disks, average of left and right side)
Chromatic (Ordinal)	EBL	Black line surrounding the eyelids scales (0 = absent; 1 = present)
	DBF	Dark bands along the flanks (0 = absent; 1 = fragmented; 2 = continuous)
	PSDBF	Pale spots inside the dark bands along the flanks (0 = absent; 1 = small pale spots 2 = ocelli)
	PDLL	Pale dorsolateral line (0 = absent; 1 = fragmented; 2 = continuous)
	SPDLL	No. of scales included into the width of the pale dorsolateral line
	DDSSL	Dark supra-dorsolateral line (0 = absent; 1 = fragmented; 2 = continuous)
	SDDLB	No. of scales included into the width of the dark supra-dorsolateral line
	PSDDSSL	Pale spots within the dark supra-dorsolateral line (0 = absent; 1 = small pale spots 2 = ocellus)
	DSO	Small ocelli arranged in rows along the mid dorsum 0 = absent; 1 = small pale spots 2 = ocelli)
	TC	Under tail coloration (0 = white; 1 = yellowish; 2 = yellow)
Morphological (Ordinal)	TE	Tail enlargement (from 0 to 2)
	RN	Raised nostrils (from 0 to 2)
	PS	Pointed snout (from 0 to 2)
	DS	Shape of the dorsal scales (0 = flat; 1 = pointed; 2 = weakly carinated (tectiform); 3 = well carinated)

Note: Variables were selected according to their relevance as diagnostic characters in the genus *Mesalina* (Hosseiniyan Yousefkhani et al., 2015; Trape et al., 2012) or based on our own examination of specimens of the various lineages.

an area of approximately 1,979,127 km² (varying between 28°N, 17°W to 14°N, 4°W) that includes southern Morocco, South-western Algeria, the full extent of Mauritania, South-western Mali, and North-eastern Senegal, comprising the whole distribution of the potential new species (known to date). Models were based on the 28 presence records confirmed by genetic or morphological assignment. Morphological identifications of unsequenced specimens were based on pictures of live unvouchered animals or from the direct examination of specimens deposited in museum collections. Only records based on adult specimens exhibiting distinctive characteristics of the ADR lineage were treated as valid. To remove duplicated observations from the same geographic locations, data were thinned reducing to 20 the number of observations to build models. Models were built using a spatial resolution of 1 km.

Variables used for the modeling were: (a) Terrain Roughness Index (TRI) calculated by upscaling a digital elevation model (USGS, 2006) from 90 meters to 1 km; (b) 18 land-cover categories (Table S6) adapted from Campos and Brito (2018) and up-scaled from 30 m to 1 km; (c) four bioclimatic variables, maximum temperature of warmest month (BIO5), minimum temperature of coldest month (BIO6), temperature annual range (BIO7), and annual total precipitation (BIO12) from Hijmans et al. (2005). All variables were uncorrelated ($r < 0.75$).

The models were developed using the Maximum Entropy approach implemented in Maxent v.3.3 (Phillips et al., 2006) with the following settings: 5000 maximum number of iterations; regularization multiplier equal to 1; 10,000 maximum number of background points; 20 replicates selected by bootstrap. The area under the receiver-operating curve (AUC) of each replicate run was taken as a measure of model accuracy and ensemble models were generated by averaging the 20 model replicates. Response curves and jackknife analyses were performed to assess the importance of each variable in each model replicate (e.g., Vale et al., 2014). Finally, the minimum training presence threshold was applied to the ensemble model given that less restrictive thresholds should be applied for conservation purposes (Liu et al., 2005). The resulting binary map (depicting presence/absence areas) was used to calculate the extent of occurrence and area of occupancy following IUCN guidelines for assessing Red List categories (IUCN, 2017).

The percentage of presences of each lineage of the *olivieri* complex in each land-cover unit was taken as a measure of the biogeographic affinities of each group (Brito et al., 2009). Selection among land-cover units was quantified from the percentages of training observations using the Standardized Levin's *B* measure of niche breadth: $B = \frac{1}{n} \sum_{i=1}^n \frac{1}{p_i}$, where *B* is the Levin's index and *n* the total number of land-cover units. "*B*" is given by $1/P(p_2)$, where *p* is the proportion of observations in each land-cover unit. The standardized index was used because of unbalanced sample size among groups. Eight land-cover units selected were sandy areas (51.1% of the study area), compact soil (6.1%), rocky plateaus (16.8%), bare rocks (6.3%), gravel and sand floodplains (1.9%), grasslands (9.1%), savannah (2.9%), and croplands (5.7%).

2.3.3 | Taxonomic ranking

We (the authors) do not necessarily adhere to the same species concept. While some follow the Unified Species Concept (USC) of De Queiroz (2007), some prefer the general framework of the Biological Species Concept (BSC; Mayr, 1970). However, we all recognize reproductive isolation as the primary operational criterion for the delimitation of species and we all agree that, while every species is a lineage, not every lineage is a species. The approach used in this paper can be defined either as following the BSC framework, or as applying a Biological Species Criterion under the USC. We thus treated sympatric or parapatric lineages that do not exchange genes when they are not isolated by extrinsic geographical barriers as species. Moreover, this study adopts the framework of integrative taxonomy based on the assumption that divergences in any of the attributes can provide evidence for the species' existence (Dayrat, 2005; Padial et al., 2010). We have divided our dataset into six categories that can each be regarded as distinct lines of evidence. They can be combined and compared in order to assess the congruence of the putative species limits among the *olivieri* complex: (a) the mtDNA data can be used to test the criteria of reciprocal monophyly and the presence/absence of barcoding gaps, (b) the multilocus nucDNA data can be used to test, independently from the mtDNA set, the criteria of reciprocal monophyly, notably in coalescence theory framework, (c) the morphological data allows to test the criteria of morphological divergence, and (d) habitat and v) distribution range and vi) land-cover datasets can be used as a complementary approach to test the criteria of isolation and distinct habitat requirements.

3 | RESULTS

3.1 | Phylogenetic relationships within the *Mesalina olivieri* species complex

Since not all samples were successfully amplified for all genes (see Table S1), some samples were absent from the concatenated mt + nucDNA dataset and/or not included in the comparison between nuclear and mtDNA results. Consequently, some of the mtDNA *M. olivieri* lineages (see Figure 2a, Figure S2 and Table 1) are absent from the mt + nucDNA results (Figure 3 and Figure S4). The trees based on concatenated mtDNA and nuDNA recover several lineages that occupy distinct regions of the distribution of the *M. olivieri* complex (including *M. simoni* and *M. pastouri*). These lineages are depicted in Figures 2–4 (see also Table 1) and identified by acronyms corresponding with their distribution: ADR from Adrar and adjacent areas in Mauritania and southern Morocco; TAG from the Tagant mountains in Mauritania; SOUS from the Sous-Massa region (Morocco); SIM the *terra typica* lineage of *M. simoni* from north and west of the Atlas Mountains in Morocco; AM from south and south-east Morocco; AS from Atlantic Sahara, ALG1 from Algeria; ISR from Israel; the *terra typica* lineage of *M. olivieri* from Egypt (EGY1); TUN1/TUN2/TUN3 from Tunisia; ALG2/ALG3 from western Algeria; MOR2

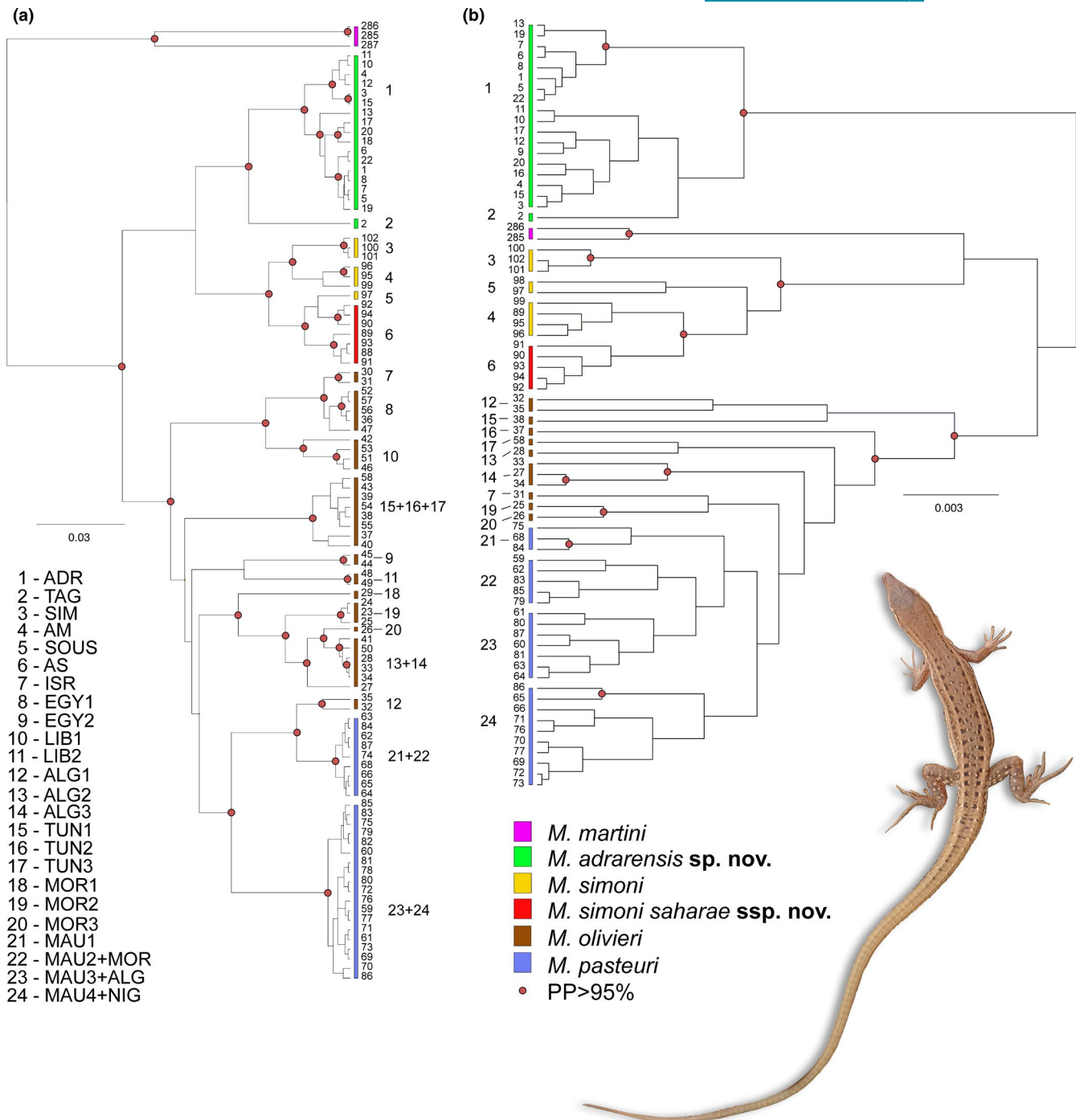


FIGURE 2 Mirrored results of the BI analysis of multilocus nuclear Dataset S2 (a) and mitochondrial Dataset S1 (b). Red dots represent nodes where $PP \geq 0.95$. Sample codes are shown in the complete trees in Figures S2 and S3. Number on the tree tips correspond to the samples in the Table 2 and Table S1; bigger numbers on the right of the tree correspond to the lineages. Inset picture shows a male specimen of *Mesalina adrarensis* sp. nov. from Mauritania

and MOR3 from eastern Morocco; a *pastouri* clade from the center of Mauritania (MAU1); a *pastouri* clade from the Atlantic Sahara region (MAU2 + MOR); a *pastouri* clade from the Atlantic coast of Mauritania and inland Algeria (MAU3 + ALG); a *pastouri* clade from the Atlantic coast of Mauritania and inland Niger (MAU4 + NIG).

All the species used as outgroup always clustered outside the *olivieri* complex, except for *M. martini*. The latter was recovered as: (a) basal to the *olivieri* complex when mtDNA was analyzed alone

(Dataset S1, Figure 2a and Figure S2), and for the mt + nucDNA results (Dataset S3; Figure 3 and Figure S4); (b) sister to the *M. simoni* clade (*M. simoni* and *olivieri* lineages AS/AM) for the nucDNA Dataset S2 (Figure 2b and Figure S3).

In all the trees that include mtDNA (Figures 2a and 3, Figures S2 and S4), the *olivieri* species complex is divided into two deep and well-supported clades: (a) one clade including the ADR and TAG lineages, *M. simoni* and the two *olivieri* lineages AS and AM (sister taxa

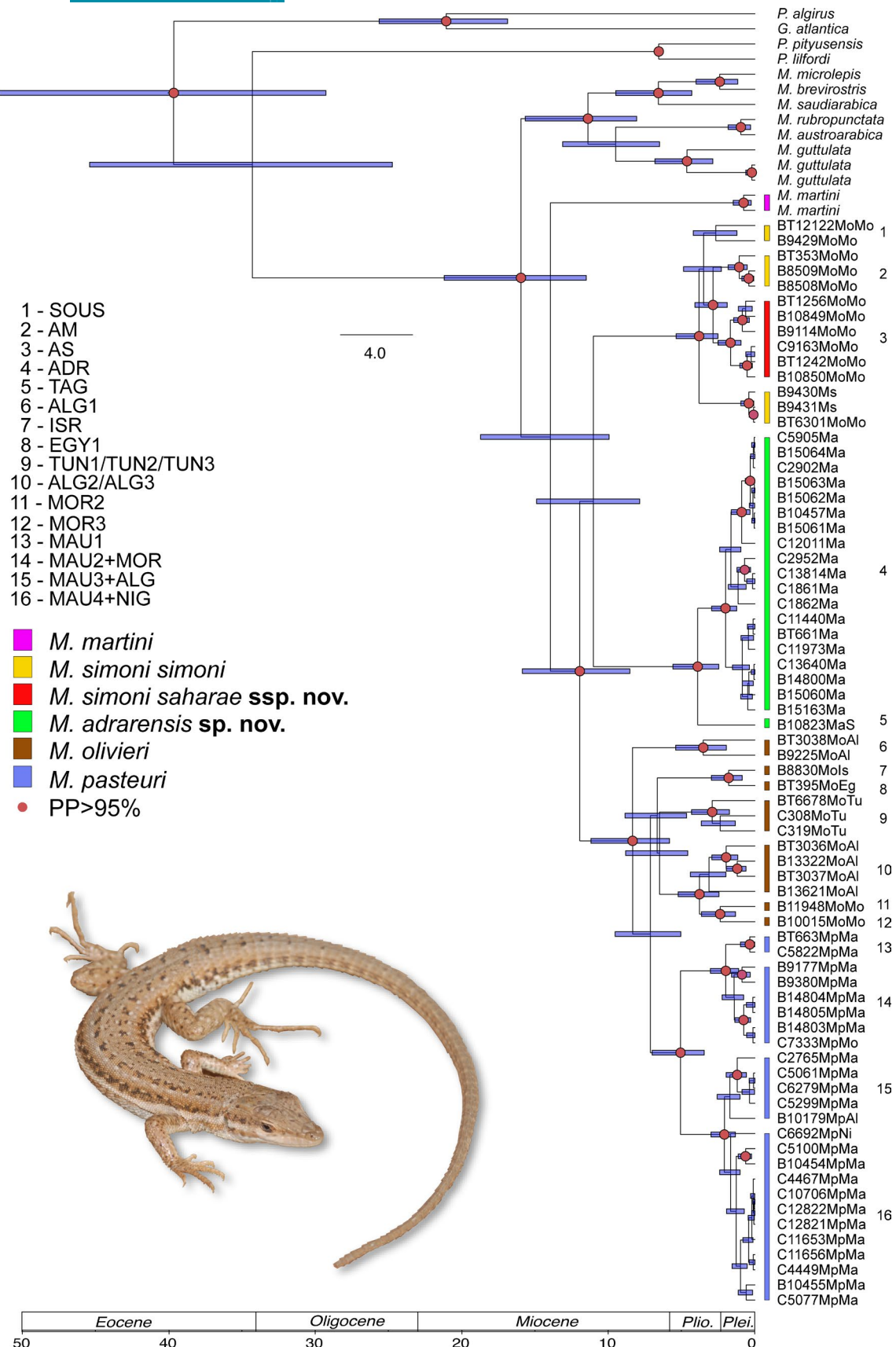


FIGURE 3 Calibrated phylogenetic mt + nucDNA tree (Dataset S3). Values represent Mya. Red dots represent nodes where PP ≥ 0.95. Blue horizontal bars represent the 95% confidence intervals for age estimated. Number on the tree tips correspond to the samples in the Table 2 and Table S1; bigger numbers on the right of the tree correspond to the lineages. Inset picture shows a specimen of *Mesalina simoni saharae* ssp. nov. from Atlantic Sahara

of *M. simoni*), and (b) one clade including the remaining *M. olivieri* and *M. pasteurii*. In all trees the AS and AM lineages are well-defined, except for the sample BEV.10849 (sample number 89). This sample (collected 76 km past Laayoune toward Smara) clusters in the AS lineage in all trees (Figures 2a and 3 and Figures S2 and S4) with the exception of the concatenated nucDNA tree (Figure 2b and Figure S3). The position of the clade made of the ADR and TAG lineages also differs between nuclear and mtDNA: basal to the *M. olivieri* species complex for the nuclear dataset (Dataset S2, Figure 2b and Figure S3) or sister to the *M. simoni* clade for the mitochondrial and for the mt + nucDNA datasets (Datasets S1 and S3, Figures 2a and 3, Figures S2 and S4).

The results also revealed a case of discordance between markers: the *olivieri* lineage ALG1 was recovered (with strong support, PP > 95%) as sister to the continental lineage of *M. pasteurii* in mtDNA (Figure 2a and Figure S2), but basal to *M. pasteurii* and *M. olivieri* (together with a sample from Tunisia, 308 = TUN1) when nucDNA was analyzed alone (Figure 2b and Figure S3). As a result, its position (basal to *M. pasteurii* and *M. olivieri*) in the mt + nucDNA concatenated tree is not meaningful (Figure 3 and Figure S4).

3.2 | Nuclear haplotype networks and mitochondrial genetic divergence

Haplotype network reconstructions for nuclear loci (Figure 5) indicate that none of the alleles found in the ADR and TAG lineages (marked in green in Figure 5) is shared with the other lineages. However, haplotype sharing was detected between *M. simoni* and the two *olivieri* lineages AS and AM for all markers. All the haplotypes found in *M. simoni* + AS and AM lineages are private and completely separated from the other species in β -fib7 and PgD7 networks. A connection between *M. simoni*, AS and AM lineages and the other species is recovered in MC1R and OD where they still diverge from the other *M. olivieri* by one and two mutational steps, respectively. In the network analysis for MC1R, the *terra typica* lineage of *M. simoni* and the SOUS lineage (yellow dot detached from the other haplotypes in the MC1R network, Figure 5) shows a divergence from the two *olivieri* lineages AS and AM of five mutational steps.

The level of mitochondrial genetic divergence (*p*-distance) between ADR and TAG lineages and the other species of the complex was recorded to be always above 8.9%. The genetic divergence between the *olivieri* lineages AS and AM and *M. simoni* was always below 5% (Table 4).

3.3 | Time of divergence

Based on the mtDNA + nuDNA concatenated tree (Figure 3 and Figure S4), estimation of divergence times indicates that the *olivieri* complex started to diversify in the Late Miocene, ca. 9.6 Mya (6.92–12.87 Mya, 95% highest posterior densities [HPD]; Figure 3) in two main clades: (a) one including the ancestor of *M. simoni* and the lineages ADR, TAG, AS, and AM and (b) the other one including

the ancestor of *M. olivieri* and *M. pasteurii*. Our estimation shows that the latter has undergone a first split (ca. 6.77 Mya) between the *olivieri* lineage ALG1 and the ancestor of *M. olivieri* and *M. pasteurii*, and that these two species diversify afterward from each other around 5 Mya. The clade made of *M. simoni* and the lineages AS, AM, ADR, and TAG started its diversification around 8.94 Mya (6.30–12.8 Mya, 95% HPD). Moreover, most of the intraspecific diversification of the complex took place during the Plio-Pleistocene transition (Figure 3). For instance: (a) the split between *M. simoni* and the lineages AS and AM is dated to 3.09 Mya (2.05–4.37 Mya 95% HPD); (b) the north-south diversification between the lineages ADR and TAG occurred ca. 3.17 Mya (2.01–4.54 Mya 95%); (c) a second, more recent and well-supported split delineated the eastern (samples no.: 1, 5–8, 13, 16–20) and the north-western (samples no: 3, 4, 9–12, 15) lineages, ca. 1.63 Mya (1.01–2.4 Mya 95% HPD).

3.4 | Additional results for the species description

3.4.1 | Morphological analyses

Measurements of all individuals examined for this work are given in Tables S3–S5. Descriptive statistics of the morphological data are shown in Tables 5–7 and Table S7. Morphological differences were found between the two lineages (ADR and TAG) representing the putative new species from Mauritania, and the remaining species of the complex (Figures S5–S8; Tables 5–7 and Table S7).

Compared with the other species of the *M. olivieri* complex, individuals of the ADR and TAG lineages have: (a) a narrower and more pointed snout (Figures S5 and S6; Table 6 and Table S7), (b) more protuberant nostrils (Figures S5 and S6; Table 5 and Table S7), (c) more dorsal and gular scales (Figure 7 and Figure S7; Table 6 and Table S7), (d) more femoral pores (Figure S7; Table 6 and Table S7), and (e) a higher number of lamellae beneath the fourth toe (Figure S7; Table 6 and Table S7). Moreover, (f) the shape and disposition of the scales composing the eyelid in the new species resemble those of *Mesalina guttulata* (Lichtenstein, 1823) (1–2 clearly enlarged, transparent scales in the lower eyelids versus several sub-equal scales in the *M. olivieri* complex) although most of the specimens of the ADR and TAG lineages lack the well-defined dark lines edging the large eyelid scales found in *M. guttulata*.

Major differences were also found in the dorsal coloration. The PCAs on these characters including specimens of *M. olivieri* and the putative new species highlights the presence of pale dorsal spots on the dorsum (PSDDSSL, more obvious in both male and females of the potential new species) and the pattern of dark bands on the dorsum (SDDLDB) and on the flanks (DBF) both thicker and better defined in *M. olivieri* than in the putative new species. Similarly, the dorsal pattern differs between the new species and *M. pasteurii*: in *M. pasteurii* the dorsal patterns is mostly made of obvious pale and dark continuous longitudinal stripes, whereas in the putative new species the two dark supra-dorsolateral lines are highly fragmented

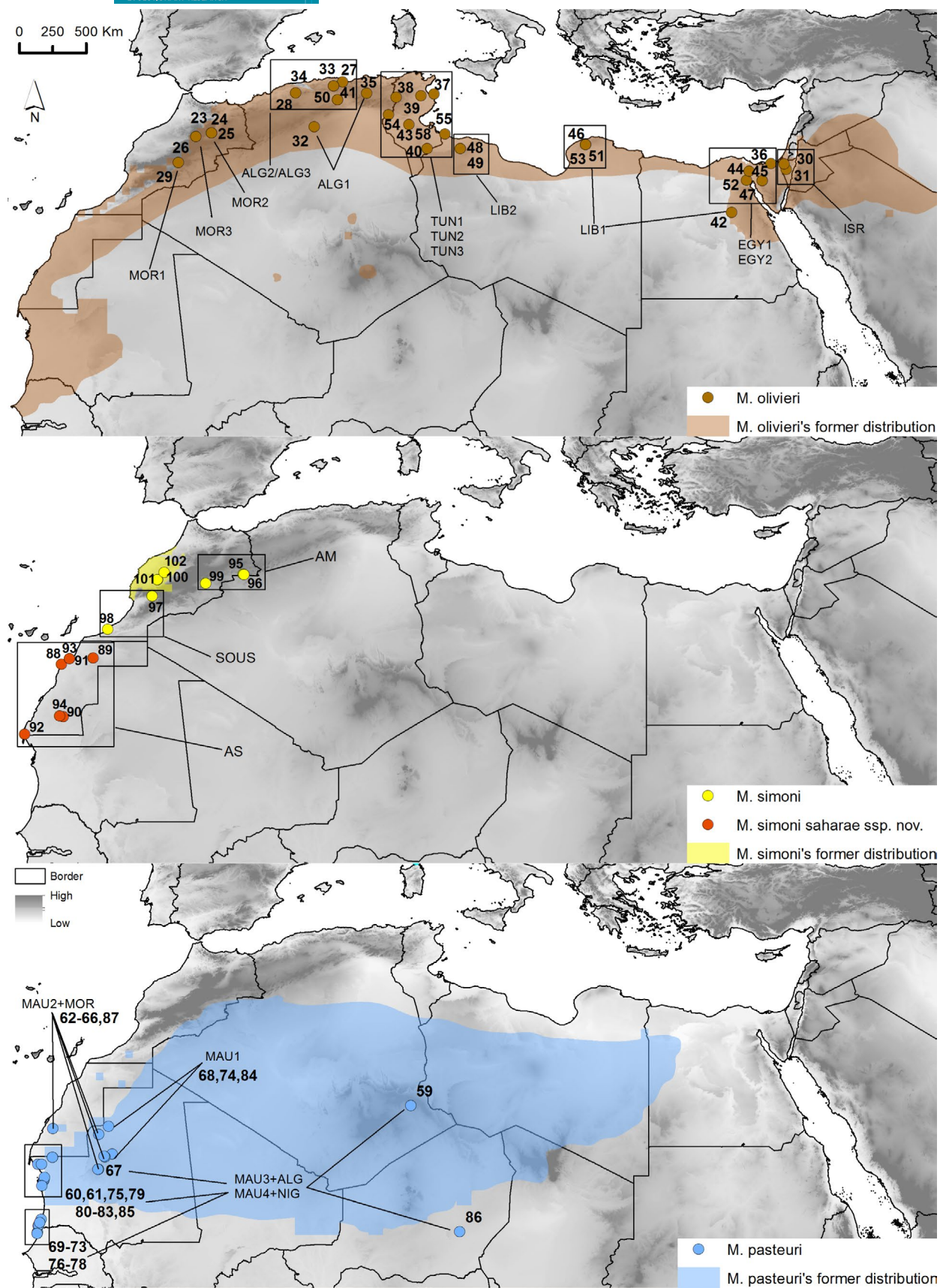


FIGURE 4 (a) The brown polygon represents the former known distribution of *Mesalina olivieri*, brown dots within it the localities of the samples used in this study; (b) The blue polygon and dots within it, represent the known distribution of *Mesalina pastouri*, blue dots outside the polygon the new localities provided in this study; (c) The yellow polygon represents the current known distribution of *Mesalina simoni* yellow dots within it the localities of *Mesalina simoni*, in red the localities of *Mesalina simoni saharae* ssp. nov.

(forming irregular small patches) and the two pale dorsolateral lines are thin and fragmented (Figures S5 and S8; Table 7).

3.4.2 | Distribution modeling and habitat comparison

The 20 replicate ecological models exhibited good predictive accuracy (average AUC = 0.906, Table S8). The most important environmental predictors were terrain ruggedness index (42.6% contribution) and land-cover category (35.4%) (Figure S9; Table S8). The highest probability of occurrence is in the intermediate levels of terrain ruggedness and in bare rock habitats (Figure 6 and Figure S9). These findings fit well with our field observations, as samples of the ADR and TAG lineages were always collected in rocky habitats on slopes or plateaus, while *M. pastouri* was only found in the adjacent plains (pers. obs.).

We found significant differences in number of observations in each land-cover category (χ^2 ; $p = 0.006$; $df = 21$; Figure 6; Table S9) for the area considered in this study: (a) the lineage representing the putative new species from Mauritania (ADR-TAG) was mostly found (70% of observations) in bare rocks, a restricted land-cover category in the study area (6.3% of the area) but showing similarities with *M. guttulata* habitat; (b) *M. simoni* and the *olivieri* lineages AS and AM were most frequently found in rocky plateaus; (c) *M. olivieri* occurred in almost all units; and (d) *M. pastouri* appeared to be most related to sandy areas. The niche breadth estimation was under 0.5 in all cases indicating that all taxa are specialized in habitat selection, and that the *olivieri* lineages ADR and TAG are the most specialized ones.

3.4.3 | Taxonomic implications

The ADR and TAG lineages form a well-supported, monophyletic clade. In all datasets and all analyses, they share the same morphological features and habitat that distinguish them from the other species of *Mesalina* from northwest Africa. We thus treat them as one evolutionary unit for the time being, pending further studies and larger sampling of the TAG lineage. Given the observed divergences in genetics, morphology, and ecology from the other species of the genus *Mesalina*, and the lack of alleles sharing with the sympatric *M. pastouri* and parapatric *M. simoni* (Figure 5 and Figure S10) demonstrating reproductive isolation, we treat the evolutionary unit made of the ADR and TAG lineages as a valid species that we describe here.

Although the current taxonomy of the genus *Mesalina* assigns populations of the complex from southern Morocco and the Atlantic Sahara to *M. olivieri*, both mtDNA and nucDNA data unambiguously assign the lineages AS and AM to *M. simoni* rather than to *M. olivieri sensu stricto* (s.s.). We, thus, formally assign, here, all the populations of the *M. olivieri* complex from southern and southwestern Morocco to the Atlantic Sahara to *M. simoni*. We thus restrict *M. olivieri* to the populations distributed from central and eastern Morocco to Israel (in brown in Figure 4; see also Figures

2, 3 and 5). We suspect that *M. olivieri*, as restricted here, is itself a species complex and that several species-level units are still merged under this name.

In the concatenated mtDNA + nucDNA trees, there are four reciprocal monophyletic lineages within *M. simoni*: (a) SOUS, (b) AS, (c) AM, and (d) *M. simoni* s.s. (Figures 3 and 4). We have sequenced or examined very few specimens of the SOUS and AM lineages and thus refrain from proposing a distinct taxonomic status for the time being. From now on, we will refer to these lineages as *M. simoni* ssp. "SOUS" and *M. simoni* ssp. "AM". On the contrary, the AS lineage exhibits a distinct morphology, with most sub-adult or adult specimens being diagnosable from *M. simoni* s.s. (Figure S5). However, the four lineages are not distinct on the nuclear networks and specimens from the northern Atlantic Sahara or extreme south-western Morocco appear intermediate morphologically between *M. simoni* s.s. and AS (pers. obs.). We thus refrain from treating the AS lineage as a distinct species and formally recognize it as a new subspecies of *M. simoni*.

The nomen *simoni* was based on seven specimens collected "inter urbes Mogador et Marocco" (= between the cities of Mogador and Marocco) and one specimen from "prope urbem Casablanca" (= not far from the city of Casablanca, see Böttger, 1880). Mogador is the city currently known as Essaouira and Marocco was used at the time for the city of Marrakech. As far as we know, there has been no type locality restriction for this nomen so the type locality of *M. simoni* remains as "between Essaouira and Marrakech and near Casablanca." This area is inhabited by the lineage currently designed as *M. simoni* s.s. All the nomina currently allocated to the synonymy of *M. olivieri* were based on specimens from the eastern clade of *M. olivieri*, and we were unable to identify any nomen available for the lineages of the *M. olivieri* complex inhabiting Mauritania or south-western Morocco. We, thus, need to create new nomina to name the new species from Mauritania (ADR and TAG linages) and the new subspecies from south-western Morocco (AS lineage).

Consequently, we suggest the following nomenclatural and taxonomic actions: (a) designate all the populations of the lineages ADR and TAG as a new species here described as *Mesalina adrarensis* sp. nov.; (b) designate as subspecies of *M. simoni* all the *M. olivieri* present in the Atlantic Sahara region, here described as *Mesalina simoni saharae* ssp. nov.; (c) allocate all populations of *M. simoni* SOUS and AM (from north of the High Atlas and west of the Middle Atlas) to *M. simoni*. The two subspecies *Mesalina simoni simoni* and *M. simoni saharae* ssp. nov. are bridged by populations of intermediate morphology and genetic background between the High Atlas and the north of the Atlantic Sahara; specimens of *M. simoni* 'SOUS' (inhabiting the area around Tan-Tan and El Ouatia) are morphologically close to typical *saharae* but seem already admixed genetically with *M. s. simoni* (see specimen B9429 Figure 2a and Figure S2). The populations currently treated as *M. simoni* 'AM' could conceivably be included in *M. simoni saharae* ssp. nov., as they are genetically grouped with this taxon, but we prefer to analyses more specimens before we can conclude.

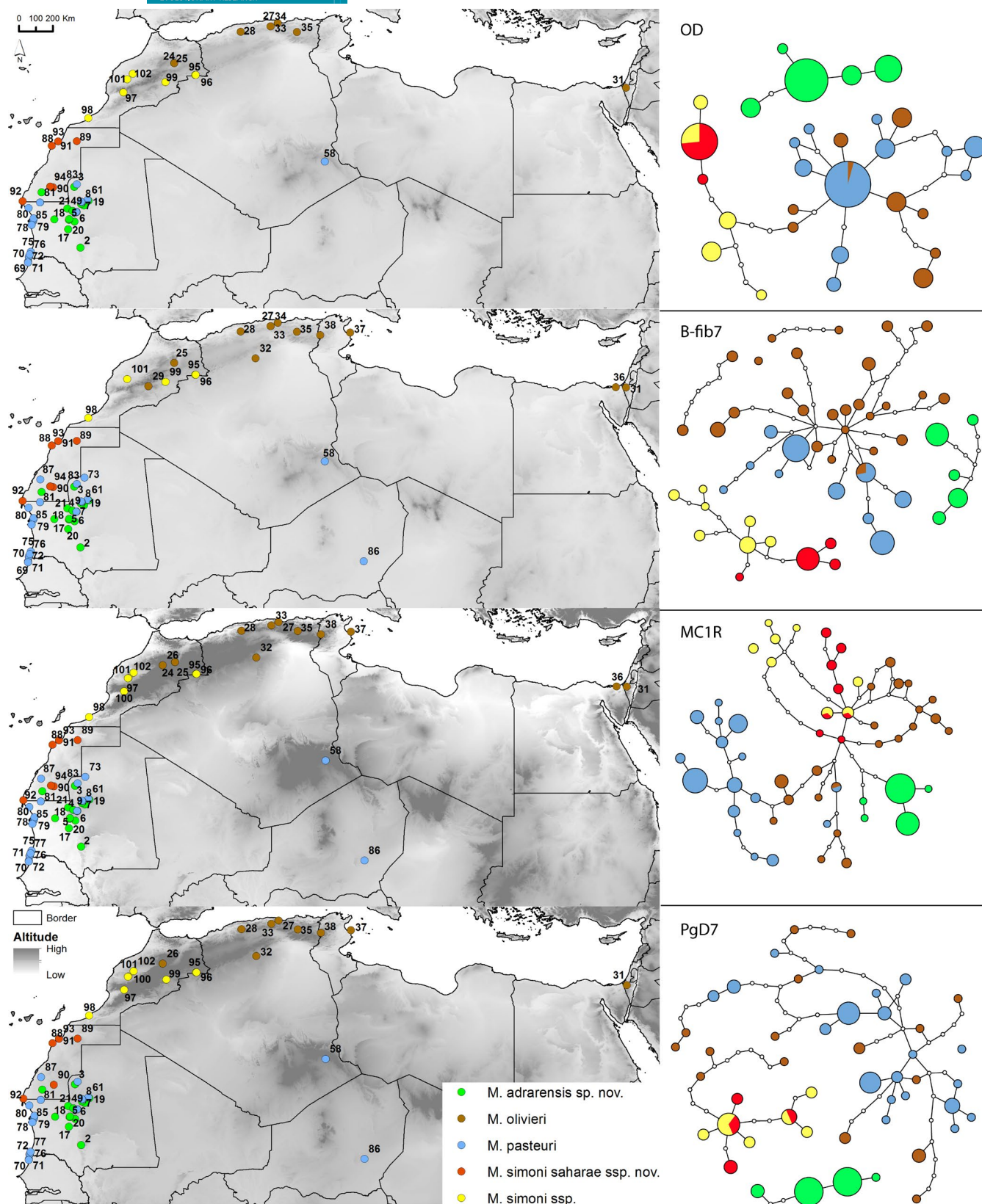


FIGURE 5 Geographical distribution and unrooted haplotype networks of the nuclear markers (OD, β -fib7, MC1R, PgD7) of the *Mesalina olivieri* species complex. Circle size is proportional to the number of alleles. Small circles show the number of mutational steps between two haplotypes. Dots numbers correspond to the samples in Table 1 and Table S1

TABLE 4 Estimates of evolutionary divergence between *Mesalina* species present in NW Africa (above) and between the different lineages of *Mesalina simoni* ssp. (below)

	<i>Mesalina adrarensis</i> sp. nov.	<i>Mesalina olivieri</i>	<i>Mesalina pasteurii</i>	<i>Mesalina simoni</i> ssp.	<i>Mesalina guttulata</i>
<i>Mesalina olivieri</i>	0.14				
<i>Mesalina pasteurii</i>	0.13	0.11			
<i>Mesalina simoni</i> ssp.	0.08	0.11	0.11		
<i>Mesalina guttulata</i>	0.20	0.19	0.22	0.18	
<i>Mesalina rubropunctata</i>	0.21	0.19	0.18	0.21	0.16
<i>Mesalina simoni</i>					<i>Mesalina simoni</i> ssp. AM
<i>Mesalina simoni</i> AM		0.03			
<i>Mesalina simoni saharae</i> ssp.nov. (AS lineage)		0.04			0.05

Note: Analyses were conducted using the Maximum Composite Likelihood model. This analysis involved 118 nucleotide sequences of the Cyt-b fragment. Codon positions included were 1st + 2nd + 3rd + Noncoding. All ambiguous positions were removed for each sequence pair (pairwise deletion option). There was a total of 286 positions in the final dataset. Distances in *Mesalina simoni* ssp. include the two subspecies.

TABLE 5 Results of the Principal Components Analysis using biometric characters

	<i>Mesalina adrarensis</i> sp. nov. vs. <i>Mesalina olivieri</i>		<i>Mesalina adrarensis</i> sp. nov. vs. <i>Mesalina pasteurii</i>		<i>Mesalina adrarensis</i> sp. nov. vs. <i>Mesalina simoni</i> ssp.	
	Males	PC 1	PC 2	PC 1	PC 2	PC 1
SVL	-0.039	-0.295	-0.133	-0.125	-0.060	-0.134
HL	0.118	0.711	0.150	0.013	0.139	0.349
HW	-0.107	0.390	0.176	0.569	-0.112	0.421
HH	-0.301	0.322	-0.096	0.206	-0.182	-0.012
TE	-0.059	0.364	0.199	0.725	-0.030	-0.436
RN	0.448	0.138	0.599	-0.290	0.333	0.649
PS	0.824	0.004	0.722	-0.096	0.905	-0.266
% variance	66.773	19.973	66.209	17.556	74.348	13.783
Females	PC 1	PC 2	PC 1	PC 2	PC 1	PC 2
SVL	-0.002	-0.232	-0.134	-0.216	-0.166	-0.216
HL	0.074	0.480	0.260	0.400	0.345	0.626
HW	-0.220	0.475	0.299	0.403	0.168	0.475
HH	-0.283	0.208	0.546	0.405	0.026	0.362
TE	-0.107	0.622	0.441	-0.242	0.398	0.062
RN	0.469	-0.002	-0.413	0.421	0.225	-0.136
PS	0.797	0.245	-0.404	0.481	0.785	-0.427
% variance	52.963	39.385	70.650	21.405	45.815	31.321

Notes: Loading scores and percentage of variance explained in the first three principal components extracted. Comparison between male and female individuals of *Mesalina adrarensis* sp. nov. with the other species of the *Mesalina olivieri* species complex.

Significant values are indicated in bold.

Mesalina adrarensis sp. nov.
(Figures 1–8; Tables 1, 3–6)

Zoobank registration. <http://zoobank.org/NomenclaturalActs/dc6c167b-8138-4017-82a4-513d8244072a>

Holotype. Adult female (Figure 7) with code MNHN-RA-2020.0017 preserved in the Muséum national d'Histoire naturelle, in Paris, France. Collected in the Tiris Zemmour (Mauritania) by Philippe Geniez, Olivier Peyre, Pierre-André Crochet and José Carlos Brito on 7th April 2017.

TABLE 6 Results of the Principal Components Analysis using pholidotic characters

	<i>Mesalina adrarensis</i> sp. nov. vs. <i>Mesalina olivieri</i>		<i>Mesalina adrarensis</i> sp. nov. vs. <i>Mesalina simoni</i> ssp.		<i>Mesalina adrarensis</i> sp. nov. vs. <i>Mesalina pasteurii</i>	
Males	PC 1	PC 2	PC 1	PC 2	PC 1	PC 2
V	0.311	0.012	0.078	0.008	0.067	0.234
D	-0.713	-0.050	0.892	-0.158	0.897	-0.182
DS	0.049	-0.158	0.039	0.254	0.174	-0.231
TR	0.213	0.179	0.092	-0.072	0.039	0.085
SL(Sx)	0.046	0.074	-0.015	0.000	-0.099	0.059
SL(Dx)	0.067	0.100	-0.024	0.011	-0.077	0.082
IL(Sx)	0.051	0.049	-0.003	-0.006	0.020	-0.090
IL(Dx)	0.064	0.059	-0.038	-0.022	-0.014	-0.052
G	0.425	-0.693	0.191	0.667	0.103	0.477
Col	0.190	0.048	0.235	-0.159	0.111	-0.055
EL	0.161	0.385	0.010	-0.316	0.112	-0.080
NTS	0.100	-0.031	0.154	-0.130	0.228	0.023
Pf(Sx)	-0.024	0.112	0.201	0.097	0.137	0.416
Pf(Dx)	-0.059	-0.011	0.162	0.450	0.165	0.303
Lam	0.271	0.522	-0.068	0.325	-0.090	-0.572
%variance	43.31	17.31	52.948	19.840	62.349	12.411
Females	PC 1	PC 2	PC 1	PC 2	PC 1	PC 2
V	0.231	0.015	0.627	0.403	0.231	0.015
D	0.699	-0.495	0.482	-0.582	0.699	-0.495
DS	0.033	0.013	-0.079	0.043	0.033	0.013
TR	0.061	-0.210	0.185	0.199	0.061	-0.210
SL(Sx)	-0.033	0.011	-0.159	0.032	-0.033	0.011
SL(Dx)	-0.058	0.027	-0.168	0.029	-0.058	0.027
IL(Sx)	0.048	-0.080	0.108	0.033	0.048	-0.080
IL(Dx)	0.031	-0.032	0.056	0.137	0.031	-0.032
G	0.210	0.374	-0.373	-0.164	0.210	0.374
Col	0.166	0.104	-0.108	-0.132	0.166	0.104
EL	0.047	-0.559	-0.003	0.489	0.047	-0.559
NTS	0.106	0.073	0.193	0.106	0.106	0.073
Pf(Sx)	0.299	0.311	-0.157	0.252	0.299	0.311
Pf(Dx)	0.324	0.203	-0.222	0.273	0.324	0.203
Lam	0.406	0.309	-0.047	0.029	0.406	0.309
%variance	35.895	19.620	94.81	2.50	35.895	19.620

Notes: Loading scores and percentage of variance explained in the first three principal components extracted. Comparison between male and female individuals of *Mesalina adrarensis* sp. nov. with the other species of the *Mesalina olivieri* species complex.

Significant values are indicated in bold.

Type locality. Mauritania, 440 m south-west of the Guelta Oumm el Habâl, 17.4 km east-southeast of F'derick. 22.60636°N/-12.55743°W/372 m a.s.l.

Paratypes. BEV.15163, adult female collected in the Adrar Atar, 44 km before Chinguetti coming from Atar (Mauritania, 20.5537°N/12.6916°W) by F. Martínez-Freiría, J.C. Brito, D.V. Gonçalves, J.C. Campos, Z. Boratyński, C.G. Vale, T.L. Silva, X. Santos, J.M. Pleguezuelos, M. Feriche

and A.S. Sow on the 29th October 2011; BEV.15060, adult male, same locality, collected by J.C. Brito, Z. Boratyński, S. Lopes, J. Marques and F. Martínez-Freiría on the 12th September 2015; BEV.15061, adult female, BEV.15062, adult male, BEV.15063, adult male, BEV.16064, adult male, all collected in the Adrar Atar, Oumm Lekhterat (Mauritania, 21.1596°N/11.9362°W) by J.C. Brito, Z. Boratyński, S. Lopes, J. Marques and F. Martínez-Freiría on the 13th September 2015, all preserved in the BEV collection in Montpellier.

TABLE 7 Results of the Principal Components Analysis using coloration characters

	<i>Mesalina adrarensis</i> sp. nov. vs. <i>Mesalina olivieri</i>		<i>Mesalina adrarensis</i> sp. nov. vs. <i>Mesalina pasteurii</i>		<i>Mesalina adrarensis</i> sp. nov. vs. <i>Mesalina simoni</i> ssp.	
Males	PC 1	PC 2	PC 1	PC 2	PC 1	PC 2
EBL	0.255	-0.201	0.326	-0.182	-0.035	0.262
DBF	0.555	-0.031	0.098	-0.116	-0.046	0.465
PSDBF	-0.262	-0.003	0.000	0.556	0.165	-0.329
PDLL	-0.210	0.232	-0.332	0.146	0.030	-0.213
SPDLL	-0.122	0.746	-0.110	-0.062	0.114	-0.087
DDSSL	0.298	-0.110	-0.176	-0.395	0.052	0.318
SDDL	0.340	-0.165	0.852	-0.012	0.956	0.206
PSDDSSL	-0.452	-0.511	0.000	0.000	0.127	-0.592
DSO	0.300	0.217	0.078	0.680	-0.152	0.243
%variance	38.513	23.754	61.52	18.176	54.423	23.086
Females	PC 1	PC 2	PC 1	PC 2	PC 1	PC 2
EBL	-0.006	0.159	0.249	-0.174	-0.033	0.057
DBF	0.422	0.114	0.000	0.000	-0.082	0.032
PSDBF	-0.153	0.227	0.000	0.000	0.122	0.051
PDLL	-0.320	0.268	-0.433	0.429	0.504	0.033
SPDLL	-0.213	0.486	0.000	0.000	0.619	-0.017
DDSSL	0.285	-0.143	-0.036	0.485	-0.183	-0.037
SDDL	0.663	0.588	0.858	0.194	-0.147	0.965
PSDDSSL	-0.306	0.454	0.000	0.000	0.525	0.226
DSO	0.192	-0.175	-0.111	-0.716	-0.095	-0.096
%variance	62.727	24.348	82.388	15.487	37.915	24.499

Notes: Loading scores and percentage of variance explained in the first three principal components extracted. Comparison between male and female individuals of *Mesalina adrarensis* sp. nov. with the other species of the *Mesalina olivieri* species complex.

Significant values are indicated in bold.

Etymology. The species epithet “*adrarensis*” refers to the Adrar Atar region because the new species was first suspected when seeing specimens from this region.

Diagnosis. A species of the *M. olivieri* complex characterized by the following combination of characters: (a) low number of eyelid scales (5–6); (b) with two clearly larger scales, like *M. guttulata* (several sub-equal scales or rarely 1–2 larger scales in the other species of the *M. olivieri* complex); (c) small black dots on the edge of the eyelids (mostly visible in dead animals preserved in ethanol); (d) more elongated snout with more prominent nostrils than the other species of the *olivieri* complex; (e) adult coloration in life (Figure 7) different from all other species of the complex (see Figure S5 and comparison below).

Coloration in life (adults). Dorsum coloration mostly brown, from sandy-brown to dark-brown or rufous-brown, with a dorsal pattern made of two central longitudinal lines of small whitish spots (usually partially edged with dark-brown or black) then two supra-dorsolateral longitudinal rows of black blotches edged externally by narrow dorsolateral fragmented whitish lines, sometimes nearly continuous,

sometimes reduced to series of small elongated dots; the flanks show small pale spots partially edged by dark coloration, sometimes fusing in a near complete dark band; on the lower part of the flanks a more continuous longitudinal white line separates the dorsal and ventral parts of the body. The pattern from the center of the back fades on the anterior part of the dorsum, especially on the nape, then disappears on the head. Dorsal pattern more contrasted in females than in some males; in some males, this pattern is reduced to a series of whitish and dark-brown spots aligned along the body. The color of the head is similar to the body coloration with faintly spotted pileus and a dark line running though the sides of the head through the eye, bordered below by a pale line reaching to the eye. Forelimbs coloration uniformly brown, hind legs brownish with whitish ocelli. Uniformly brown tail with a median dark stripe, more or less visible, disappearing at the first third of its length, this median stripe is externally edged on each side by a light stripe resulting from the prolongation of each light dorsolateral stripe. Underparts of the head and the legs pinkish-beige, belly overall similar but paler on central belly, underparts of the tail whitish, sometimes yellowish especially in males. Juveniles present a pale background coloration, striped with wide and continuous pale and dark (sometimes white and pure black) bands along the body,

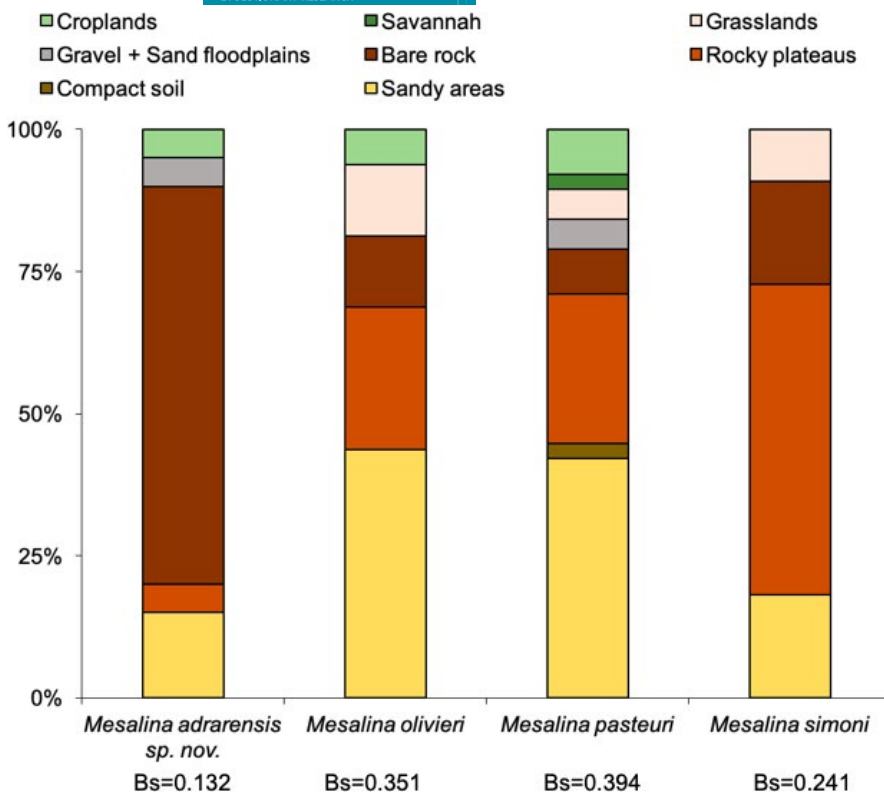


FIGURE 6 Results on the habitat analysis on the five species of the *Mesalina olivieri* complex in North West Africa. Bs is the standardized Levin's measure ranging from 0.0 to 1.0; high B means no discrimination between land-cover units, meanwhile low Bs value means selection among land-cover units

then very much like *M. pasteurii* (this pattern is probably common to all juveniles of the *M. olivieri* species complex).

Comparison. *Mesalina adrarensis* sp. nov. resembles (sometimes strongly) *M. guttulata*, possibly due to adaptation to similar environmental conditions. In comparison with *M. guttulata*, *M. adrarensis* sp. nov. has a browner background coloration and a less densely spotted dorsal pattern that often fades on the neck without exhibiting the remarkable pattern of irregularly arranged ocelli that characterizes *M. guttulata*. Contrary to *M. guttulata*, *M. adrarensis* sp. nov. has small light spots and dark marks organized in longitudinal lines. In both species, the eyelids are composed of 2 (rarely 1) large translucent scales, situated above 0 to 8 smaller ones; while in *M. guttulata* these scales are always edged with a continuous black stripe, in *M. adrarensis* sp. nov. this black coloration is mostly absent or made of spots along the edges of the scales. Compared with *M. olivieri* and *M. simoni*, *M. adrarensis* sp. nov. has more prominent nostrils, a longer snout, and more flattened head. Dorsal coloration in juveniles of all species of the *M. olivieri* species complex is characterized by continuous stripes. Meanwhile *M. olivieri* and *M. pasteurii* (but less frequent in *M. simoni*) maintain this striped coloration in their adult forms, these dorsal stripes in adults of *M. adrarensis* sp. nov. are fragmented. The eyelids of *M. simoni* and *M. olivieri* are made of 6–12 medium and small scales but no or (rarely) 1–2 clearly larger scales (cf. Figure 7i).

Adults of *M. adrarensis* sp. nov. can be easily distinguished from the sympatric *M. pasteurii* by the lack of obvious dorsal and dorsolateral stripes that characterize the adults of the latter species, and by the

brownish coloration typical of *M. adrarensis* sp. nov. (*M. pasteurii* has a typical sand color in accordance with its sandy habitat; Figure S5).

Genetic and phylogenetic remarks. The phylogenetic analyses by Kapli et al. (2015), Simó-Riudalbas et al. (2019) and the phylogenetic and nuclear network analyses performed in this study (Figures 2, 3 and 5 and Figures S2–S4; Table 4) validate the specific status of *M. adrarensis* sp. nov.. The amount of genetic divergence (p-distance) for the Cyt-b gene between the new species and the other members of the *M. olivieri* complex ranges from 9% (from its sister species *M. simoni*) to 14% *M. olivieri* (Table 4). The network analysis of the nuclear genes indicates that, despite the large number of samples of the *M. olivieri* species complex included in the analysis (70, 85, 71, and 69 for β -fib7, MC1R, PgD7, and OD, respectively), all haplotypes of *M. adrarensis* sp. nov. are private (Figure 5).

Description of the holotype. Adult female (Figure 7). Slender body slightly depressed in the caudal part. Long and pointed snout with slightly prominent nostrils; SVL = 44 mm, Tail length (entire, not regenerated) = 86 mm, total length = 130 mm, Head length = 10 mm, Head width = 6.4 mm, Head height = 4.3 mm, midbody dorsal scales = 44, small smooth, and regular temporal and dorsal scales, transverse rows of ventral plates = 32 arranged in eight longitudinal rows, enlarged plates in collar = 7, supralabials = 4, infralabials = 7, gular scales (counted along a line from the infrasupralabials to the collar) = 24, femoral pores 15 + 14, lamellae beneath the 4th toe = 19 (slightly keeled). Eyelid disks with five barely translucent scales (two large + three small) not edged with black.

FIGURE 7 *Mesalina adrarensis* sp. nov., holotype (MNHN-RA-2020.0017). (a) Live specimen; (b) Detail of the head in vivo; (c) Ventral view in vivo; (d) Dorsal pattern; (e) upper (dorsal) part of the head; (f) ventral (gular) side of the head; (g) right side of the head; (h) left side of the head; (i) Detail of the eyelid scales; (j) Type locality. Photo credits to P. Geniez (a–c) and C. Pizzigalli (c–g, i and j)



Distribution and habitat. The known range of *M. adrarensis* sp. nov. encompasses the mountain rocky areas of the Adrar Atar in Mauritania, further extending to the north up to the plateau of Zednes (Observation 13758; Table S10), to the Northwest up to Koudiet Laghnem (Morocco), and to the south down to the central Tagant Mountain (Figure 8). The observation 13758 is a sight record that is unsupported by any photo or tissue sample but has been identified in the field by its typical habitus and habitat (J. C. Brito pers. obs.)

The Area of Occupancy (AOO) calculated from the ecological models was of 34,766 km², while the Extent of Occurrence (EOO) was of 175,445 km² (Table S8).

The highest probability of occurrence is at an intermediate levels of terrain ruggedness and in bare rock habitats (Figure 6 and Figure S9). The type locality is a flat and rocky area located on the top of a plateau in the Adrar Atar (Figure 8 and Figure S10b,c). The area is very scarcely vegetated with many stones, mostly low and sparse shrubs and, rarely, *Acacia* sp. trees (Figure 7j).

Ecology. Specimens were observed active among stones mostly from 11:00 am to 17:00 pm. If threatened it usually seeks shelter under a rock or in spiny bushes. Diet and reproductive features are still unknown.

Conservation status. The AOO calculated from the ecological models was 34,766 km², while the EOO was 175,445 km². Most of the habitats are for the moment devoid of major human impact and we are not aware of any direct threat to the species such as direct destruction of human exploitation. Although we do not have any information on the species' population trends, we do not suspect any marked decline based on the lack of direct or indirect menace. Following IUCN guidelines (2017), we thus propose here that the conservation status of *M. adrarensis* sp. nov. should be Least Concern (LC), based on the high values for the area of occupancy and extend of occurrence and the lack of observed or forecasted population decline. However, the area of occupancy is highly fragmented due to the ecology of the species (Figure 8) and the amount of knowledge currently available for this species remain limited.

Notes. The specimens BEV.10823 (GenBank code KM411138) and CIBIO2952 (GeneBank code KM411139) correspond to a juvenile (BEV.10823) and to a sub-adult (CIBIO2952) *M. adrarensis* sp. nov., previously identified as *M. pastouri* in Kapli et al. (2015) and Simó-Riudalbas et al. (2019). The assignment of these two specimens to *M. pastouri* was due to their striped color pattern, typical of *M. pastouri*. However, both our, Kapli et al. (2015) and Simó-

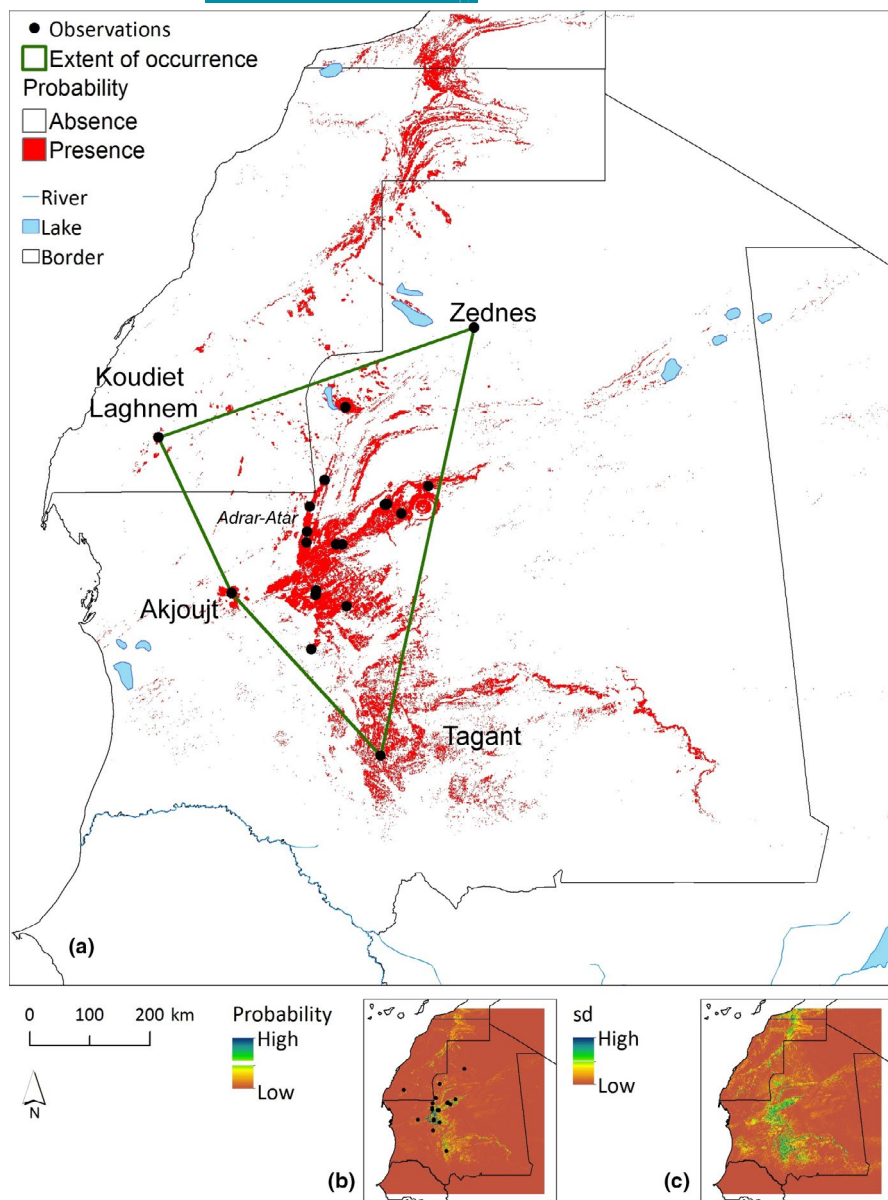


FIGURE 8 Ecological modeling of *Mesalina adrarensis* sp. nov. (a) Binary predictions of suitable habitats for the taxon; the green perimeter represents the current known distribution. (b) Average probability of occurrence and (c) standard deviation from 20 individual model replicates. Black dots represent the currently known localities of the species

Riudalbas et al. (2019) genetic results assign these two specimens to *M. adrarensis* sp. nov.. The difference in coloration between these two specimens and the other specimens of *M. adrarensis* sp. nov. results from strong ontogenetic variation of coloration in *M. adrarensis* sp. nov. (contrastingly striped coloration in juveniles).

Mesalina simoni saharae ssp. nov.
(Figures 1–5 and 9; Tables 1, 3–6)

Zoobank registration. <http://zoobank.org/NomenclaturalActs/30f33118-ec56-48a6-87b9-1d811dac016>

Holotype. Adult male (Figure 9), with code MNHN-RA-2020.0018 (ex BEV.9114) preserved in the Muséum national d'Histoire naturelle, in Paris, France. Collected by Pierre-André Crochet and Julien Renoult on 10th September 2006.

Type locality. Morocco, Atlantic Sahara, road N1, 69 km past Boujdour toward Laayoune, 26.4925°N/-13.9198°W/60 m a.s.l.

Paratypes. Adult male BEV.10849, from 6 km E of Sidi Kathari, 26.5298°N/-12.3364°W, collected by Pierre-André Crochet on 21st March 2010; adult female BEV.10850, from 4 km past Awserd toward Dakhla, 22.5709°N/-14.3544°W, collected by Pierre-André Crochet on the 18th March 2010, all preserved in the BEV collection in Montpellier.

Etymology. The epithet “*saharae*” refers to the Atlantic Sahara region where this new subspecies is distributed.

Diagnose. A member of the *M. olivieri* species complex closely related to the nominotypical *M. simoni*, but with the following combination of characters: (a) eyelids with 5–6 large transparent scales (b) not edged in black (rarely indistinct spots on their edges), (c) dorsal coloration in life generally sandy, sandy-brown, or sandy

gray with (d) a poorly marked dorsal pattern mostly composed of longitudinal rows of whitish spots; spots narrowly edged internally by dark coloration (dark inner edge typically 1–2 or 2–3 scales wide), sometimes bordered by a pale grayish dorsolateral line, (e) a dark continuous or near continuous band from the nostril along the flanks to the hind legs constituting the darkest element in the pattern and often including pale spots and their dark edges, (f) a distinctive delicate habitus with elongated body and neck and flattened head (Figure 9 and Figure S5).

Genetic and phylogenetic remarks. The phylogenetic analyses by Kapli et al. (2015), Simó-Riudalbas et al. (2019) and the phylogenetic and nuclear network analyses performed in this study (Figures 2, 3 and 5 and Figures S2–S4; Table 4) support the hypothesis that the populations of *M. simoni saharae* ssp. nov. belong to the species *M. simoni* and not to the species *M. olivieri*. A network analysis of the nuclear genes indicates that, despite the large number of samples of the *M. olivieri* species complex included in the analysis (70, 85, 71, and 69 for β -fib7, MC1R, PgD7, and OD, respectively), all haplotypes of *M. simoni saharae* ssp.

nov. are shared with *M. s. simoni* and not with *M. olivieri* (Figure 5). The amount of genetic divergence (*p*-distance) in the Cyt-b gene between the new subspecies and the other members of the *M. olivieri* complex ranges between 4% from *M. simoni* and 11% from *M. olivieri* (Table 4). One specimen from the Souss valley, geographically located between the ranges of both subspecies, is morphologically similar to *M. s. simoni* but is somewhat intermediate in the nuclear and concatenated trees, suggesting a lack of reproductive isolation between *simoni* and *saharae*. Based on this and on their level of genetic divergence, we treat *saharae* and *simoni* as conspecific pending more detailed analyses of their interactions in contact zones.

Description of the holotype. An adult male (Figure 9) with well-developed femoral pores. Slender and elongated body and slender head; SVL = 41 mm, regenerated tail, Head length = 9.6 mm, Head width = 5.9 mm, Head height = 4.2 mm, midbody dorsal scales = 34, medium sized, slightly pointed, not shining; transverse rows of ventral = 28, longitudinal rows of ventral = 8, enlarged plates in collar = 6, supralabials = 4 + 5, infralabials = 7 + 9, gular

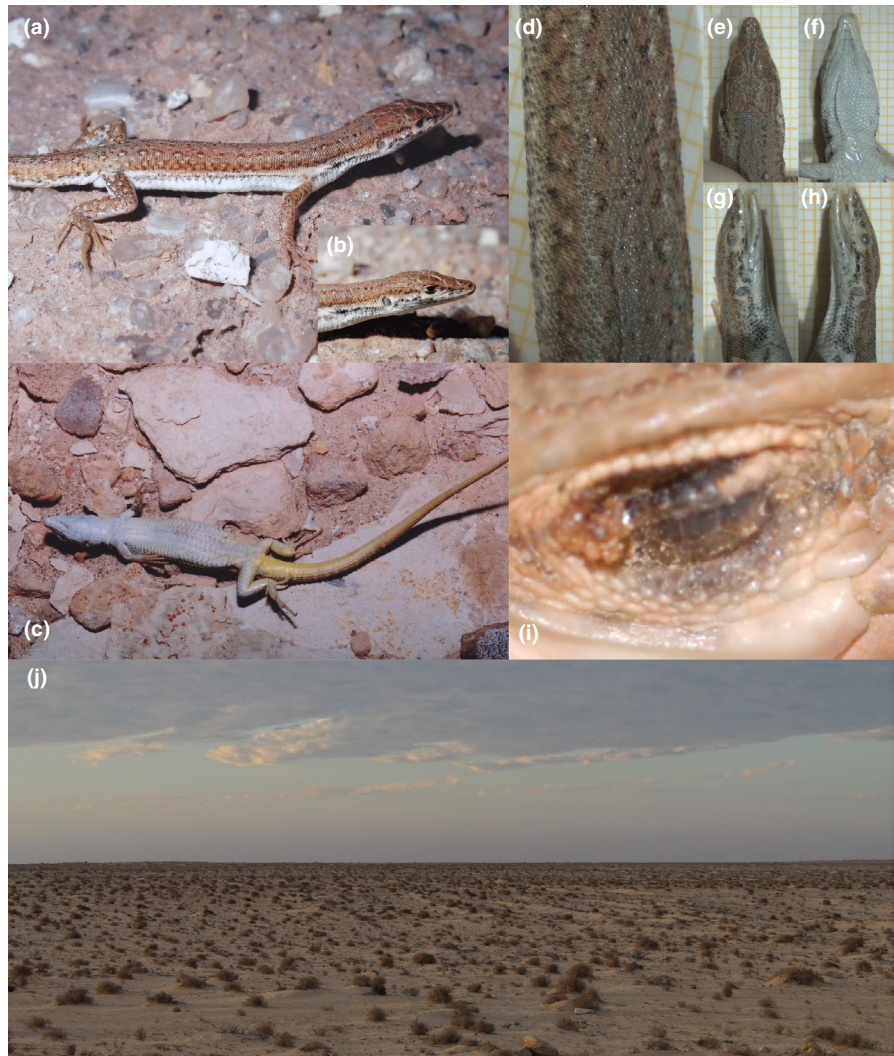


FIGURE 9 *Mesalina simoni saharae* ssp. nov., holotype (MNHN-RA-2020.0018). (a) Live specimen; (b) Detail of the head in vivo; (c) Ventral view in vivo; (d) Dorsal pattern; (e) upper (dorsal) part of the head; (f) ventral (gular) side of the head; (g) right side of the head; (h) left side of the head; (i) Detail of the eyelid scales; (j) Type locality. Photo credits to P.-A. Crochet (a, b and c) and C. Pizzigalli (c-i and j)

scales (counted along a line from the infrasupralabials to the collar) = 25, femoral pores = 10 + 13, lamellae beneath the 4th toe = 20. Eyelid disks with five translucent scales not edged with black.

Coloration in life. See diagnose above. In addition, pileus almost uniform, with faded spots, sometimes distinctly spotted with small dark spots. Fore limbs uniformly sandy-brown, hind legs brownish with faded whitish ocelli. Almost uniform sandy/brown tail with indistinct spots disappearing in the second half of its length. Ventral coloration white, sometimes turning to yellow on the undertail, at least in the specimens from the north of the range.

Distribution and habitat. As understood here, this subspecies' distribution encompasses approximately 173,970 Km² across the west of the Sahara, from the Mauritanian border to the Tan-Tan area, and as far inland as Awserd (see Figure 4). The current knowledge on this distribution is clearly constrained by the reduced accessibility of the region and is doubtless more extensive than currently known. In its distribution range, this subspecies mostly dwells semi-deserts and coastal steppes with scattered low bushes on loess, coarse sand, or gravel substratum (Figure 9).

Notes. Individuals from Tan-Tan to the Sous-Massa region (Morocco; 1-SOUS in Figures 2–4 and Table 1), seem to be genetically admixed between *M. simoni saharae* ssp. nov. and *M. s. simoni*; morphologically, specimens from the Tan-Tan area are rather typical of *M. simoni saharae* ssp. nov. though while our specimen from the Souss is rather typical of *M. s. simoni*. More detailed studies are needed to clarify the extant of gene flow between these two subspecies and the taxonomy of these populations that inhabit the area between the cores of the range of the two subspecies.

Taxonomic notes and updated distribution for *Mesalina simoni*
 Our results provide the first direct evidence that *M. olivieri* and *M. simoni* are valid, reproductively isolated species (based on lack of allele sharing for nuclear markers in the parapatry area in Morocco, see below). The taxon *simoni* was recognized as a valid subspecies of *M. olivieri* by Pasteur and Bons (1960) but was restricted to the population of the *M. olivieri* complex inhabiting Morocco north and west of the Atlas Mountains (corresponding with our *M. s. simoni* here). *Mesalina simoni* was first elevated to species rank by Arnold (1986) based on considerable differences in hemipenial structure between specimens assigned to either *M. s. simoni* or *Mesalina simony olivieri*. Further genetic data (e.g., Kapli et al., 2015) failed to recover *M. olivieri* and *M. simoni* as reciprocally monophyletic in mtDNA, suggesting an inadequate taxonomy for the complex. Our new taxonomy (which includes in *M. simoni* most populations of the *M. olivieri* complex from Morocco) solves these issues as *M. simoni* and *M. olivieri* become reciprocally monophyletic. Our nuclear data suggest that there is reproductive isolation in their contact zone in south-eastern Morocco: localities 29 (*M. olivieri*) and 99 (*M. simoni*) do not share any alleles in *OD* or β -*fib7* despite their distribution

overlapping. The distribution of *M. olivieri* now stops in the west on the eastern and southern foothills of the High Atlas of Morocco, reaching as far west as the surroundings of Boumalne Dades (see Figure 4). Our understanding of the distribution limits of *M. simoni* and *M. olivieri* in north-western Africa is still hampered by the lack of diagnostic external morphological features to separate them. We have examined numerous specimens of the two species and have failed to find any stable morphological difference. Clearly, the morphological characters reported in the literature (see for ex. Hosseiniyan Yousefkhani et al., 2015) were based on an inadequate appraisal of the considerable morphological variation in *M. simoni* (see for ex. Figure S5). While *M. simoni saharae* ssp. nov. is usually reasonably easy to identify, *M. s. simoni* (north and west of the Atlas Mountains in Morocco) and the various populations of *M. simoni* ssp. (Sous and AM) -currently unassigned to any subspecies- are, based on current knowledge, impossible to distinguish morphologically from *M. olivieri*.

4 | DISCUSSION

4.1 | Phylogenetic relationships and cytonuclear discordance

Our revision of the *M. olivieri* species complex relies on several phylogenetic approaches to address the previously reported paraphyly of *M. olivieri* and *M. pastouri* (Kapli et al., 2015; Simó-Riudalbas et al., 2019). We used our concatenated mtDNA and nucDNA tree (Figure 3 and Figure S4) as the best hypothesis to delineate the species-level units in the complex; this results in (at least) four species being part of the *olivieri* species complex, with *M. adrarensis* sp. nov. and *M. simoni* now fully monophyletic relative to all the other members of the complex. The relationships between these four species and *M. martini* are not fully resolved yet and differ between our datasets (mtDNA or nucDNA). This lack of resolution can stem from the (non-exclusive) action of rapid species divergence resulting in short internodes in the species-tree and incongruence among gene trees due to incomplete lineage sorting, interspecific gene flow during or after the speciation processes and/or lack of power due to short sequence data.

Our results are also affected by an instance of cytonuclear discordance. The position of the Algerian clade ALG1 is poorly supported in nucDNA but is recovered as basal to and highly divergent from all *M. olivieri* and *M. pastouri* samples. This same lineage is closely related to and poorly divergent from some of the *M. pastouri* samples in mtDNA, resulting in its embedded position in the *M. pastouri* mitochondrial diversity (see Figure 2a and Figure S2). Such incongruences in phylogenetic position and amount of divergence in mtDNA and nucDNA may have been due to past introgression of *M. pastouri* mtDNA into the nuclear background of the lineage ALG1, resulted in cytonuclear discordance. Incongruences on the genetic divergence between mtDNA and nucDNA have been reported in other taxa, like *Podarcis hispanicus* species complex (Renoult et al., 2009), *Tarentola*

mauritanica (Rato et al., 2010), in the genus *Plethodon* (Fisher-Reid & Wiens, 2011) and *Salamandra* (Burgon et al., 2021) mostly pointing to incomplete lineage sorting or past gene flow between the lineages (Fisher-Reid & Wiens, 2011; Rato et al., 2010).

4.2 | Hidden diversity within *M. olivieri* and *M. pastouri*: Linnean and Darwinian shortfalls

None of our datasets (mtDNA, nucDNA, or combined mt + nucDNA trees) recover *M. olivieri* and *M. pastouri* as reciprocally monophyletic. The Algerian clade of *M. olivieri* ALG1 is recovered as basal to a *pastouri*-*olivieri* group in our concatenated tree (Figure 3), and it has a different position when mtDNA and nucDNA are analyzed separately (Figure 2a,b and Figures S2 and S3). Indeed, lack of monophyly relative to *M. pastouri* as well as deep divergences in both mtDNA and nucDNA datasets in *M. olivieri* are strong evidence that *M. olivieri*, as understood here, is made of several biological species. For example, the Algerian populations of *M. olivieri* harbor two highly divergent lineages: ALG1 and ALG2/ALG3, the latter closely related to the Moroccan lineages MOR2 and MOR3. Most of the other deep lineages in *M. olivieri* have allopatric distributions, from Israel and Egypt to eastern Morocco, based on our still limited sampling. Interestingly, Arnold (1986) already pointed out variation in hemipenal morphology between populations of what we still treat as *M. olivieri*, suggestive of several species. Beddek et al. (2018) conducted an exhaustive phylogeographic study comparing North African species with an East–West phylogeographic divide, and highlighted several sutures lines and refugia (e.g., the Rifian corridor and the Kabylia mountain region) that generated vicariance events in the Maghreb. The clade subdivision of *M. olivieri* recovered in our study mirrors some of the suture lines and refugia uncovered in Beddek et al. (2018), reinforcing the idea that, for this species (a Mediterranean or mesic species), longitudinal fragmentation of ancestral areas was the main force shaping its diversification. We are thus convinced that *M. olivieri*, even after we restricted it here, still contains several valid biological species distributed along an East–West longitudinal diversification pattern. Regarding *M. pastouri*, two well-supported (PP = 100%) lineages have been unveiled in North West Africa (Figure 3 and Figure S4): (a) one mostly distributed on the Atlantic Sahara region (13-MAU1 and 14-MAU2 + MOR); (b) one including specimens from inland Mauritania, Algeria, and Niger (15-MAU3 + ALG and 16-MAU4 + NIG). This noteworthy amount of diversity within *M. olivieri* and *M. pastouri* has already been reported in previous studies (Kapli et al., 2015; Simó-Riudalbas et al., 2019). The first step in identifying these candidate species would be to increase both the number of specimens genotyped and the number of nuclear loci employed. This would allow to generate more robust delimitations of candidate species (i.e., using species delimitation methods such as in Rato et al., 2016), and to better understand their distribution before explicit tests of reproductive isolation in contact zones can be realized (as in Dufresnes et al., 2020). The second step to

a correct identification of these candidate species would be a redaction of a new dichotomous key. The keys currently available (Hosseiniyan Yousefkhani et al., 2015; Trape et al., 2012) were found to be incomplete or, sometimes, inaccurate, probably due to the difficulty of the analysis of old and poorly preserved samples and/or because the *M. olivieri* species complex is composed of several cryptic species (Bickford et al., 2007). Unfortunately, sampling gaps from the central and west regions of North Africa still hampers the identification and analysis of contact zones between these lineages and preclude assessing the species status of many putative species still “hidden” in the *M. olivieri* complex. Incomplete species inventory (Linnean shortfall; Brown & Lomolino, 1998) is the first obstacle in biodiversity studies (Hortal et al., 2015). This shortfall can be the reason of incomplete phylogenetic knowledge on the evolution of lineages, species, and traits (Darwinian shortfall, Diniz-Filho et al., 2013). Species affected by these shortfalls generally inhabit large and unsurveyed regions of the world (Bush & Lovejoy, 2007; Hopkins, 2007), such as the cases of *M. pastouri* or *M. olivieri*. The distribution of these species encompasses some of the most remote and politically instable regions in the Sahara Desert, where sample collection is very difficult (Brito et al., 2014, 2018).

4.3 | Ecological differences and distribution: Wallacean shortfalls

Following the description of *M. adrarensis* sp. nov. and the revision of the species limits of *M. simoni*, we have narrowed the distribution of *M. olivieri*, which now reaches its western limit in eastern Morocco (Figure 4a). We also extended the distribution of *M. simoni* (previously endemic to Morocco west and north of the Atlas; see Joger et al., 2006 and Martínez del Mármol et al., 2019), which now occupies most of the Saharan climate regions of Morocco from extreme SE Morocco to the north-western border of Mauritania (Figure 4b). The previous southern limit of *M. pastouri* in Mauritania was in the Banc d’Arguin National Park (Sow et al., 2014). Our study provides new records for *M. pastouri* (Figure 4c), in south-western Mauritania (Diawling National Park), and south of the previously known distribution in south-eastern Niger. We also identified a wide area of sympatry between *M. pastouri* and *M. adrarensis* sp. nov. (Figure S10), extending about 200 km on either side of the north-western Mauritanian border. While no actual syntopy was detected, certainly because the two species have very different habitat requirement (rocky substratum for *M. adrarensis* sp. nov., sandy substratum for *M. pastouri*, see below), populations of both species were found less than 20 km apart in the north-eastern part of the Adrar Atar plateau (Figure S10). We also identified a potential contact zone between *M. pastouri*, *M. adrarensis* sp. nov., and *M. simoni saharae* ssp. nov. in extreme southern Morocco (Atlantic Sahara; Figure S10). The known distribution limits of these three species are, to date, around 100 km apart, but with no unsuitable habitats in between. This area is still severely under-sampled, and clearly, it is likely that the three species meet in this area (Figure S10). Further sampling efforts are needed

to establish accurate range limits and extent of sympatry, but there are obviously no extrinsic barriers to gene flow between *M. adrarensis* sp. nov., *M. pastouri*, and *M. simoni* in northern Mauritania and southern Atlantic Sahara. This lack of knowledge in species distribution has been named Wallacean shortfall (Lomolino, 2004). This shortfall is particularly accentuated in remote and inaccessible regions (Hortal et al., 2015), such as Mauritania and southern Atlantic Sahara, and North Africa in general (Brito et al., 2018).

The results of the habitat comparisons revealed clear ecological differences between *M. adrarensis* sp. nov. and the other species of the complex. *Mesalina adrarensis* sp. nov. exhibits a narrow niche breadth, inhabiting almost exclusively slopes, wadis and plateaus on rocky substratum (Table S9 and Figures 6 and 7j). This distinction is obvious when *M. adrarensis* sp. nov. is compared to *M. olivieri* and *M. pastouri*, the two species to which the ADR and TAG lineages were associated until now. *Mesalina olivieri* and *M. simoni* are soft substratum specialists inhabiting mostly loess or other soil substratum, normally not sand or rocks, although they can locally inhabit stony areas (i.e., soil with scattered stones), mostly on flat grounds. The presence of *M. pastouri* in rocky habitat types (Figure 6 and Figure S10; samples 63, 64 and 65), including rocky plateaus, is an artifact of the land-cover upscaling process (from 30 m to 1 km); *M. pastouri* is a well-known sand specialist (Bons, 1960; Trape et al., 2012; pers. obs.), which can persist in sandy micro-habitats scattered inside rocky plateaus (Figure S10b,c), but such micro-habitats are mostly overlooked at the geographic scale we used in the habitat analyses.

4.4 | Biogeography of *Mesalina adrarensis* sp. nov.

The diversification of the *olivieri* complex started in the Late Miocene (ca. 12.08–6.38 Mya; Figure 3) in concomitance with the beginning of the arid period responsible of the formation of the current Sahara Desert dated approximately 7–6 Mya in Chad (Holmes, 2008; Swezey, 2009) or even more recently further west (Schuster et al., 2006), when a gradual decrease in precipitation and increase of the dust flow led to vegetation collapse (Claussen, 2009; Wang et al., 2008). During the Pliocene (5.3–2.6 Mya), multiple dry-wet cycles affected the region and induced a succession of dry-humid periods (reviewed in Brito et al., 2014). Previous studies identified mountains, highlands and coastal areas as refugia during the arid cycles of the Sahara-Sahel (Brito et al., 2014; Gonçalves, Pereira, et al., 2018). We hypothesize that periods of desertification in the area forced the ancestor of the *olivieri* complex (probably a mesic species) to contract its distribution in several refugia, possibly centered around the Adrar Atar, Tagant (and other Mauritanian massifs) and the Atlantic coastal areas. Eventually, this isolation resulted in a series of vicariance events that led to speciation giving rise to *M. adrarensis* sp. nov. and *M. simoni*. In addition, the low elevation of several regions of the Sahara and the presence of sand before the Sahara's desertification started (Swezey, 2009) suggest that parts of the west and center of the Sahara flooded due to the formation of extended hydrological networks (e.g., Tamanrasset paleo river; Skonieczny

et al., 2015). In this scenario, today's plateaus (i.e., Adrar Atar) may have been isolated either by dry areas or flooded areas and acted as "islands" were the ancestors of the current species were trapped (see also Gonçalves, Martínez-Freiría, et al., 2018; Velo-Antón et al., 2018). The latitudinal genetic structure recorded for *M. adrarensis* sp. nov. and *M. simoni* (i.e., ADR versus TAG or AS, AM, and SOUS, Figures 2 and 3, and Figures S2–S4) could represent more recent range fragmentation due to varying climatic conditions (Brito et al., 2014) and/or dynamic geographical features (such as river basins; e.g., Gonçalves, Martínez-Freiría, et al., 2018; Velo-Antón et al., 2018) or be the result of isolation by distance in continuous populations. Indeed, vicariance and isolation by distance can be difficult to separate when geographical and/or genomic sampling is sparse (Bradburd et al., 2018).

ACKNOWLEDGEMENTS

This work was funded by National Geographic Society (CRE 7629-04/8412-08), Mohamed bin Zayed Species Conservation Fund (11052709, 11052707, 11052499), Fundação para a Ciência e a Tecnologia (PTDC/BIA-BEC/099934/2008 and PTDC/BIA-BIC/2903/2012), FEDER funds through the Operational Programme for Competitiveness Factors - COMPETE (FCOMP-01- 0124-FEDER-008917/028276), and by AGRIGEN-NORTE-01-0145-FEDER-000007, supported by Norte Portugal Regional Operational Programme (NORTE2020), under the PORTUGAL 2020 Partnership Agreement, through the European Regional Development Fund (ERDF). F.M.F., G.V.A. and J.C.B. were supported by FCT (DL57/2016/CP1440/CT0010, IF/01425/2014, and CEECINST/00014/2018/CP1512/CT0001, respectively), C.P. was supported by the Municipality of Martinengo (Determinazione del 16–11–2020 Settore IV – Servizi Socio Culturali; no. generale:872 – No. settoriale 212). Capture permits were issued by the Haut Commissariat aux Eaux et Forêts (278/2012 and 20/2013/HCEFLCD/DLCDPN/DPRN/CFF) and Ministère de l'Environnement et du Développement Durable of Mauritania (460/MDE/PNBA). Logistic support for fieldwork was given by Pedro Santos Lda (Trimble GPS), Off Road Power Shop, P.N. Banc d'Arguin (Mauritania), Association Nature Initiative (Morocco), and Université des Sciences, de Technologie et de Médecine de Nouakchott. We thank BIODESERTS group members for their assistance during fieldwork and A. Pagan and I. Freitas for the support during the analysis. We are also grateful to P. Kapli and P. Lymberakis from the Natural History Museum of Crete for providing additional tissue samples. We also thank O. Peyre, B. Allegrini, J. Marques, J.M. Pleguezuelos, M. Feriche, A.S. Sow, Y. Hingrat, A. Miralles, M. Beddek, M. Siol, G. Léotard, E. Didner, J. Renoult for help with collecting samples.

ORCID

Cristian Pizzigalli  <https://orcid.org/0000-0002-0140-8660>

Pierre-André Crochet  <https://orcid.org/0000-0002-0422-3960>

Fernando Martínez-Freiría  <https://orcid.org/0000-0003-2311-8960>

Guillermo Velo-Antón  <https://orcid.org/0000-0002-9483-5695>

José Carlos Brito  <https://orcid.org/0000-0001-5444-8132>

REFERENCES

- Arnold, E. N. (1986). The hemipenis of lacertid lizards (Reptilia: Lacertidae): Structure, variation and systematic implication. *Journal of Natural History*, 20, 1221–1257. <https://doi.org/10.1080/00222938600770811>
- Arnold, E. N., Arribas, O., & Carranza, S. (2007). Systematics of the Palaearctic and oriental lizard tribe *Lacertini* (Squamata: Lacertidae: *Lacertinae*), with descriptions of eight new genera. *Zootaxa*, 1430, 1–86. <https://doi.org/10.11646/zootaxa.1430.1.1>
- Beddek, M., Zenboudji-Beddek, S., Geniez, P., Fathalla, R., Sourouille, P., Arnal, V., Dellaoui, B., Koudache, F., Telailia, S., Peyre, O., & Crochet, P.-A. (2018). Comparative phylogeography of amphibians and reptiles in Algeria suggests common causes for the east-west phylogeographic breaks in the Maghreb. *PLoS One*, 13(8), e0201218. <https://doi.org/10.1371/journal.pone.0201218>
- Bickford, D., Lohman, D. J., Sodhi, N. S., Ng, P. K. L., Meier, R., Winker, K., Ingram, K. K., & Das, I. (2007). Cryptic species as a window on diversity and conservation. *Trends in Ecology and Evolution*, 22(3), 148–155. <https://doi.org/10.1016/j.tree.2006.11.004>
- Bons, J. (1960). Description d'un nouveau lézard du Sahara: *Eremias pasteurii* sp. nov. (Lacertidés). C. R. Séances mens. Société des Sciences Naturelles et Physiques du Maroc, 4, 69–71.
- Bons, J., & Geniez, P. (1995). Contribution to the systematics of the lizard *Acanthodactylus erythrurus* (Sauria, Lacertidae) in Morocco. *Herpetological Journal*, 5, 271.
- Böttger, O. (1880). *Die Reptilien und Amphibien von Syrien, Palaestina und Cypern*. Mahlau & Waldschmidt.
- Bradbard, G. S., Graham, M. C., & Peter, L. R. (2018). Inferring continuous and discrete population genetic structure across space. *Genetics*, 210(1), 33–52.
- Brito, J. C., Acosta, A. L., Álvares, F., & Cuzin, F. (2009). Biogeography and conservation of taxa from remote regions: An application of ecological-niche based models and GIS to North-African Canids. *Biological Conservation*, 142, 3020e3029. <https://doi.org/10.1016/j.biocon.2009.08.001>
- Brito, J. C., Durant, S. M., Pettorelli, N., Newby, J., Canney, S., Algadafi, W., Rabeil, T., Crochet, P.-A., Pleguezuelos, J. M., Wacher, T., de Smet, K., Gonçalves, D. V., da Silva, M. J. F., Martínez-Freiría, F., Abáigar, T., Campos, J. C., Comizzoli, P., Fahd, S., Fellous, A., ... Carvalho, S. B. (2018). Armed conflicts and wildlife decline: Challenges and recommendations for effective conservation policy in the Sahara-Sahel. *Conservation Letters*, 11(5), e12446. <https://doi.org/10.1111/conl.12446>
- Brito, J. C., Godinho, R., Martínez-Freiría, F., Pleguezuelos, J. M., Rebelo, H., Santos, X., Vale, C. G., Velo-Antón, G., Boratyński, Z., Carvalho, S. B., Ferreira, S., Gonçalves, D. V., Silva, T. L., Tarroso, P., Campos, J. C., Leite, J. V., Nogueira, J., Álvares, F., Sillero, N., ... Carranza, S. (2014). Unravelling biodiversity, evolution and threats to conservation in the Sahara-Sahel. *Biological Reviews*, 89, 215–231. <https://doi.org/10.1111/brv.12049>
- Brito, J. C., & Pleguezuelos, J. M. (2019). Desert biodiversity—World's hot spots/globally outstanding biodiverse deserts. In: *Earth systems and environmental sciences* (pp. 10–22). <https://doi.org/10.1016/B978-0-12-409548-9.11794-4>
- Brown, J. H., & Lomolino, M. V. (1998). *Biogeography*, 2nd ed. Sinauer.
- Bryson, R. W. Jr, García-Vázquez, U. O., & Riddle, B. R. (2012). Relative roles of Neogene vicariance and Quaternary climate change on the historical diversification of bunchgrass lizards (*Sceloporus scalaris* group) in Mexico. *Molecular Phylogenetics and Evolution*, 62(1), 447–457. <https://doi.org/10.1016/j.ympev.2011.10.014>
- Burgos, J. D., Vences, M., Steinfartz, S., Bogaerts, S., Bonato, L., Donaire-Barroso, D., Martínez-Solano, I., Velo-Antón, G., Vieites, D. R., Mable, B. K., & Elmer, K. R. (2021). Phylogenomic inference of species and subspecies diversity in the Palearctic salamander genus *Salamandra*. *Molecular Phylogenetics and Evolution*, 157, 107063.
- Bush, M. B., & Lovejoy, T. E. (2007). Amazonian conservation: Pushing the limits of biogeographical knowledge. *Journal of Biogeography*, 34(8), 1291–1293. <https://doi.org/10.1111/j.1365-2699.2007.01758.x>
- Campos, J. C., & Brito, J. C. (2018). Mapping underrepresented land cover heterogeneity in arid regions: The Sahara-Sahel example. *ISPRS Journal of Photogrammetry and Remote Sensing*, 146, 211–220. <https://doi.org/10.1016/j.isprsjprs.2018.09.012>
- Claussen, M. (2009). Late Quaternary vegetation-climate feedbacks. *Climate in the Past*, 5, 203–216. <https://doi.org/10.5194/cp-5-203-2009>
- Clement, M., Posada, D., & Crandall, K. A. (2000). TCS: A computer program to estimate gene genealogies. *Molecular Ecology*, 9, 1657–1660. <https://doi.org/10.1046/j.1365-294x.2000.01020.x>
- Dayrat, B. (2005). Towards integrative taxonomy. *Biological Journal of the Linnean Society*, 85, 407–417. <https://doi.org/10.1111/j.1095-8312.2005.00503.x>
- De Queiroz, K. (2007). Species concepts and species delimitation. *Systematic Biology*, 56(6), 879–886. <https://doi.org/10.1080/10635150701701083>
- Diniz-Filho, J. A. F., Loyola, R. D., Raia, P., Mooers, A. O., & Bini, L. M. (2013). Darwinian shortfalls in biodiversity conservation. *Trends in Ecology and Evolution*, 28(12), 689–695. <https://doi.org/10.1016/j.tree.2013.09.003>
- Dufresnes, C., Nicieza, A. G., Litvinchuk, S. N., Rodrigues, N., Jeffries, D. L., Vences, M., Perrin, N., & Martínez-Solano, I. (2020). Are glacial refugia hotspots of speciation and cytonuclear discordances? Answers from the genomic phylogeography of Spanish common frogs. *Molecular Ecology*, 29(5), 986–1000. <https://doi.org/10.1111/mec.15368>
- Fisher-Reid, M. C., & Wiens, J. J. (2011). What are the consequences of combining nuclear and mitochondrial data for phylogenetic analysis? Lessons from *Plethodon* salamanders and 13 other vertebrate clades. *BMC Evolutionary Biology*, 11, 300. <https://doi.org/10.1186/1471-2148-11-300>
- Friesen, V. L., Congdon, B. C., Kidd, M. G., & Birt, T. P. (1999). Polymerase chain reaction (PCR) primers for the amplification of five nuclear introns in vertebrates. *Molecular Ecology*, 8, 2147–2149. <https://doi.org/10.1046/j.1365-294x.1999.00802-4.x>
- Gonçalves, D. V., Martínez-Freiría, F., Crochet, P.-A., Geniez, P., Carranza, S., & Brito, J. C. (2018). The role of climatic cycles and trans-Saharan migration corridors in species diversification: Biogeography of *Psammophis schokari* group in North Africa. *Molecular Phylogenetics and Evolution*, 118, 64–74. <https://doi.org/10.1016/j.ympev.2017.09.009>
- Gonçalves, D. V., Pereira, P., Velo-Antón, G., Harris, D. J., Carranza, S., & Brito, J. C. (2018). Assessing the role of aridity-induced vicariance and ecological divergence in species diversification in Northwest Africa using *Agama* lizards. *Biological Journal of the Linnean Society*, 124, 363–380. <https://doi.org/10.1093/biolinnean/bly055>
- Hammer, Ø., Harper, D. A. T., & Ryan, P. D. (2001). PAST: Paleontological Statistics software package for education and data analysis. *Palaeontologia Electronica*, 4(1), 9.
- Hijmans, R. J., Cameron, S. E., Parra, J. L., Jones, P. G., & Jarvis, A. (2005). Very high resolution interpolated climate surfaces for global land areas. *International Journal of Climatology*, 25, 1965–1978. <https://doi.org/10.1002/joc.1276>
- Holmes, J. A. (2008). How the Sahara became dry. *Science*, 320, 752–753. <https://doi.org/10.1126/science.1158105>
- Hopkins, M. J. (2007). Modelling the known and unknown plant biodiversity of the Amazon Basin. *Journal of Biogeography*, 34(8), 1400–1411. <https://doi.org/10.1111/j.1365-2699.2007.01737.x>
- Hortal, J., de Bello, F., Diniz-Filho, J. A. F., Lewinsohn, T. M., Lobo, J. M., & Ladle, R. J. (2015). Seven shortfalls that beset large-scale knowledge of biodiversity. *Annual Review of Ecology, Evolution, and Systematics*, 46, 523–549. <https://doi.org/10.1146/annurev-ecolsys-112414-054400>

- Hosseiniyan Yousefkhani, S. S., Marmol Marin, G. M. D., Rastegar-Pouyani, N., & Rastegar-Pouyani, E. (2015). A bibliographical recompilation of the genus *Mesalina* Gray, 1838 (Sauria: Lacertidae) with a key to the species. *Russian Journal of Herpetology*, 22(1), 23–34.
- IUCN (2017). *Guidelines for using the IUCN red list categories and criteria. Version 13*. IUCN Standards and Petitions Subcommittee
- Joger, U., Slimani, T., El Mouden, H., & Geniez, P. (2006). *Mesalina simoni. The IUCN Red list of threatened species 2006* (p. e.T61535A12509619).
- Kapli, P., Lymberakis, P., Crochet, P.-A., Geniez, P., Brito, J. C., Almutairi, M., Ahmadzadeh, F., Schmitz, A., Wilms, T., Pouyani, N. R., & Poulakakis, N. (2015). Historical biogeography of the lacertid lizard *Mesalina* in North Africa and the Middle East. *Journal of Biogeography*, 42, 267–279.
- Kapli, P., Lymberakis, P., Poulakakis, N., Mantziou, G., Parmakelis, A., & Mylonas, M. (2008). Molecular phylogeny of three *Mesalina* (Reptilia: Lacertidae) species (*M. guttulata*, *M. brevirostris* and *M. bahaeldini*) from North Africa and the Middle East: Another case of paraphyly? *Molecular Phylogenetics and Evolution*, 49, 102–110.
- Katoh, K., Rozewicki, J., & Yamada, K. D. (2019). MAFFT online service: Multiple sequence alignment, interactive sequence choice and visualization. *Briefings in Bioinformatics*, 20, 1160–1166.
- Kumar, S., Stecher, G., Li, M., Knyaz, C., & Tamura, K. (2018). MEGA X: Molecular evolutionary genetics analysis across computing platforms. *Molecular Biology and Evolution*, 35, 1547–1549. <https://doi.org/10.1093/molbev/msy096>
- Lanfear, R., Calcott, B., Ho, S. Y., & Guindon, S. (2012). PartitionFinder: Combined selection of partitioning schemes and substitution models for phylogenetic analyses. *Molecular Biology and Evolution*, 29(6), 1695–1701. <https://doi.org/10.1093/molbev/mss020>
- Librado, P., & Rozas, J. (2009). DnaSP v5: A software for comprehensive analysis of DNA polymorphism data. *Bioinformatics*, 25(11), 1451–1452. <https://doi.org/10.1093/bioinformatics/btp187>
- Liu, C., Berry, P. M., Dawson, T. P., & Pearson, R. G. (2005). Selecting thresholds of occurrence in the prediction of species distributions. *Ecography*, 28, 385–393. <https://doi.org/10.1111/j.0906-7590.2005.03957.x>
- Lomolino, M. V. (2004). Conservation biogeography. *Frontiers of Biogeography: New Directions in the Geography of Nature*, 293, 293–296.
- Martínez del Mármlor, G. M., Harris, D. J., Geniez, P., de Pous, P., & Salvi, D. (2019). *Amphibians and reptiles of Morocco*. Edition Chimaira.
- Mayr, E. (1970). *Populations, species, and evolution: an abridgment of animal species and evolution*, Vol. 19. Harvard University Press.
- Múrias dos Santos, A., Cabezas, M. P., Tavares, A. I., Xavier, R., & Branco, M. (2016). tcsBU: A tool to extend TCS network layout and visualization. *Bioinformatics*, 32(4), 627–628. <https://doi.org/10.1093/bioinformatics/btv636>
- Padial, J. M., Miralles, A., De la Riva, I., & Vences, M. (2010). The integrative future of taxonomy. *Frontiers in Zoology*, 7, 16. <https://doi.org/10.1186/1742-9994-7-16>
- Phillips, S. J., Anderson, R. P., & Schapire, R. E. (2006). Maximum entropy modeling of species geographic distributions. *Ecological Modelling*, 190(3–4), 231–259. <https://doi.org/10.1016/j.ecolmodel.2005.03.026>
- Pinho, C., Harris, D. J., & Ferrand, N. (2008). Non-equilibrium estimates of gene flow inferred from nuclear genealogies suggest that Iberian and North African wall lizards (*Podarcis* spp.) are an assemblage of incipient species. *BMC Evolutionary Biology*, 8, 63. <https://doi.org/10.1186/1471-2148-8-63>
- Pinho, C., Kaliontzopoulou, A., Carretero, M. A., Harris, D. J., & Ferrand, N. (2009). Genetic admixture between the Iberian endemic lizards *Podarcis bocagei* and *Podarcis carbonelli*: Evidence for limited natural hybridization andimodal hybrid zone. *Journal of Zoological Systematics and Evolutionary Research*, 47, 368–377.
- Rato, C., Carranza, S., Perera, A., Carretero, M. A., & Harris, D. J. (2010). Conflicting patterns of nucleotide diversity between mtDNA and nucDNA in the Moorish gecko, *Tarentola mauritanica*. *Molecular Phylogenetics and Evolution*, 56(3), 962–971.
- Rato, C., Harris, D. J., Carranza, S., Machado, L., & Perera, A. (2016). The taxonomy of the *Tarentola mauritanica* species complex (Gekkota: Phyllodactylidae): Bayesian species delimitation supports six candidate species. *Molecular Phylogenetics and Evolution*, 94, 271–278. <https://doi.org/10.1016/j.ympev.2015.09.008>
- Renoult, J. P., Geniez, P., Bacquet, P., Benoit, L., & Crochet, P. A. (2009). Morphology and nuclear markers reveal extensive mitochondrial introgressions in the Iberian Wall Lizard species complex. *Molecular Ecology*, 18(20), 4298–4315. <https://doi.org/10.1111/j.1365-294X.2009.04351.x>
- Schuster, M., Düringer, P., Ghienne, J. F., Vignaud, P., Mackaye, H. T., Likius, A., & Brunet, M. (2006). The age of the Sahara desert. *Science*, 311, 821. <https://doi.org/10.1126/science.1120161>
- Sequeira, F., Ferrand, N., & Harris, D. J. (2006). Assessing the phylogenetic signal of the nuclear β -Fibrinogen intron 7 in salamanders (Amphibia: Salamandridae). *Amphibia-Reptilia*, 27, 409–418. <https://doi.org/10.1163/156853806778190114>
- Simó-Riudalbas, M., Tamar, K., Šmid, J., Mitsi, P., Sindaco, R., Chirio, L., & Carranza, S. (2019). Biogeography of *Mesalina* (Reptilia: Lacertidae), with special emphasis on the *Mesalina adramitana* group from Arabia and the Socotra Archipelago. *Molecular Phylogenetics and Evolution*, 137, 300–312. <https://doi.org/10.1016/j.ympev.2019.04.023>
- Sindaco, R., Jeremčenko, V. K., Venchi, A., & Grieco, C. (2008). *The reptiles of the Western Palearctic: Annotated checklist and distributional atlas of the turtles, crocodiles, amphisbaenians and lizards of Europe, North Africa, Middle East and Central Asia* (p. 589). Edizioni Belvedere.
- Sindaco, R., Simó-Riudalbas, M., Sacchi, R., & Carranza, S. (2018). Systematics of the *Mesalina guttulata* species complex (Squamata: Lacertidae) from Arabia with the description of two new species. *Zootaxa*, 4429(3), 513–547. <https://doi.org/10.11646/zootaxa.4429.3.4>
- Skonieczny, C., Paillou, P., Bory, A., Bayon, G., Biscara, L., Crosta, X., Eynaud, F., Malaizé, B., Revel, M., Aleman, N., Barousseau, J. P., Vernet, R., Lopez, S., & Grouset, F. (2015). African humid periods triggered the reactivation of a large river system in Western Sahara. *Nature Communications*, 6, 8751. <https://doi.org/10.1038/ncomms9751>
- Šmid, J., Moravec, J., Gvodík, V., Štundl, J., Frynta, D., Lymberakis, P., Kapli, P., Wilms, T., Schmitz, A., & Shobrak, M. (2017). Cutting the Gordian Knot: Phylogenetic and ecological diversification of the species *Mesalina brevirostris* complex (Squamata, Lacertidae). *Zoologica Scripta*, 46, 649–664.
- Sow, A. S., Martínez-Freiría, F., Dieng, H., Fahd, S., & Brito, J. C. (2014). Biogeographical analysis of the Atlantic Sahara reptiles: Environmental correlates of species distribution and vulnerability to climate change. *Journal of Arid Environments*, 109, 65–73.
- Suchard, M. A., Lemey, P., Baele, G., Ayres, D. L., Drummond, A. J., & Rambaut, A. (2018). Bayesian phylogenetic and phylodynamic data integration using BEAST 1.10. *Virus Evolution*, 4, veyle016. <https://doi.org/10.1093/ve/vey016>
- Swezey, C. S. (2009). Cenozoic stratigraphy of the Sahara, Northern Africa. *Journal of African Earth Sciences*, 53, 89–121. <https://doi.org/10.1016/j.jafrearsci.2008.08.001>
- Trape, J. F., Chirio, L., & Trape, S. (2012). *Lézards, Crocodiles et Tortues d'Afrique occidentale et du Sahara*. IRD éditions.
- Uetz, P., Goll, J., & Hallerman, J. (2020). *The reptile database*. <http://www.reptile-database.org>
- USGS (2006). *Shuttle Radar Topography Mission (SRTM): Mapping the world in 3 dimensions*. United States Geological Survey. <http://srtm.usgs.gov/index.html>

- Vale, C. G., Tarroso, P., & Brito, J. C. (2014). Predicting species distribution at range margins: Testing the effects of study area extent, resolution and threshold selection in the Sahara-Sahel transition zone. *Diversity and Distributions*, 20, 20–33. <https://doi.org/10.1111/ddi.12115>
- Velo-Antón, G., Martínez-Freiría, F., Pereira, P., Crochet, P.-A., & Brito, J. C. (2018). Living on the edge: Ecological and genetic connectivity of the Spiny-footed lizard, *Acanthodactylus aureus*, confirms the Atlantic Sahara desert as biogeographic corridor and centre of lineage diversification. *Journal of Biogeography*, 45, 1031–1042.
- Wang, Y., Notaro, M., Liu, Z., Gallimore, R., Levis, S., & Kutzbach, J. H. (2008). Detecting vegetation-precipitation feedbacks in mid-Holocene North Africa from two climate models. *Climate in the Past*, 4, 59–67. <https://doi.org/10.5194/cp-4-59-2008>

SUPPORTING INFORMATION

Additional supporting information may be found online in the Supporting Information section.

Figure S1. Sampling localities and sources.

Figure S2. Results of the BI analysis of mtDNA (Dataset S1).

Figure S3. Results of the BI analysis of nDNA (Dataset S2).

Figure S4. Results of the BI analysis on cytonuclear (Dataset S3).

Figure S5. Phenotypic diversity in the *Mesalina olivieri* species complex.

Figure S6. Principal Component Analysis (PCA) of the biometric variables.

Figure S7. Principal Component Analysis (PCA) of the pholidotic variables.

Figure S8. Principal Component Analysis (PCA) of the coloration variables.

Figure S9. Response curves for the most important environmental predictors.

Figure S10. Possible contact zone.

Table S1. GenBank accession codes and samples information.

Table S2. Information on all datasets used in the analyses.

Table S3. Material examined for biometric comparisons.

Table S4. Material examined for pholidotic characters comparisons.

Table S5. Material examined for coloration characters comparisons.

Table S6. Categories of the variable Land-cover used in the ecological models.

Table S7. Descriptive statistics.

Table S8. Details and metrics of the 20 model replicates developed.

Table S9. Number of observations and Standardized Levin's *B* measure of niche breadth.

Table S10. Known localities of *Mesalina adrarensis* sp. nov.

Alignment S1. Sequences alignment for *Cyt-b* gene.

Alignment S2. Sequences alignment for *β-fib7* gene.

Alignment S3. Sequences alignment for *MC1R* gene.

Alignment S4. Sequences alignment for *PgD7* gene.

Alignment S5. Sequences alignment for *OD* gene.

Dataset S1. Mitochondrial dataset, 378 sequences (285 bp).

Dataset S2 Concatenated multilocus nuclear dataset, 78 sequences (1700 bp).

Dataset S3. Concatenated mt + nucDNA dataset, 86 sequences (1986 bp)

How to cite this article: Pizzigalli, C., Crochet, P.-A., Geniez, P., Martínez-Freiría, F., Velo-Antón, G., & Carlos Brito, J. (2021). Phylogeographic diversification of the *Mesalina olivieri* species complex (Squamata: Lacertidae) with the description of a new species and a new subspecies endemic from North West Africa. *Journal of Zoological Systematics and Evolutionary Research*, 00, 1–29. <https://doi.org/10.1111/jzs.12516>

**Phylogeographic diversification of the *Mesalina olivieri* species complex
(Squamata: Lacertidae) with the description of a new species and a new subspecies
endemic from North West Africa**

Cristian Pizzigalli, Pierre-André Crochet, Philippe Geniez, Fernando Martínez-Freiría,
Guillermo Velo-Antón, José Carlos Brito

SUPPORTING INFORMATION

Fig S1 Sampling localities and sources	Pg.3
Fig S2 Results of the BI analysis of mtDNA (Dataset 1)	Pg.4
Fig S3 Results of the BI analysis of nDNA (Dataset 2)	Pg.7
Fig S4 Results of the BI analysis on cytonuclear (Dataset 3)	Pg.8
Fig S5 Phenotypic diversity in the <i>Mesalina olivieri</i> species complex	Pg.9
Fig S6 Principal Component Analysis (PCA) of the biometric variables	Pg.10
Fig S7 Principal Component Analysis (PCA) of the pholidotic variables	Pg.11
Fig S8 Principal Component Analysis (PCA) of the coloration variables	Pg.12
Fig S9 Response curves for the most important environmental predictors	Pg.13
Fig S10 Possible contact zone	Pg.14
Table S1 GenBank accession codes and samples information	Pg.15
Table S2 Information on all datasets used in the analyses	Pg.28
Table S3 Material examined for biometric comparisons	Pg.29
Table S4 Material examined for pholidotic characters comparisons	Pg.31
Table S5 Material examined for colouration characters comparisons	Pg.34
Table S6 Categories of the variable Land Cover used in the ecological models	Pg.37
Table S7 Descriptive statistics	Pg.38
Table S8 Details and metrics of the 20 model replicates developed	Pg.41
Table S9 Number of observations and Standardised Levin's B measure	Pg.42
Table S10 Known localities of <i>M. adrarensis</i> sp. nov.	Pg.43
Alignment S1	Provided separately from this file
Alignment S2	Provided separately from this file
Alignment S3	Provided separately from this file
Alignment S4	Provided separately from this file
Alignment S5	Provided separately from this file
Dataset 1	Provided separately from this file

Dataset 2

Provided separately from this file

Dataset 3

Provided separately from this file

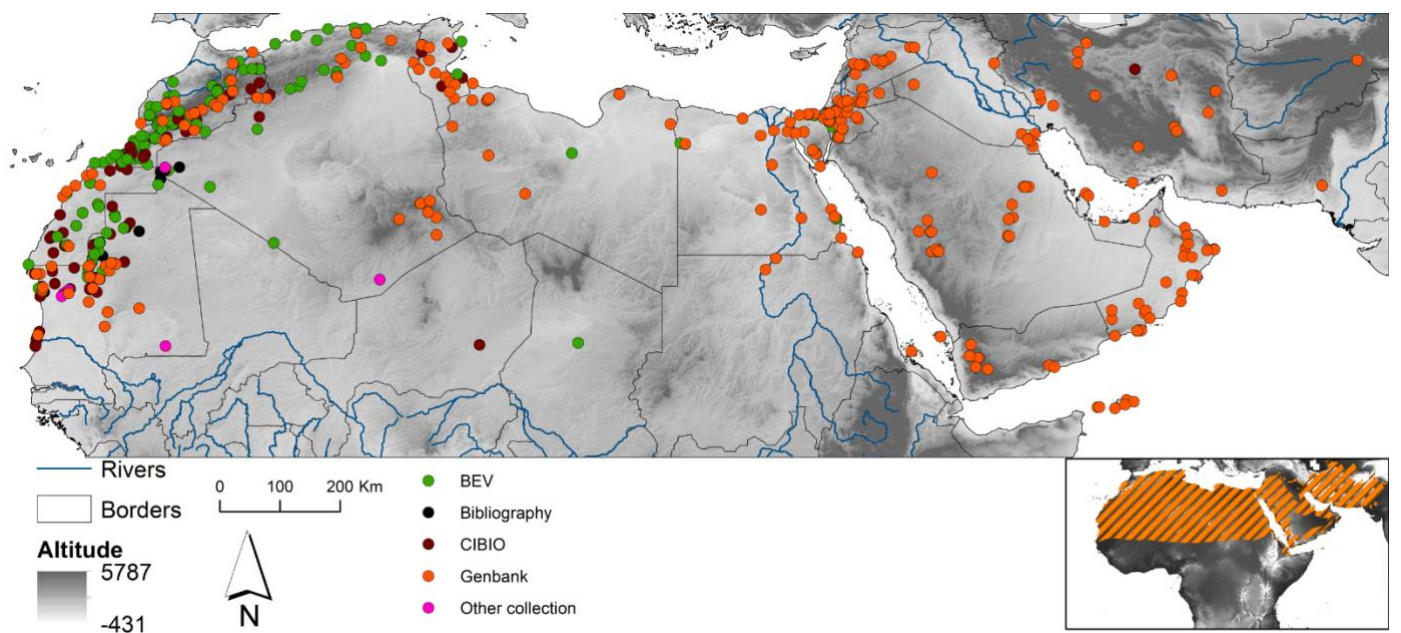
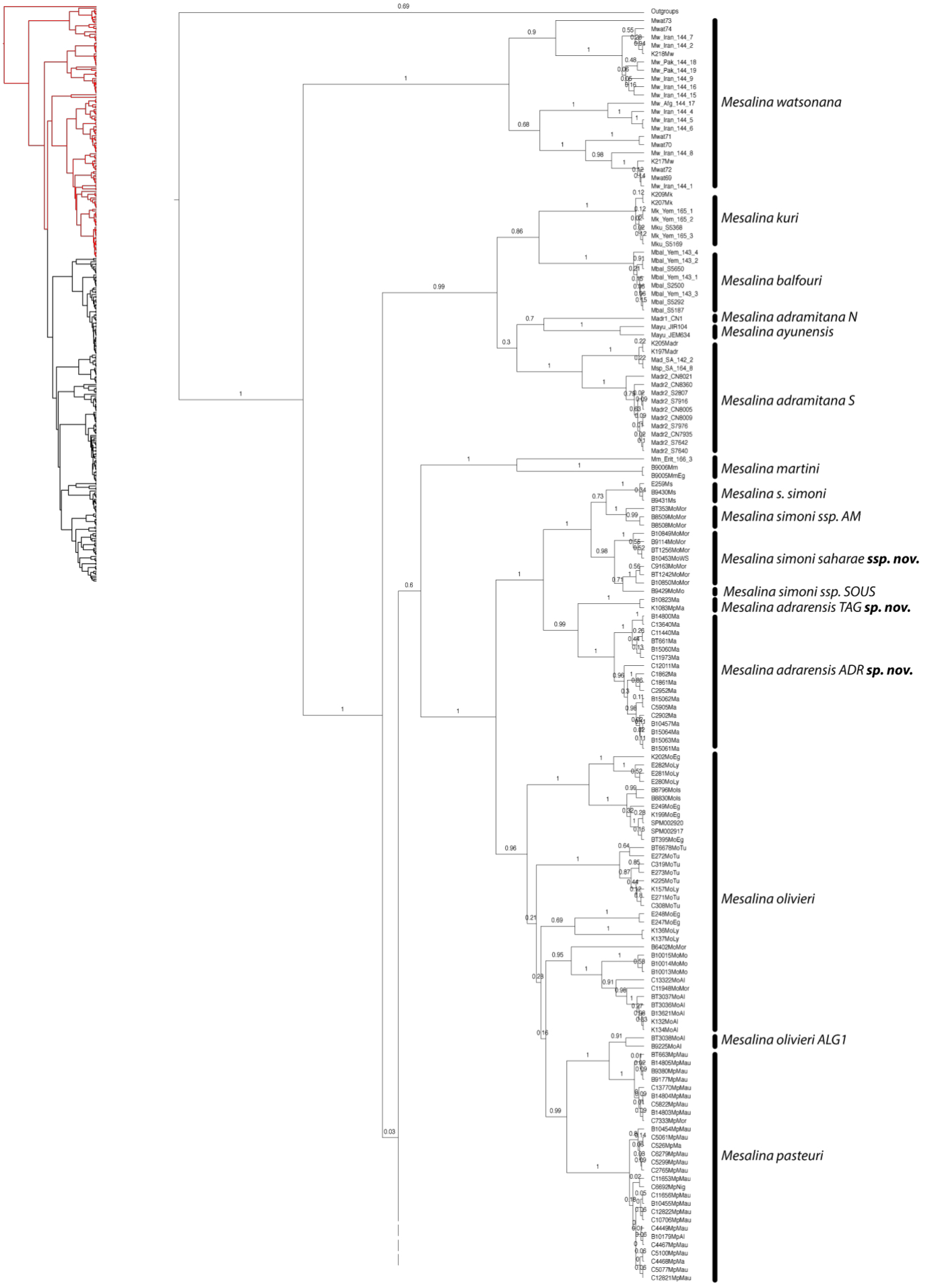
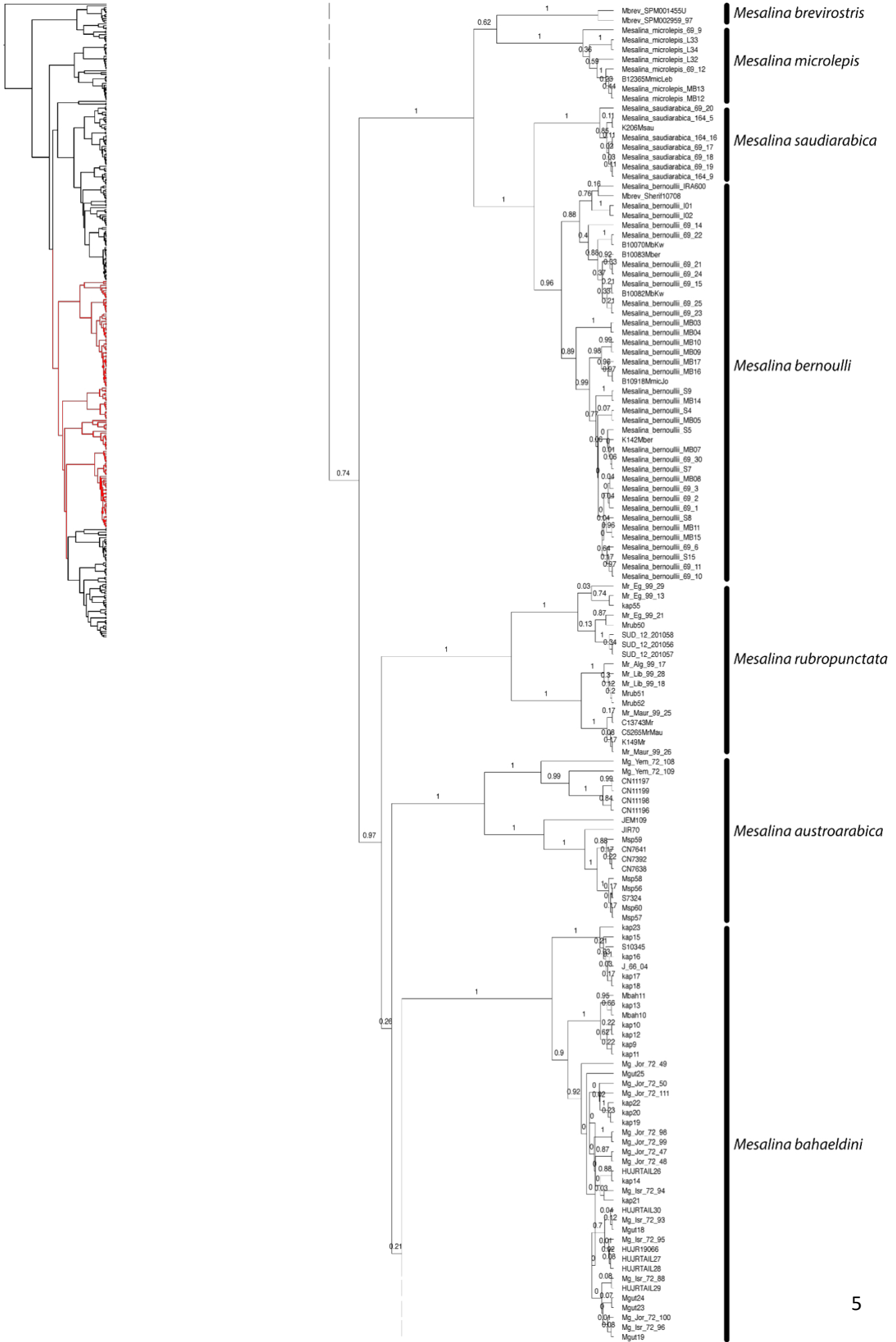


Fig S1. Sampling localities and sources of the *Mesalina* specimens used in this study. The map on the bottom right represents the current distribution of the genus *Mesalina*.





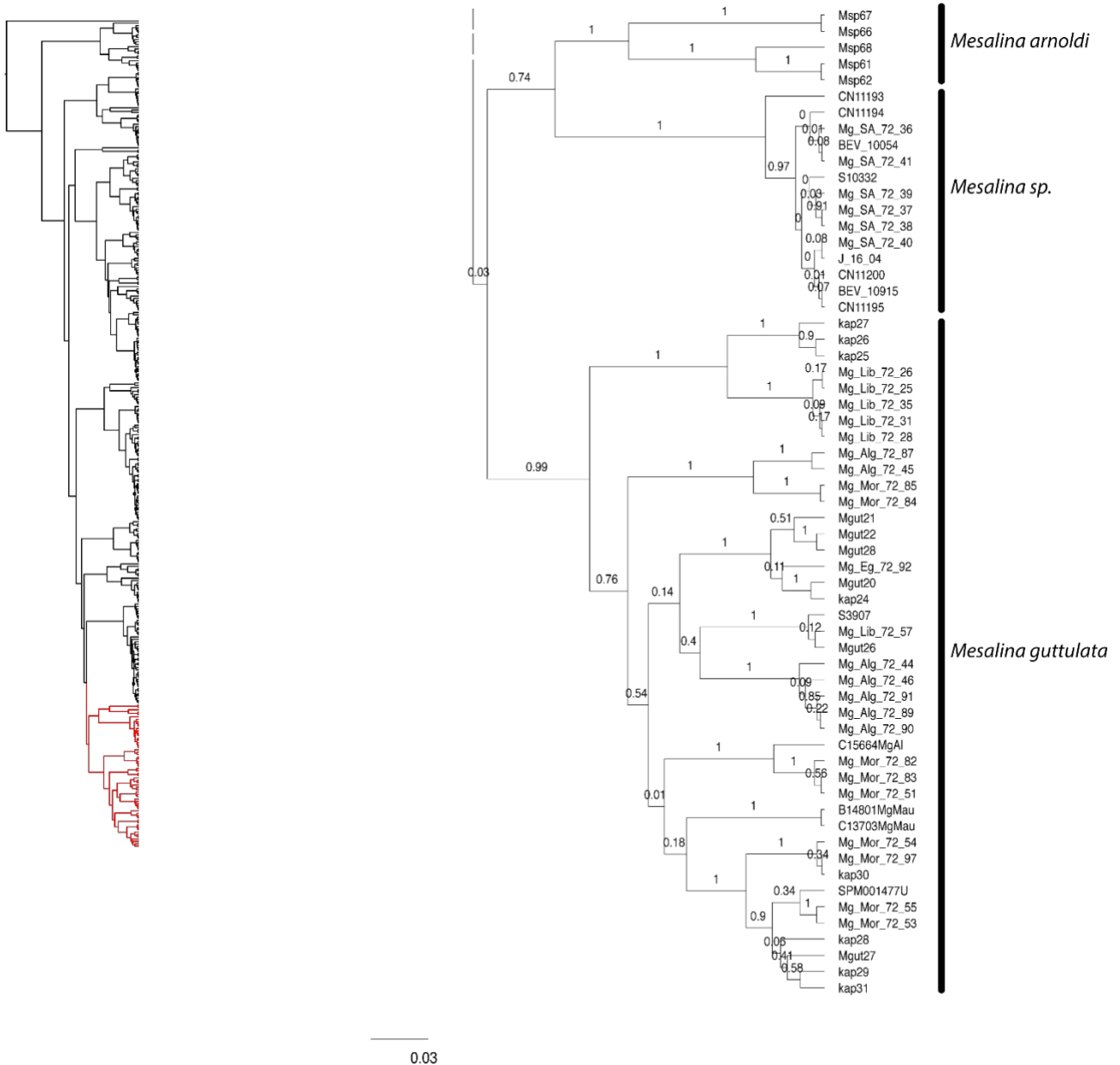


Fig S2. Results of the BI analysis of mtDNA (Dataset 1). Only posterior probabilities ≥ 0.95 are shown in the branches. Sample codes correspond to those in Tables 1 and S1.

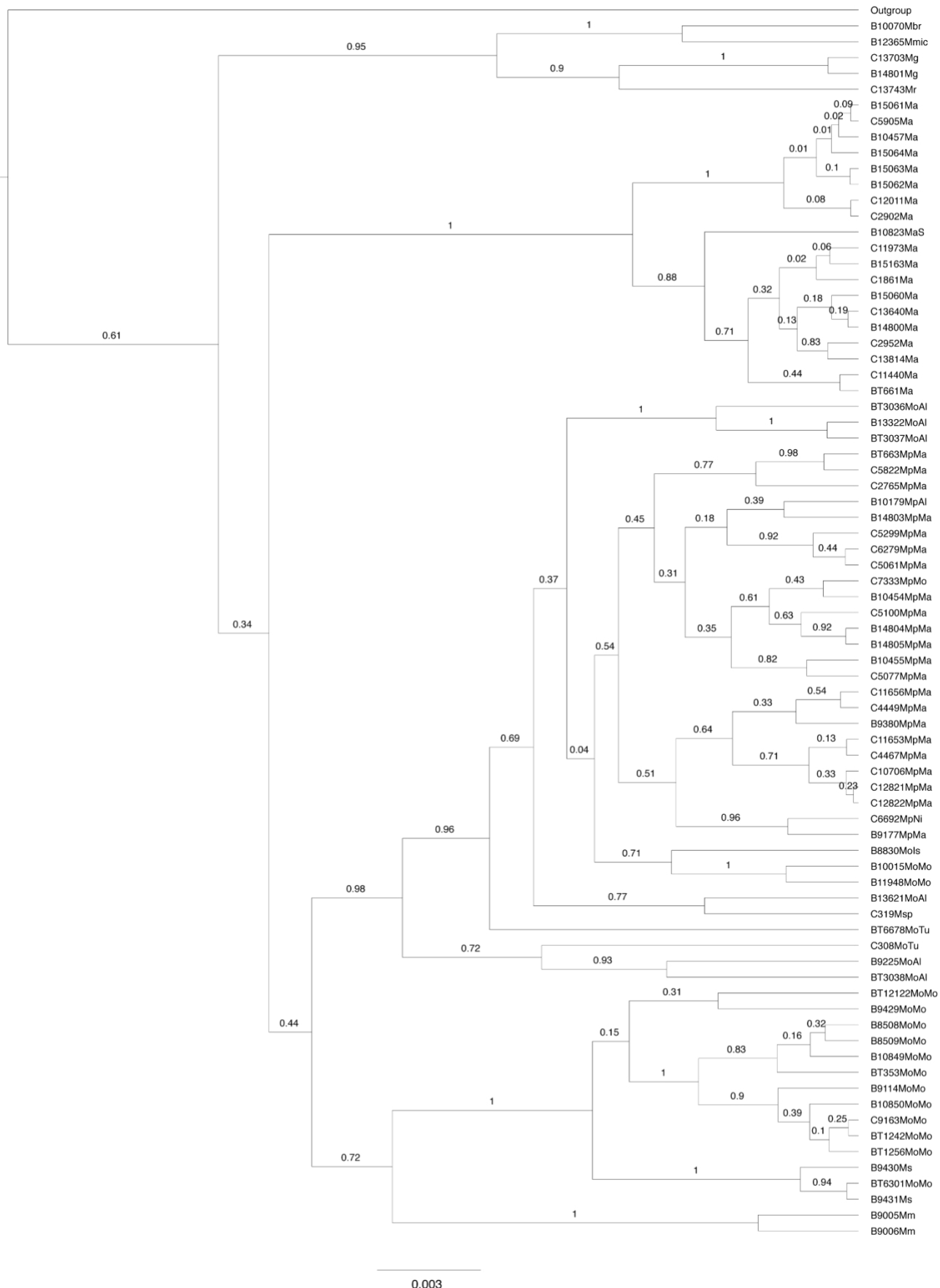


Fig S3. Results of the BI analysis of nDNA (Dataset 2). Sample codes correspond to those in Tables 1 and S1.

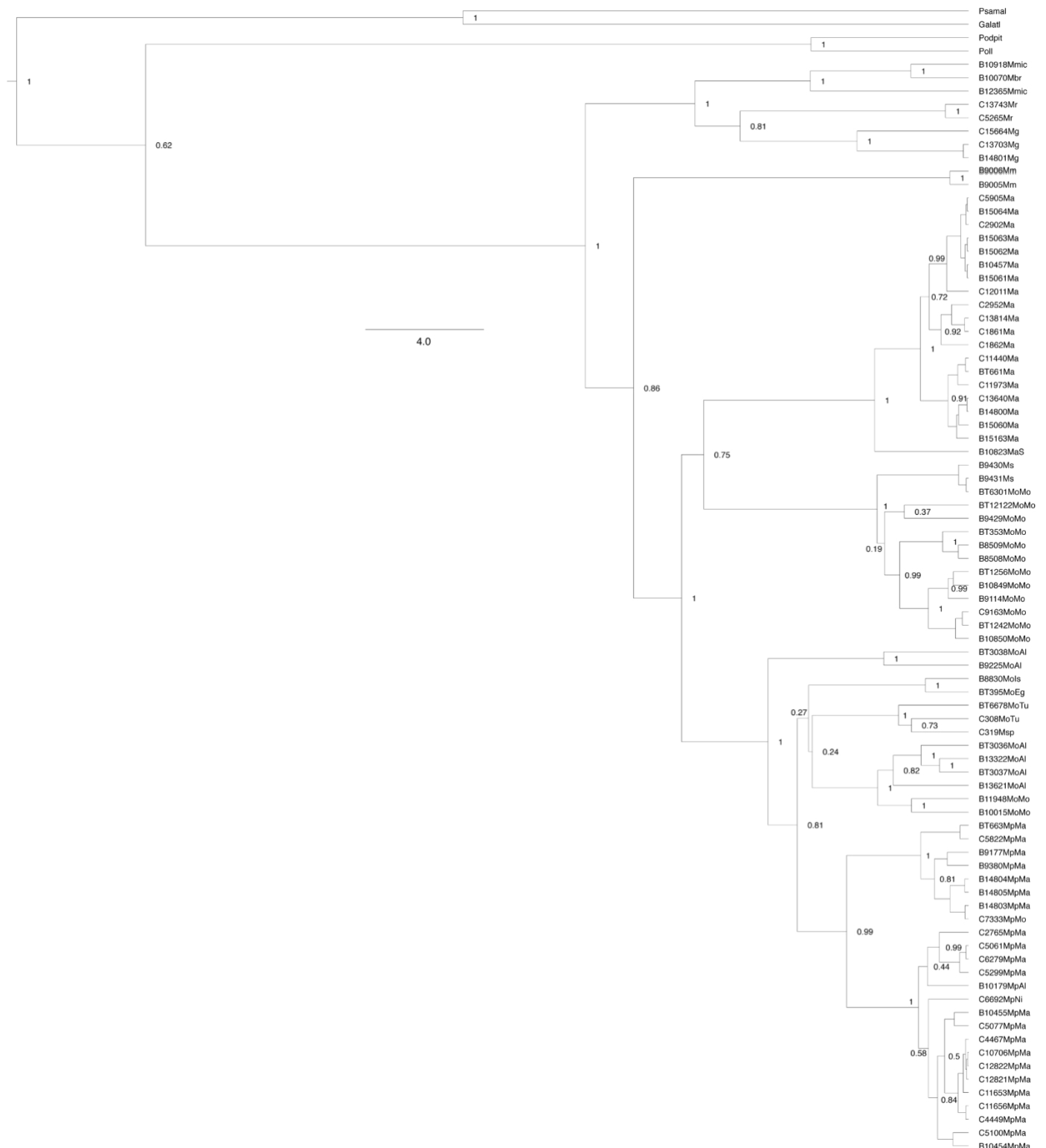


Fig S4. Results of the BI analysis on cytonuclear (Dataset 3). Sample codes correspond to those in Tables 1 and S1.



M. simoni saharae ssp. nov.



M. s. simoni



M. adrarensis sp. nov.



M. olivieri



M. pasteurii



Fig S5. Phenotypic diversity in the *Mesalina olivieri* species complex.

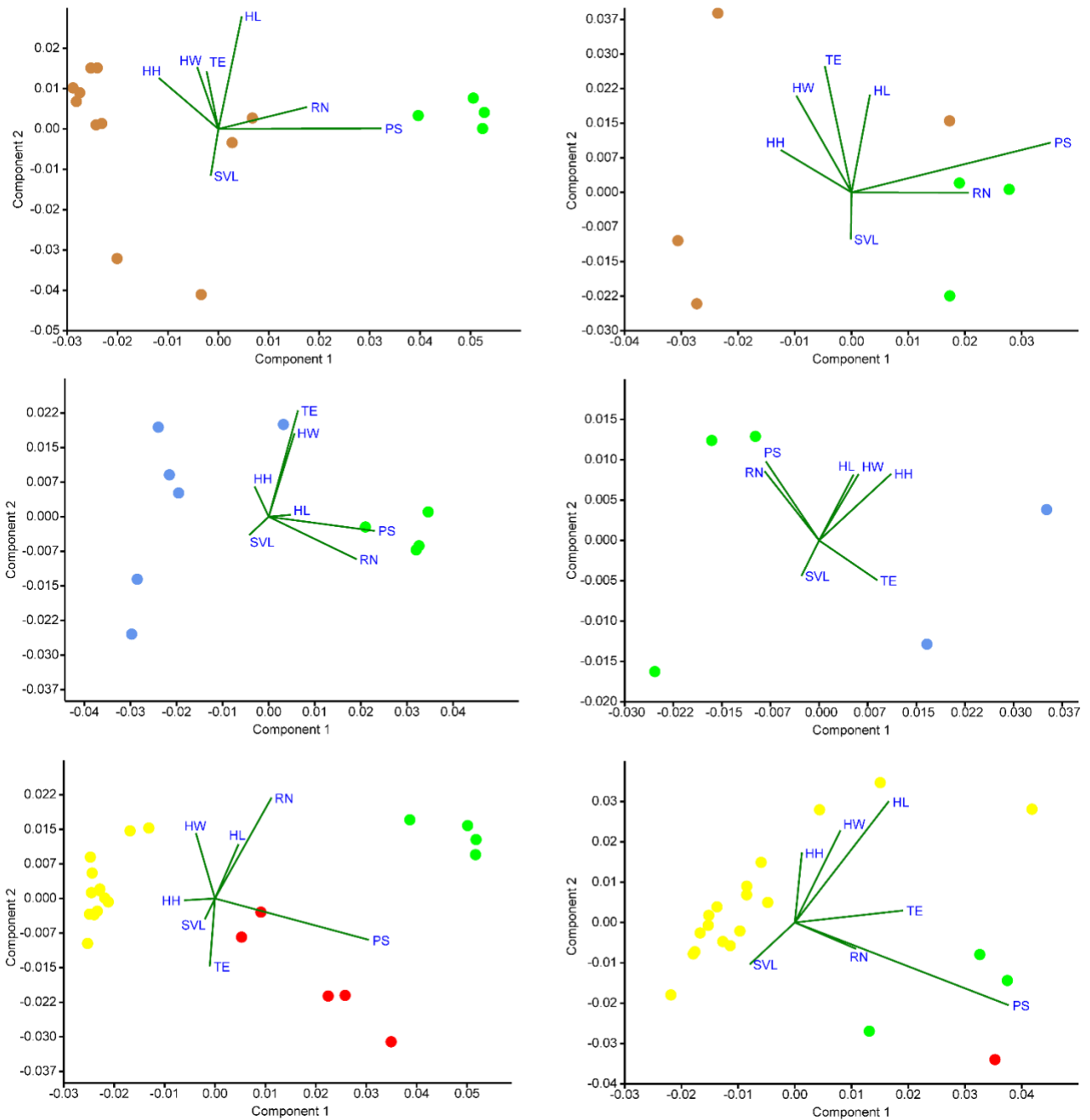


Fig. S6. Principal Component Analysis (PCA) of the biometric variables. Variables selected from the heating map analysis from male (left) and female (right) individuals of *Mesalina olivieri* species complex. The main morphological variables are superimposed to the graphs. Colours are the same previously used in other figures, and represent *M. adrarensis* sp. nov. (green), *M. olivieri* (brown), *M. pastorei* (blue), *M. simoni* (yellow), and *M. simoni saharae* ssp. nov. (red).

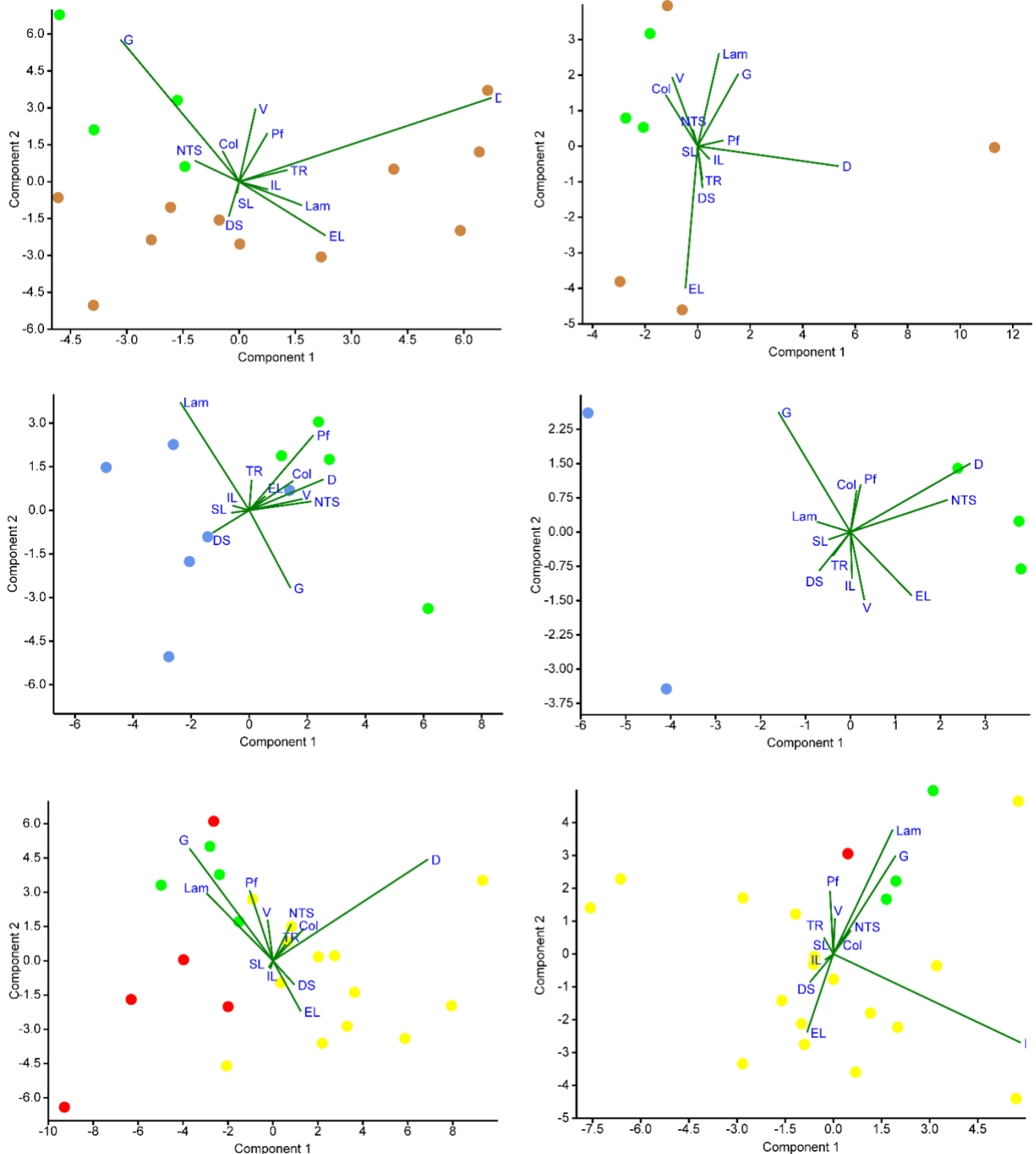


Fig. S7. Principal Component Analysis (PCA) of the pholidotic variables. Variables selected from the heating map analysis from male (left) and female (right) individuals of *Mesalina olivieri* species complex. The main morphological variables are superimposed to the graphs. Colours are the same previously used in other figures, and represent *M. adrarensis* sp. nov. (green), *M. olivieri* (brown), *M. pasteurii* (blue), *M. simoni* (yellow), and *M. simoni saharae* ssp. nov. (red).

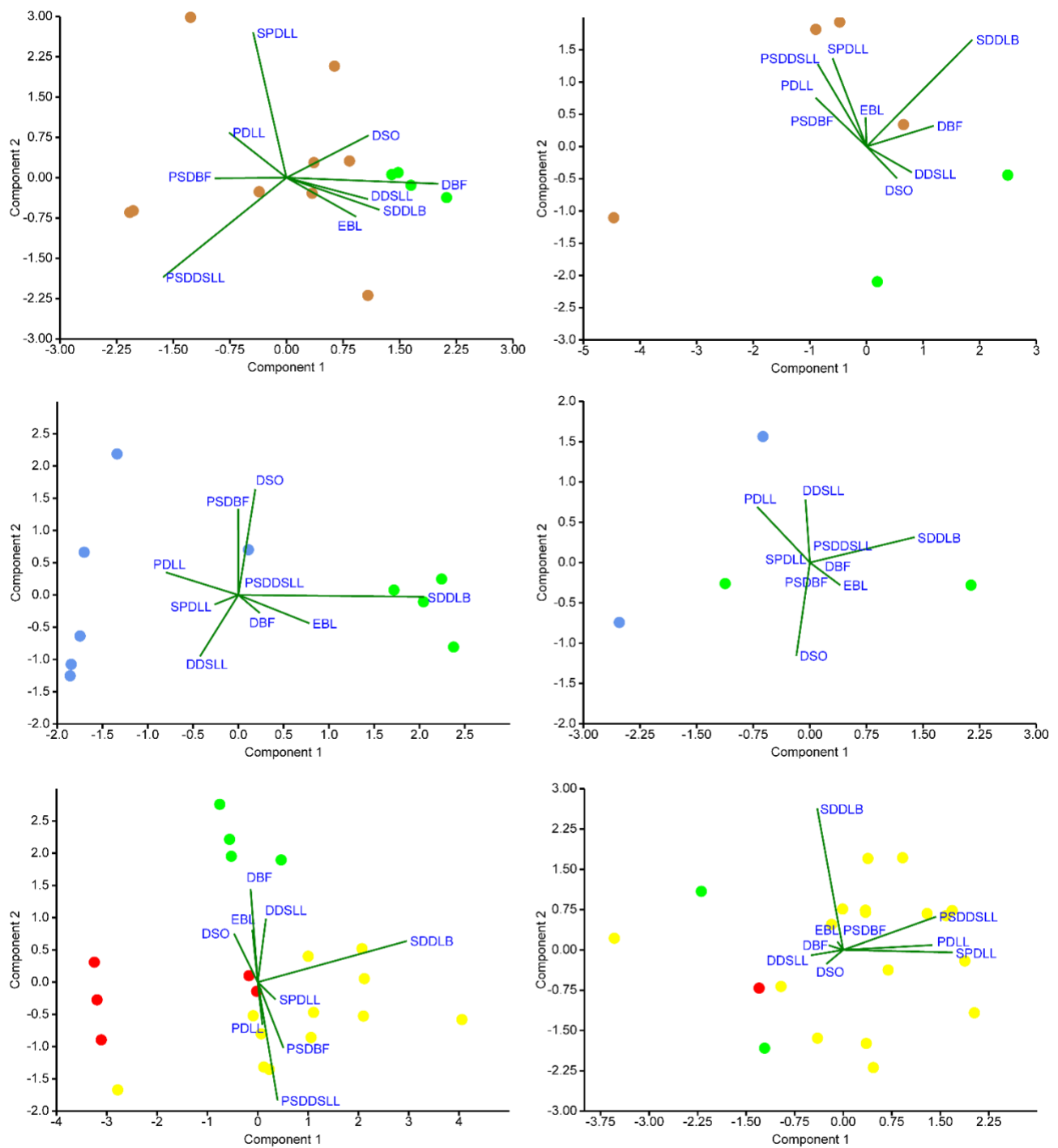


Fig. S8. Principal Component Analysis (PCA) of the coloration variables. Variables selected from the heating map analysis from male (left) and female (right) individuals of *Mesalina olivieri* species complex. The main morphological variables are superimposed to the graphs. Colours are the same previously used in other figures, and represent *M. adrarensis* sp. nov. (green), *M. olivieri* (brown), *M. pastouri* (blue), *M. simoni* (yellow), and *M. simoni saharae* ssp. nov. (red).

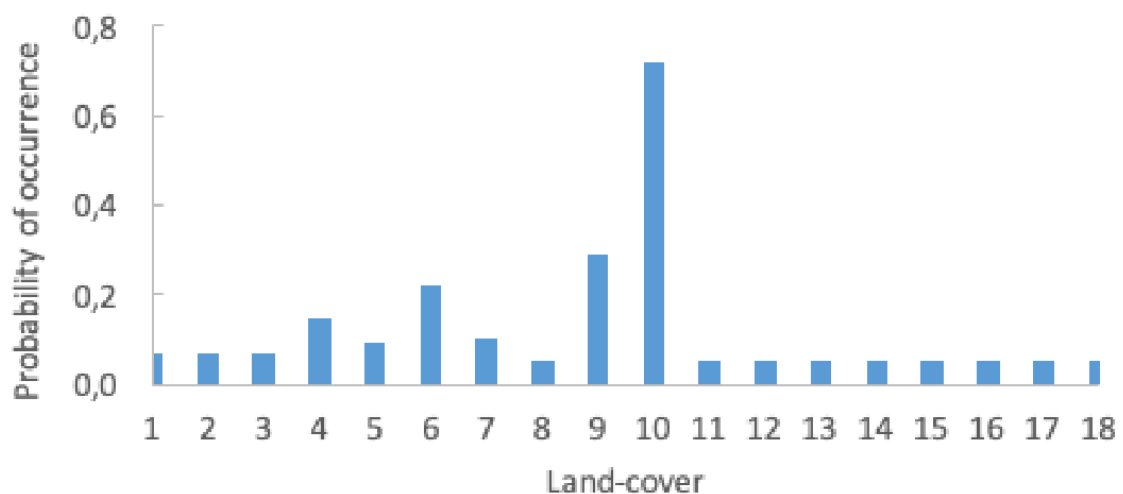
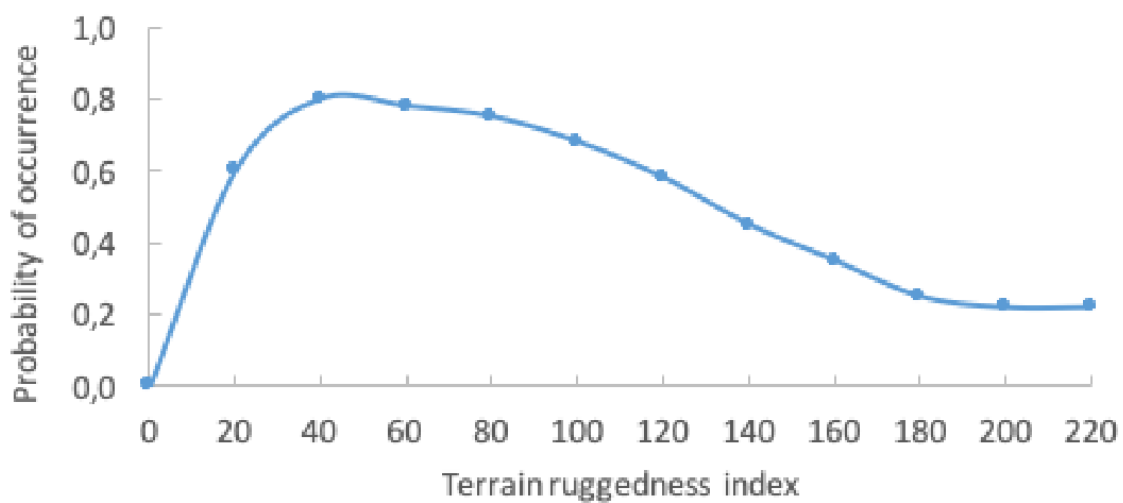


Fig S9. Response curves for the most important environmental predictors related to the distribution of *M. adrarensis* sp. nov.

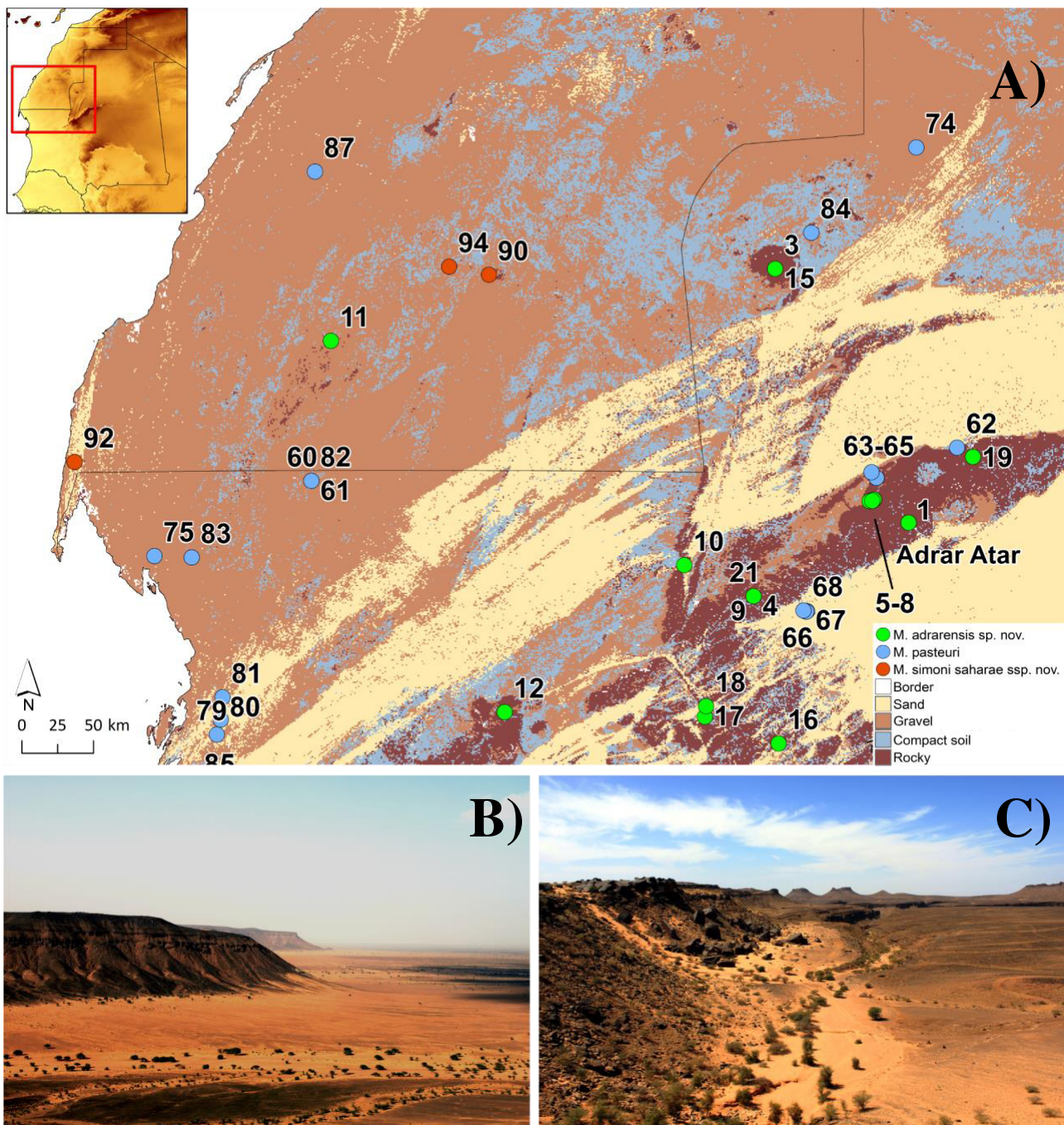


Fig. S10 A) Possible contact zone between *Mesalina adrarensis* sp. nov. (green), *M. pastorei* (blue), and *M. simoni saharae* ssp. nov. (red). The main land-cover categories (adapted from Campos and Brito, 2018) in the Adrar Atar (Mauritania) and adjacent northern regions. Pictures **B)** and **C)** show the proximity of dunes and sandy areas to the Mauritanian plateau. In picture C it is possible to notice some sand patches extending from the bottom to the top the plateau.

Table S1. Information about the samples used for the genetic analyses including GenBank accession codes. GeneBank accession codes in bold refer to sequences produced for this work.

Nº	Sample code	Species	Country	Latitude	Longitude	Cyt-b	B-fib7	OD	MC1R	PgD7
1	BEV.10457	<i>M. adrarensis</i> sp. nov.	Mauritania	21.0150	-11.7180	MZ223743	--	MZ223562	MZ223529	MZ223679
2	BEV.10823	<i>M. adrarensis</i> sp. nov.	Mauritania	17.3982	-12.0305	MZ223776	MZ223824	--	MZ223547	MZ223686
3	BEV.14800	<i>M. adrarensis</i> sp. nov.	Mauritania	22.6086	-12.5569	MZ223754	--	MZ223568	MZ223539	MZ223687
4	BEV.15060	<i>M. adrarensis</i> sp. nov.	Mauritania	20.5537	-12.6916	MZ223756	--	MZ223572	MZ223540	MZ223688
5	BEV.15061	<i>M. adrarensis</i> sp. nov.	Mauritania	21.1596	-11.9362	MZ223744	MZ223830	MZ223573	MZ223538	MZ223680
6	BEV.15062	<i>M. adrarensis</i> sp. nov.	Mauritania	21.1596	-11.9362	MZ223745	MZ223831	MZ223574	MZ223530	MZ223681
7	BEV.15063	<i>M. adrarensis</i> sp. nov.	Mauritania	21.1596	-11.9362	MZ223746	MZ223832	MZ223575	MZ223531	MZ223693
8	BEV.15064	<i>M. adrarensis</i> sp. nov.	Mauritania	21.1596	-11.9362	MZ223747	MZ223833	MZ223576	MZ223532	MZ223682
9	BEV.15163	<i>M. adrarensis</i> sp. nov.	Mauritania	20.5537	-12.6916	--	MZ223825	MZ223577	MZ223544	--
10	BEV.T661	<i>M. adrarensis</i> sp. nov.	Mauritania	20.7485	-13.1276	MZ223757	MZ223829	MZ223596	MZ223533	MZ223689
11	CIBIO11440	<i>M. adrarensis</i> sp. nov.	Morocco	22.1557	-15.3468	MZ223758	--	MZ223600	MZ223534	MZ223690
12	CIBIO11973	<i>M. adrarensis</i> sp. nov.	Mauritania	19.8265	-14.2555	MZ223759	MZ223828	MZ223603	MZ223545	--
13	CIBIO12011	<i>M. adrarensis</i> sp. nov.	Mauritania	21.1596	-11.9362	MZ223753	--	MZ223604	MZ223535	MZ223683
14	CIBIO12018	<i>M. adrarensis</i> sp. nov.	Mauritania	21.1502	-11.9623	--	--	--	--	--
15	CIBIO13640	<i>M. adrarensis</i> sp. nov.	Mauritania	22.6086	-12.5569	MZ223755	--	MZ223607	MZ223541	MZ223691
16	CIBIO13814	<i>M. adrarensis</i> sp. nov.	Mauritania	19.6289	-12.5344	--	MZ223826	MZ223609	MZ223542	MZ223692
17	CIBIO1861	<i>M. adrarensis</i> sp. nov.	Mauritania	19.7972	-12.9980	MZ223750	MZ223827	MZ223610	MZ223546	--
18	CIBIO1862	<i>M. adrarensis</i> sp. nov.	Mauritania	19.8632	-12.9909	MZ223751	--	MZ223611	--	MZ223694
19	CIBIO2902	<i>M. adrarensis</i> sp. nov.	Mauritania	21.4282	-11.3139	MZ223748	MZ223834	MZ223613	MZ223536	MZ223684
20	CIBIO2952	<i>M. adrarensis</i> sp. nov.	Mauritania	18.9849	-13.0647	MZ223752	MZ223835	MZ223614	MZ223543	MZ223695
21	CIBIO5865	<i>M. adrarensis</i> sp. nov.	Mauritania	20.5537	-12.6916	--	--	--	--	--
22	CIBIO5905	<i>M. adrarensis</i> sp. nov.	Mauritania	21.1521	-11.9470	MZ223749	--	MZ223622	MZ223537	MZ223685
23	BEV.10013	<i>M. olivieri</i>	Morocco	33.1860	-3.9900	MZ223702	--	MZ223556	--	--
24	BEV.10014	<i>M. olivieri</i>	Morocco	33.1860	-3.9900	MZ223703	--	--	MZ223522	--
25	BEV.10015	<i>M. olivieri</i>	Morocco	33.1860	-3.9900	MZ223704	MZ223787	MZ223557	MZ223474	--
26	BEV.11948	<i>M. olivieri</i>	Morocco	32.9297	-5.0465	MZ223708	--	MZ223565	MZ223527	MZ223657

N°	Sample code	Species	Country	Latitude	Longitude	Cyt-b	B-fib7	OD	MC1R	PgD7
27	BEV.13322	<i>M. olivieri</i>	Algeria	36.6245	4.8517	MZ223709	MZ223815	MZ223566	MZ223523	MZ223645
28	BEV.13621	<i>M. olivieri</i>	Algeria	35.8802	1.6841	MZ223705	MZ223789	MZ223567	MZ223490	MZ223646
29	BEV.6402	<i>M. olivieri</i>	Morocco	31.1940	-6.2100	MZ223710	MZ223788	--	--	--
30	BEV.8796	<i>M. olivieri</i>	Israel	30.7077	34.7845	MZ223773	--	--	--	--
31	BEV.8830	<i>M. olivieri</i>	Israel	31.0858	34.6310	MZ223774	MZ223823	MZ223582	MZ223526	MZ223653
32	BEV.9225	<i>M. olivieri</i>	Algeria	33.5914	2.9508	MZ223722	MZ223836	--	MZ223491	MZ223652
33	BEV.T3036	<i>M. olivieri</i>	Algeria	36.3413	4.2509	MZ223706	MZ223816	MZ223591	MZ223525	MZ223656
34	BEV.T3037	<i>M. olivieri</i>	Algeria	36.3413	4.2509	MZ223707	MZ223817	MZ223592	MZ223524	--
35	BEV.T3038	<i>M. olivieri</i>	Algeria	35.8585	6.4908	MZ223723	MZ223844	MZ223593	MZ223492	MZ223649
36	BEV.T395	<i>M. olivieri</i>	Egypt	31.1200	33.7600	MZ223775	MZ223822	--	MZ223521	--
37	BEV.T6678	<i>M. olivieri</i>	Tunisia	35.8006	11.0361	--	MZ223790	--	MZ223493	MZ223655
38	CIBIO308	<i>M. olivieri</i>	Tunisia	35.5822	8.4826	MZ223711	MZ223791	--	MZ223488	MZ223658
39	NHMC80.3.119.29	<i>M. olivieri</i>	Tunisia	35.6895	10.1501	KM411225	--	--	--	--
40	NHMC80.3.119.10	<i>M. olivieri</i>	Tunisia	32.1287	10.5638	KM411225	--	--	--	--
41	NHMC80.3.119.108	<i>M. olivieri</i>	Algeria	35.4151	4.5190	KM411132	--	--	--	--
42	NHMC80.3.119.109	<i>M. olivieri</i>	Egypt	27.8300	31.1068	KM411202	--	--	--	--
43	NHMC80.3.119.14	<i>M. olivieri</i>	Tunisia	33.7531	9.3350	EF555315	--	--	--	--
44	NHMC80.3.119.16	<i>M. olivieri</i>	Egypt	29.9651	33.1606	EF555289	--	--	--	--
45	NHMC80.3.119.19	<i>M. olivieri</i>	Egypt	29.9651	33.1606	EF555290	--	--	--	--
46	NHMC80.3.119.2	<i>M. olivieri</i>	Libya	32.3912	21.2404	EF555322	--	--	--	--
47	NHMC80.3.119.20	<i>M. olivieri</i>	Egypt	29.9797	32.1187	EF555291	--	--	--	--
48	NHMC80.3.119.21	<i>M. olivieri</i>	Libya	32.1247	12.8068	KM411136	--	--	--	--
49	NHMC80.3.119.22	<i>M. olivieri</i>	Libya	32.1247	12.8068	KM411137	--	--	--	--
50	NHMC80.3.119.23	<i>M. olivieri</i>	Algeria	35.4151	4.5190	KM411134	--	--	--	--
51	NHMC80.3.119.3	<i>M. olivieri</i>	Libya	32.3912	21.2404	EF555323	--	--	--	--
52	NHMC80.3.119.40	<i>M. olivieri</i>	Egypt	30.5965	32.2715	KM411199	--	--	--	--
53	NHMC80.3.119.5	<i>M. olivieri</i>	Libya	32.3912	21.2404	EF555324	--	--	--	--
54	NHMC80.3.119.9	<i>M. olivieri</i>	Tunisia	34.4076	7.9448	EF555313	--	--	--	--
55	NHMC80.3.164.19	<i>M. olivieri</i>	Libya	33.0956	11.7626	KM411157	--	--	--	--

N°	Sample code	Species	Country	Latitude	Longitude	Cyt-b	B-fib7	OD	MC1R	PgD7
56	SPM002917	<i>M. olivieri</i>	Egypt	-	-	--	--	--	--	--
57	SPM002920	<i>M. olivieri</i>	Egypt	-	-	--	--	--	--	--
58	CIBIO319	<i>M. olivieri</i>	Tunisia	32.9974	10.6080	MZ223712	MZ223818	--	MK551641	MZ223654
59	BEV.10179	<i>M. pasteurii</i>	Algeria	24.7839	8.8719	MZ223724	MZ223792	MZ223559	MK551638	MZ223626
60	BEV.10454	<i>M. pasteurii</i>	Mauritania	21.2777	-15.4703	MZ223736	MZ223794	MZ223560	MK551646	MZ223631
61	BEV.10455	<i>M. pasteurii</i>	Mauritania	21.2777	-15.4703	MZ223725	--	MZ223561	MK551642	MZ223638
62	BEV.14803	<i>M. pasteurii</i>	Mauritania	21.4866	-11.4139	MZ223713	MZ223800	MZ223570	MK551640	MZ223647
63	BEV.14804	<i>M. pasteurii</i>	Mauritania	21.2970	-11.9199	MZ223714	MZ223795	MZ223571	MZ223509	--
64	BEV.14805	<i>M. pasteurii</i>	Mauritania	21.2970	-11.9199	MZ223715	MZ223797	--	MZ223510	MZ223643
65	BEV.9177	<i>M. pasteurii</i>	Mauritania	21.3321	-11.9512	MZ223716	MZ223814	MZ223584	MZ223511	MZ223635
66	BEV.9380	<i>M. pasteurii</i>	Mauritania	20.4600	-12.3560	MZ223717	MZ223806	MZ223585	MZ223513	MZ223627
67	BEV.T662	<i>M. pasteurii</i>	Mauritania	20.4563	-12.3602	--	--	MZ223597	MZ223496	--
68	BEV.T663	<i>M. pasteurii</i>	Mauritania	20.4641	-12.3790	MZ223718	--	MZ223598	MZ223514	MZ223650
69	CIBIO10706	<i>M. pasteurii</i>	Mauritania	16.2051	-16.5034	MZ223726	MZ223807	MZ223599	MZ223504	MZ223639
70	CIBIO11653	<i>M. pasteurii</i>	Mauritania	16.6072	-16.4418	MZ223727	MZ223813	MZ223601	MZ223499	MZ223632
71	CIBIO11656	<i>M. pasteurii</i>	Mauritania	16.6554	-16.4242	MZ223728	MZ223808	MZ223602	MZ223501	MZ223633
72	CIBIO12821	<i>M. pasteurii</i>	Mauritania	16.1307	-16.5112	MZ223729	MZ223809	MZ223605	MZ223500	MZ223648
73	CIBIO12822	<i>M. pasteurii</i>	Mauritania	16.1307	-16.5112	MZ223730	MZ223810	MZ223606	MZ223505	MZ223640
74	CIBIO13770	<i>M. pasteurii</i>	Mauritania	23.3699	-11.6696	MZ223721	MZ223793	--	--	--
75	CIBIO2765	<i>M. pasteurii</i>	Mauritania	20.8061	-16.4561	MZ223741	MZ223801	MZ223612	MZ223512	MZ223629
76	CIBIO4449	<i>M. pasteurii</i>	Mauritania	17.0674	-16.2555	MZ223731	MZ223811	MZ223615	MZ223502	--
77	CIBIO4467	<i>M. pasteurii</i>	Mauritania	16.8484	-16.3503	MZ223732	MZ223812	MZ223616	MZ223506	MZ223634
78	CIBIO4468	<i>M. pasteurii</i>	Mauritania	16.8484	-16.3503	MZ223733	--	--	--	--
79	CIBIO5061	<i>M. pasteurii</i>	Mauritania	19.6851	-16.0641	MZ223737	--	MZ223617	MZ223519	MZ223630
80	CIBIO5077	<i>M. pasteurii</i>	Mauritania	19.7795	-16.0390	MZ223734	MZ223803	MZ223618	MZ223516	MZ223641
81	CIBIO5100	<i>M. pasteurii</i>	Mauritania	19.9197	-16.0280	MZ223735	MZ223796	MZ223619	MZ223508	MZ223642
82	CIBIO526	<i>M. pasteurii</i>	Mauritania	21.2777	-15.4703	KM411230	--	--	--	--
83	CIBIO5299	<i>M. pasteurii</i>	Mauritania	20.7972	-16.2221	MZ223739	MZ223805	MZ223620	MZ223520	MZ223644
84	CIBIO5822	<i>M. pasteurii</i>	Mauritania	22.8350	-12.3292	MZ223719	MZ223802	MZ223621	MZ223515	MZ223651

N°	Sample code	Species	Country	Latitude	Longitude	Cyt-b	B-fib7	OD	MC1R	PgD7
85	CIBIO6279	<i>M. pasteuri</i>	Mauritania	19.3514	-16.2004	MZ223740	MZ223799	MZ223623	MZ223518	MZ223628
86	CIBIO6692	<i>M. pasteuri</i>	Niger	16.2178	12.1985	MZ223742	MZ223819	--	MZ223498	MZ223636
87	CIBIO7333	<i>M. pasteuri</i>	Morocco	23.2185	-15.4468	MZ223720	MZ223798	--	MZ223502	MZ223637
88	BEV.10453	<i>M. simoni saharae ssp. nov.</i>	Morocco	26.1256	-14.4799	KM411227	MZ223845	--	--	--
89	BEV.10849	<i>M. simoni saharae ssp. nov.</i>	Morocco	26.5298	-12.3364	MZ223763	MZ223850	MZ223563	MZ223475	MZ223659
90	BEV.10850	<i>M. simoni saharae ssp. nov.</i>	Morocco	22.5709	-14.3544	MZ223764	MZ223846	MZ223564	MZ223482	MZ223663
91	BEV.9114	<i>M. simoni saharae ssp. nov.</i>	Morocco	26.4925	-13.9198	MZ223762	MZ223847	MZ223583	MZ223478	MZ223670
92	BEV.T1242	<i>M. simoni saharae ssp. nov.</i>	Morocco	21.3963	-16.9579	MZ223765	MZ223848	MZ223589	MZ223480	MZ223660
93	BEV.T1256	<i>M. simoni saharae ssp. nov.</i>	Morocco	26.4925	-13.9198	MZ223761	MZ223851	MZ223590	MZ223481	MZ223669
94	CIBIO9163	<i>M. simoni saharae ssp. nov.</i>	Morocco	22.6215	-14.6044	MZ223766	MZ223849	MZ223624	MZ223479	--
95	BEV.8508	<i>M. simoni ssp.</i>	Morocco	32.1900	-2.2037	MZ223770	MZ223852	MZ223580	MZ223476	MZ223661
96	BEV.8509	<i>M. simoni ssp.</i>	Morocco	32.1750	-2.1650	MZ223771	MZ223853	MZ223581	MZ223477	MZ223662
97	BEV.9429	<i>M. simoni ssp.</i>	Morocco	30.7076	-8.3577	MZ223767		MZ223586	MZ223473	MZ223664
98	BEV.T12122	<i>M. simoni ssp.</i>	Morocco	28.4876	-11.3366	--	MZ223856	MZ223588	MZ223483	MZ223668
99	BEV.T353	<i>M. simoni ssp.</i>	Morocco	31.5740	-4.7380	MZ223772	MZ223855	MZ223594	--	MZ223671
100	BEV.9430	<i>M. simoni simoni</i>	Morocco	31.8301	-7.9829	MZ223768	--	MZ223587	MZ223553	MZ223665
101	BEV.9431	<i>M. simoni simoni</i>	Morocco	31.8129	-8.0138	MZ223769	MZ223857	--	MZ223554	MZ223666
102	BEV.T6301/E259	<i>M. simoni simoni</i>	Morocco	32.3011	-7.5307	--	--	MZ223595	MZ223555	MZ223667
107	CN1	<i>M. adramitana</i>	Oman	23.7861	57.7977	MK551691	--	--	MK551616	--
108	CN7935	<i>M. adramitana</i>	Oman	18.8911	54.8119	MK551683	--	--	MK551606	--
109	CN8005	<i>M. adramitana</i>	Oman	18.2627	55.1938	MH040005	--	--	MH040050	--
110	CN8009	<i>M. adramitana</i>	Oman	18.4416	55.2722	MK551684	--	--	MK551607	--
111	CN8021	<i>M. adramitana</i>	Oman	17.8778	53.0862	MK551685	--	--	MK551608	--
112	CN8360	<i>M. adramitana</i>	Oman	18.4640	53.0678	MK551690	--	--	MK551613	--
113	K197	<i>M. adramitana</i>	S. Arabia	22.2445	41.4320	KM411197	--	--	--	--
115	K205	<i>M. adramitana</i>	S. Arabia	22.2525	41.8796	KM411205	--	--	--	--
116	S2807	<i>M. adramitana</i>	Oman	19.5626	57.6233	KY967144	--	--	KY967099	--
117	S7640	<i>M. adramitana</i>	Oman	20.7264	58.2622	MK551686	--	--	MK551609	--
118	S7642	<i>M. adramitana</i>	Oman	19.0311	57.5285	MK551687	--	--	MK551610	--

Nº	Sample code	Species	Country	Latitude	Longitude	Cyt-b	B-fib7	OD	MC1R	PgD7
119	S7916	<i>M. adramitana</i>	Oman	20.2584	56.5810	MK551688	--	--	MK551611	--
120	S7976	<i>M. adramitana</i>	Oman	19.0311	57.5285	MK551689	--	--	MK551612	--
121	Msp67	<i>M. arnoldi</i>	Yemen	15.3600	44.4700	MH040006	--	--	--	--
122	Msp66	<i>M. arnoldi</i>	Yemen	15.3800	44.4500	MH040007	--	--	MH040051	--
123	Msp68	<i>M. arnoldi</i>	Yemen	15.5100	43.8800	MH040008	--	--	--	--
124	Msp61	<i>M. arnoldi</i>	Yemen	14.7800	44.2800	MH040009	--	--	MH040052	--
125	Msp62	<i>M. arnoldi</i>	Yemen	14.7800	44.2800	MH040010	--	--	MH040053	--
126	CN11196	<i>M. austroarabica</i>	S. Arabia	16.7543	41.9985	MK551727	--	--	MK551656	--
127	CN11197	<i>M. austroarabica</i>	S. Arabia	16.7543	41.9985	MK551728	--	--	MK551657	--
128	CN11198	<i>M. austroarabica</i>	S. Arabia	16.7543	41.9985	MK551729	--	--	MK551658	--
129	CN11199	<i>M. austroarabica</i>	S. Arabia	16.7543	41.9985	MK551730	--	--	MK551659	--
130	CN7392	<i>M. austroarabica</i>	Oman	17.1494	54.9757	MH040011	--	--	MH040054	--
131	CN7638	<i>M. austroarabica</i>	Oman	17.1597	54.8069	MH040012	--	--	MH040055	--
132	CN7641	<i>M. austroarabica</i>	Oman	17.1494	54.9757	MH040013	--	--	MH040056	--
133	JEM109	<i>M. austroarabica</i>	Yemen	14.9000	49.0300	MH040014	--	--	MH040057	--
134	JIR70	<i>M. austroarabica</i>	Oman	16.8014	53.2783	MH040015	--	--	MH040058	--
135	NHMC80.3.72.108	<i>M. austroarabica</i>	Yemen	16.2333	43.9667	KM411144	--	--	--	--
136	NHMC80.3.72.109	<i>M. austroarabica</i>	Yemen	14.6500	45.0500	KM411145	--	--	--	--
137	S2421	<i>M. austroarabica</i>	Oman	17.1139	54.7137	MH040016	--	--	MH040059	--
138	S2599	<i>M. austroarabica</i>	Oman	17.1139	54.7137	MH040017	--	--	MH040060	--
139	S2701	<i>M. austroarabica</i>	Oman	17.1139	54.7137	MH040018	--	--	MH040061	--
140	S2725	<i>M. austroarabica</i>	Oman	17.1139	54.7137	MH040019	--	--	MH040062	--
141	S2838	<i>M. austroarabica</i>	Oman	17.1139	54.7137	MH040020	--	--	MH040063	--
142	S7324	<i>M. austroarabica</i>	Oman	17.1214	54.7140	MH040021	--	--	MH040064	--
143	JEM634	<i>M. ayunensis</i>	Yemen	14.7800	49.3700	MK551693	--	--	MK551625	--
144	JIR104	<i>M. ayunensis</i>	Oman	17.9335	55.5275	MK551692	--	--	MK551624	--
145	HUJR-19066	<i>M. bahaeldini</i>	Israel	31.2540	35.1630	MH040022	--	--	MH040065	--
146	HUJR-TAIL-26	<i>M. bahaeldini</i>	Israel	31.9870	35.4360	MH040023	--	--	--	--
147	HUJR-TAIL-27	<i>M. bahaeldini</i>	Israel	31.2080	34.7710	MH040024	--	--	MH040066	--

Nº	Sample code	Species	Country	Latitude	Longitude	Cyt-b	B-fib7	OD	MC1R	PgD7
148	HUJR-TAIL-28	<i>M. bahaeldini</i>	Israel	31.2040	34.7930	MH040025	--	--	MH040067	--
149	HUJR-TAIL-29	<i>M. bahaeldini</i>	Israel	31.3270	35.2280	MH040026	--	--	MH040068	--
150	HUJR-TAIL-30	<i>M. bahaeldini</i>	Israel	31.3270	35.2280	MH040027	--	--	--	--
151	J66/04	<i>M. bahaeldini</i>	Jordan	30.7622	36.6803	MH040028	--	--	MH040069	--
152	NHMC80.3.108.1	<i>M. bahaeldini</i>	Egypt	28.5408	33.9810	EF555285	--	--	--	--
153	NHMC80.3.108.2	<i>M. bahaeldini</i>	Egypt	28.5408	33.9810	EF555286	--	--	--	--
154	NHMC80.3.108.3	<i>M. bahaeldini</i>	Egypt	28.5408	33.9810	EF555287	--	--	--	--
155	NHMC80.3.108.4	<i>M. bahaeldini</i>	Egypt	28.5408	33.9810	EF555288	--	--	--	--
156	NHMC80.3.108.5	<i>M. bahaeldini</i>	Egypt	28.7064	33.7480	EF555283	--	--	--	--
157	NHMC80.3.72.10	<i>M. bahaeldini</i>	Jordan	31.2531	35.6135	EF555293	--	--	--	--
158	NHMC80.3.72.100	<i>M. bahaeldini</i>	Jordan	31.5615	35.7827	KM411182	--	--	--	--
159	NHMC80.3.72.11	<i>M. bahaeldini</i>	Jordan	31.2531	35.6135	EF555294	--	--	--	--
160	NHMC80.3.72.111	<i>M. bahaeldini</i>	Jordan	30.3289	35.4426	KM411201	--	--	--	--
161	NHMC80.3.72.13	<i>M. bahaeldini</i>	Jordan	30.7022	35.5841	EF555295	--	--	--	--
162	NHMC80.3.72.14	<i>M. bahaeldini</i>	Jordan	31.9116	36.6168	EF555317	--	--	--	--
163	NHMC80.3.72.15	<i>M. bahaeldini</i>	Jordan	31.9116	36.6168	EF555318	--	--	--	--
164	NHMC80.3.72.16	<i>M. bahaeldini</i>	Jordan	31.9116	36.6168	EF555319	--	--	--	--
165	NHMC80.3.72.17	<i>M. bahaeldini</i>	Jordan	31.9116	36.6168	EF555320	--	--	--	--
166	NHMC80.3.72.20	<i>M. bahaeldini</i>	Jordan	31.2531	35.6135	EF555292	--	--	--	--
167	NHMC80.3.72.22	<i>M. bahaeldini</i>	Egypt	29.9651	33.1606	EF555284	--	--	--	--
168	NHMC80.3.72.24	<i>M. bahaeldini</i>	Jordan	29.5704	35.4113	EF555321	--	--	--	--
169	NHMC80.3.72.47	<i>M. bahaeldini</i>	Jordan	31.2149	35.9653	KM411174	--	--	--	--
170	NHMC80.3.72.48	<i>M. bahaeldini</i>	Jordan	31.2149	35.9653	KM411175	--	--	--	--
171	NHMC80.3.72.49	<i>M. bahaeldini</i>	Jordan	31.5989	35.9934	KM411176	--	--	--	--
172	NHMC80.3.72.50	<i>M. bahaeldini</i>	Jordan	31.8773	35.6834	KM411177	MZ223842	--	--	--
173	NHMC80.3.72.88	<i>M. bahaeldini</i>	Israel	30.6242	34.8233	KM411100	--	--	--	--
174	NHMC80.3.72.93	<i>M. bahaeldini</i>	Israel	30.7077	34.7845	KM411093	--	--	--	--
175	NHMC80.3.72.94	<i>M. bahaeldini</i>	Israel	30.7077	34.7845	KM411094	--	--	--	--
176	NHMC80.3.72.95	<i>M. bahaeldini</i>	Israel	31.0648	34.8406	KM411095	--	--	--	--

Nº	Sample code	Species	Country	Latitude	Longitude	Cyt-b	B-fib7	OD	MC1R	PgD7
177	NHMC80.3.72.96	<i>M. bahaeldini</i>	Israel	31.0648	34.8406	KM411096	--	--	--	--
178	NHMC80.3.72.98	<i>M. bahaeldini</i>	Jordan	29.6864	35.4260	KM411180	--	--	--	--
179	NHMC80.3.72.99	<i>M. bahaeldini</i>	Jordan	29.6470	35.4340	KM411181	--	--	--	--
180	S10345	<i>M. bahaeldini</i>	S. Arabia	27.3243	41.4300	MH040029	--	--	MH040070	--
181	S2496	<i>M. bahaeldini</i>	Egypt	28.5528	33.9492	MH040030	--	--	MH040071	--
182	S2835	<i>M. bahaeldini</i>	Egypt	28.7946	33.7321	MH040031	--	--	MH040072	--
183	S3746	<i>M. bahaeldini</i>	Jordan	30.1680	35.6730	MH040032	--	--	--	--
184	TAU.R16256	<i>M. bahaeldini</i>	Israel	31.1900	34.8050	KY967145	--	--	KY967100	--
185	TAU.R16263	<i>M. bahaeldini</i>	Israel	31.2560	35.1710	MH040033	--	--	MH040073	--
186	TAU.R16293	<i>M. bahaeldini</i>	Israel	30.8630	34.4420	MH040034	--	--	MH040074	--
187	TAU.R16294	<i>M. bahaeldini</i>	Israel	30.8500	34.4510	MH040035	--	--	MH040075	--
188	NHMC80.3.143.1	<i>M. balfouri</i>	Yemen	12.6500	54.0333	KM411213	--	--	--	--
189	NHMC80.3.143.2	<i>M. balfouri</i>	Yemen	12.6500	54.0333	KM411214	--	--	--	--
190	NHMC80.3.143.3	<i>M. balfouri</i>	Yemen	12.6500	54.0333	KM411215	--	--	--	--
191	NHMC80.3.143.4	<i>M. balfouri</i>	Yemen	12.6500	54.0333	KM411216	--	--	--	--
192	S2500	<i>M. balfouri</i>	Yemen	12.1224	53.2748	MH040036	--	--	MH040076	--
193	S5187	<i>M. balfouri</i>	Yemen	12.5460	54.4974	MK551681	--	--	MK551604	--
194	S5292	<i>M. balfouri</i>	Yemen	12.1224	53.2748	MK551680	--	--	MK551603	--
195	S5650	<i>M. balfouri</i>	Yemen	12.3635	53.9329	KY967146	--	--	KY967101	--
196	I01	<i>M. bernoullii</i>	Iran	34.3893	45.4705	KY967154	--	--	KY967112	--
197	I02	<i>M. bernoullii</i>	Iran	34.3893	45.4705	KY967155	--	--	KY967113	--
198	IRA600	<i>M. bernoullii</i>	Iran	32.0333	48.5000	KY967156	--	--	--	--
199	MB_Azraq	<i>M. bernoullii</i>	Jordan	31.8333	36.8167	KY967157	--	--	--	--
200	MB_Azraq2	<i>M. bernoullii</i>	Jordan	31.8333	36.8167	KY967158	--	--	--	--
201	MB03	<i>M. bernoullii</i>	Jordan	31.8333	36.8167	KY967159	--	--	--	--
202	MB04	<i>M. bernoullii</i>	Jordan	30.9233	36.5690	KY967159	--	--	--	--
203	MB05	<i>M. bernoullii</i>	Jordan	32.4582	38.0368	KY967160	--	--	--	--
204	MB07	<i>M. bernoullii</i>	Syria	34.6280	38.5609	KY967162	--	--	--	--
205	MB08	<i>M. bernoullii</i>	Syria	34.6280	38.5609	KY967161	--	--	--	--

N°	Sample code	Species	Country	Latitude	Longitude	Cyt-b	B-fib7	OD	MC1R	PgD7
206	MB09	<i>M. bernoullii</i>	Syria	32.7221	36.9376	KY967165	--	--	--	--
207	MB10	<i>M. bernoullii</i>	Syria	32.7221	36.9376	KY967166	--	--	--	--
208	MB11	<i>M. bernoullii</i>	Syria	34.3111	36.9072	KY967167	--	--	--	--
209	MB14	<i>M. bernoullii</i>	Syria	34.2667	37.0667	KY967163	--	--	--	--
210	MB15	<i>M. bernoullii</i>	Syria	34.2667	37.0667	KY967168	--	--	--	--
211	MB16	<i>M. bernoullii</i>	Jordan	31.9667	35.9667	KY967169	--	--	--	--
212	MB17	<i>M. bernoullii</i>	Jordan	31.9667	35.9667	KY967170	--	--	--	--
213	NHMC80.3.69.1	<i>M. bernoullii</i>	Syria	34.3619	38.1740	EF555302	--	--	--	--
214	NHMC80.3.69.10	<i>M. bernoullii</i>	Syria	35.4268	40.0278	EF555307	--	--	--	--
215	NHMC80.3.69.11	<i>M. bernoullii</i>	Syria	35.4268	40.0278	EF555308	--	--	--	--
216	NHMC80.3.69.14	<i>M. bernoullii</i>	S. Arabia	26.4185	47.4792	KM411190	--	--	--	--
217	NHMC80.3.69.15	<i>M. bernoullii</i>	S. Arabia	26.4147	47.4773	KM411191	--	--	--	--
218	NHMC80.3.69.2	<i>M. bernoullii</i>	Syria	34.6000	37.8315	EF555303	--	--	--	--
219	NHMC80.3.69.21	<i>M. bernoullii</i>	Kuwait	29.3678	47.8102	KM411234	--	--	--	--
220	NHMC80.3.69.22	<i>M. bernoullii</i>	Kuwait	29.0144	47.9773	KM411235	--	--	--	--
221	NHMC80.3.69.23	<i>M. bernoullii</i>	Kuwait	29.8433	48.1131	KM411236	--	--	--	--
222	NHMC80.3.69.24	<i>M. bernoullii</i>	Kuwait	29.3794	47.8422	KM411237	--	--	--	--
223	NHMC80.3.69.25	<i>M. bernoullii</i>	Kuwait	29.8236	47.2502	KM411183	--	--	--	--
224	NHMC80.3.69.3	<i>M. bernoullii</i>	Syria	34.6000	37.8315	EF555304	--	--	--	--
225	NHMC80.3.69.30	<i>M. bernoullii</i>	Syria	33.6831	36.4953	KM411142	--	--	--	--
226	NHMC80.3.69.6	<i>M. bernoullii</i>	Syria	34.8142	38.7897	EF555305	--	--	--	--
227	S15	<i>M. bernoullii</i>	Syria	34.5247	38.2856	KY967172	--	--	KY967114	--
228	S4	<i>M. bernoullii</i>	Syria	34.3111	36.9072	KY967160	--	--	KY967115	--
229	S5	<i>M. bernoullii</i>	Syria	34.3111	36.9072	KY967173	--	--	KY967115	--
230	S7	<i>M. bernoullii</i>	Syria	34.3111	36.9072	KY967174	--	--	KY967111	--
231	S8	<i>M. bernoullii</i>	Syria	34.3111	36.9072	KY967175	--	--	KY967115	--
232	S9	<i>M. bernoullii</i>	Syria	34.3111	36.9072	KY967164	--	--	KY967110	--
233	Sherif10708	<i>M. bernoullii</i>	Egypt	27.7472	34.2287	KY967171	--	--	--	--
234	BEV.10070	<i>M. brevirostris</i>	Kuwait	28.5844	18.1673	MZ223697	MZ223837	MZ223558	MZ223548	MZ223625

N°	Sample code	Species	Country	Latitude	Longitude	Cyt-b	B-fib7	OD	MC1R	PgD7
235	BEV.10082	<i>M. brevirostris</i>	Kuwait	29.5559	47.7410	MZ223698	MZ223838	--	--	--
236	SPM001455U	<i>M. brevirostris</i>	UAE	24.1719	52.6109	KY967153	--	--	KY967109	--
237	SPM002959(97)	<i>M. brevirostris</i>	Bahrain			KY967152	--	--	KY967108	--
238	BEV.14801	<i>M. guttulata</i>	Mauritania	24.4623	-11.3515	MZ223781	--	MZ223569	MZ223486	MZ223672
239	CIBIO13703	<i>M. guttulata</i>	Mauritania	25.1565	-11.5348	--	MZ223782	MZ223608	MZ223487	--
240	CIBIO15664	<i>M. guttulata</i>	Algeria	30.9237	-2.0314	--	MZ223784	MZ223578	--	MZ223673
241	NHMC80.3.72.1	<i>M. guttulata</i>	Tunisia	33.5225	9.9925	EF555310	--	--	--	--
242	NHMC80.3.72.18	<i>M. guttulata</i>	Morocco	31.0882	-6.4673	EF555299	KM411268	--	--	--
243	NHMC80.3.72.2	<i>M. guttulata</i>	Tunisia	33.5225	9.9925	EF555311	--	--	--	--
244	NHMC80.3.72.21	<i>M. guttulata</i>	Morocco	31.7146	-4.9221	EF555300	--	--	--	--
245	NHMC80.3.72.25	<i>M. guttulata</i>	Libya	32.1245	12.8076	KM411130	--	--	--	--
246	NHMC80.3.72.26	<i>M. guttulata</i>	Libya	32.1247	12.8068	KM411129	--	--	--	--
247	NHMC80.3.72.28	<i>M. guttulata</i>	Libya	31.9756	12.6724	KM411131	--	--	--	--
248	NHMC80.3.72.31	<i>M. guttulata</i>	Libya	32.0601	12.7227	KM411133	--	--	--	--
249	NHMC80.3.72.35	<i>M. guttulata</i>	Libya	32.1245	12.8076	KM411135	--	--	--	--
250	NHMC80.3.72.44	<i>M. guttulata</i>	Algeria	25.3483	8.3791	KM411165	--	--	--	--
251	NHMC80.3.72.45	<i>M. guttulata</i>	Algeria	34.4176	3.4798	KM411167	--	--	--	--
252	NHMC80.3.72.46	<i>M. guttulata</i>	Algeria	25.3500	8.3911	KM411173	--	--	--	--
253	NHMC80.3.72.5	<i>M. guttulata</i>	Morocco	32.0472	-4.4088	EF555297	--	--	--	--
254	NHMC80.3.72.51	<i>M. guttulata</i>	Morocco	32.5860	-3.7605	KM411178	KM411275	--	--	--
255	NHMC80.3.72.53	<i>M. guttulata</i>	Morocco	29.3698	-8.1993	KM411210	--	--	--	--
256	NHMC80.3.72.54	<i>M. guttulata</i>	Morocco	30.3918	-6.8817	KM411211	--	--	--	--
257	NHMC80.3.72.55	<i>M. guttulata</i>	Morocco	29.4523	-8.0597	KM411212	--	--	--	--
258	NHMC80.3.72.57	<i>M. guttulata</i>	Libya	28.4433	12.7800	KM411222	--	--	--	--
259	NHMC80.3.72.7	<i>M. guttulata</i>	Tunisia	33.1502	10.2899	EF555312	--	--	--	--
260	NHMC80.3.72.8	<i>M. guttulata</i>	Libya	30.4659	24.5366	EF555296	--	--	--	--
261	NHMC80.3.72.82	<i>M. guttulata</i>	Morocco	33.2894	-3.8437	KM411092	--	--	--	--
262	NHMC80.3.72.83	<i>M. guttulata</i>	Morocco	33.2894	-3.8437	KM411088	--	--	--	--
263	NHMC80.3.72.84	<i>M. guttulata</i>	Morocco	32.1193	-1.5799	KM411089	MZ223786	--	--	--

N°	Sample code	Species	Country	Latitude	Longitude	Cyt-b	B-fib7	OD	MC1R	PgD7
264	NHMC80.3.72.85	<i>M. guttulata</i>	Morocco	32.1193	-1.5799	KM411090	--	--	--	--
265	NHMC80.3.72.87	<i>M. guttulata</i>	Algeria	34.6805	3.2499	KM411099	--	--	--	--
266	NHMC80.3.72.89	<i>M. guttulata</i>	Algeria	24.4441	9.4138	KM411101	MZ223843	--	--	--
267	NHMC80.3.72.9	<i>M. guttulata</i>	Morocco	31.4018	-5.7276	EF555298	--	--	--	--
268	NHMC80.3.72.90	<i>M. guttulata</i>	Algeria	25.5012	8.9996	KM411102	--	--	--	--
269	NHMC80.3.72.91	<i>M. guttulata</i>	Algeria	23.3130	9.4302	KM411103	--	--	--	--
270	NHMC80.3.72.92	<i>M. guttulata</i>	Egypt	23.1141	35.5882	KM411091	--	--	--	--
271	NHMC80.3.72.97	<i>M. guttulata</i>	Morocco	30.0780	-6.2365	KM411097	--	--	--	--
272	S3612	<i>M. guttulata</i>	Libya	30.3132	10.4496	MH040037	--	--	MH040077	--
273	S3907	<i>M. guttulata</i>	Libya	30.3131	10.4495	MH040038	--	--	--	--
274	SPM001477U	<i>M. guttulata</i>	Morocco			MH040039	--	--	MH040078	--
275	SPM002367(7)	<i>M. guttulata</i>	Egypt	22.1831	36.6657	MH040040	--	--	MH040079	--
276	SPM002368(93)	<i>M. guttulata</i>	Egypt	22.1831	36.6657	MH040041	--	--	MH040080	--
277	SPM002382(8)	<i>M. guttulata</i>	Egypt	30.8320	29.2037	MH040042	--	--	MH040081	--
278	SPM003430	<i>M. guttulata</i>	Morocco	27.1400	-13.1800	MH040043	--	--	MH040082	--
279	SUD12/2010-68	<i>M. guttulata</i>	Sudan	21.0720	30.6938	MH040044	--	--	MH040083	--
280	NHMC80.3.165.1	<i>M. kuri</i>	Yemen	12.1867	52.1528	KM411207	--	--	--	--
281	NHMC80.3.165.2	<i>M. kuri</i>	Yemen	12.1867	52.1528	KM411208	--	--	--	--
282	NHMC80.3.165.3	<i>M. kuri</i>	Yemen	12.1867	52.1528	KM411209	--	--	--	--
283	S5169	<i>M. kuri</i>	Yemen	12.1996	52.2658	MK551682	--	--	MK551605	--
284	S5368	<i>M. kuri</i>	Yemen	12.1996	52.2658	KY967147	--	--	KY967102	--
285	NHMC80.3.166.1	<i>M. martini</i>	Egypt	24.9629	34.9357	KM411104	MZ223820	--	MK551653	MZ223676
286	NHMC80.3.166.2	<i>M. martini</i>	Egypt	24.4929	35.1594	KM411105	MZ223821	--	MH040084	MZ223677
287	NHMC80.3.166.3	<i>M. martini</i>	Eritrea	15.8009	40.1271	KM411204	--	--	--	--
288	BEV.10918	<i>M. microlepis</i>	Jordan	31.5989	35.9934	MZ223700	MZ223839	--	MZ223549	--
289	BEV.12365	<i>M. microlepis</i>	Lebanon	34.3164	36.4136	MZ223701	MZ223841	--	MZ223550	MZ223678
290	L32	<i>M. microlepis</i>	Lebanon	34.3656	36.4026	KY967149	--	--	KY967105	--
291	L33	<i>M. microlepis</i>	Lebanon	34.3656	36.4026	KY967150	--	--	KY967106	--
292	L34	<i>M. microlepis</i>	Lebanon	34.3656	36.4026	KY967150	--	--	KY967107	--

Nº	Sample code	Species	Country	Latitude	Longitude	Cyt-b	B-fib7	OD	MC1R	PgD7
293	MB12	<i>M. microlepis</i>	Syria	34.3111	36.9072	KY967151	--	--	--	--
294	MB13	<i>M. microlepis</i>	Syria	34.3111	36.9072	KY967151	--	--	--	--
295	NHMC80.3.69.12	<i>M. microlepis</i>	Syria	34.2931	36.7655	EF555309	--	--	--	--
296	NHMC80.3.69.9	<i>M. microlepis</i>	Syria	35.4174	40.3198	EF555306	--	--	--	--
297	CIBIO13743	<i>M. rubropunctata</i>	Mauritania	24.0811	-10.3958	MZ223777	MZ223840	--	MZ223485	MZ223674
298	CIBIO5265	<i>M. rubropunctata</i>	Mauritania	20.9758	-15.4156	MZ223778	--	--	MZ223552	MZ223675
299	NHMC80.3.99.1	<i>M. rubropunctata</i>	Egypt	24.4000	33.0170	EF555316	--	--	--	--
300	NHMC80.3.99.13	<i>M. rubropunctata</i>	Egypt	24.9294	30.3897	KM411122	--	--	--	--
301	NHMC80.3.99.17	<i>M. rubropunctata</i>	Algeria	24.3264	7.0058	KM411203	--	--	--	--
302	NHMC80.3.99.18	<i>M. rubropunctata</i>	Libya	25.9666	15.1574	KM411146	--	--	--	--
303	NHMC80.3.99.21	<i>M. rubropunctata</i>	Egypt	30.0457	31.2402	KM411147	--	--	--	--
304	NHMC80.3.99.25	<i>M. rubropunctata</i>	Mauritania	19.5518	-14.3706	KM411148	--	--	--	--
305	NHMC80.3.99.26	<i>M. rubropunctata</i>	Mauritania	19.5518	-14.3706	KM411149	--	--	--	--
306	NHMC80.3.99.27	<i>M. rubropunctata</i>	Mauritania	21.2985	-13.0674	KM411150	--	--	--	--
307	NHMC80.3.99.28	<i>M. rubropunctata</i>	Libya	25.9666	15.1574	KM411143	--	--	--	--
308	NHMC80.3.99.29	<i>M. rubropunctata</i>	Egypt	29.8734	32.6497	KM411200	--	--	--	--
309	RIM092	<i>M. rubropunctata</i>	Mauritania	21.4968	-11.6168	MK551703	--	--	MK551635	--
310	RIM093	<i>M. rubropunctata</i>	Mauritania	21.4968	-11.6168	MK551702	--	--	MK551634	--
311	SPM002355(45)	<i>M. rubropunctata</i>	Egypt	29.7095	30.3792	MK551701	--	--	MK551633	--
312	SUD12/2010-56	<i>M. rubropunctata</i>	Sudan	21.8008	31.3488	MK551699	--	--	MK551631	--
313	SUD12/2010-57	<i>M. rubropunctata</i>	Sudan	21.8008	31.3488	KY967148	--	--	KY967103	--
314	SUD12/2010-58	<i>M. rubropunctata</i>	Sudan	21.8008	31.3488	MK551700	--	--	MK551632	--
315	NHMC80.3.164.16	<i>M. saudiarabica</i>	S. Arabia	22.3952	41.7529	KM411151	--	--	--	--
316	NHMC80.3.164.5	<i>M. saudiarabica</i>	S. Arabia	22.4000	41.7333	KM411198	--	--	--	--
317	NHMC80.3.164.9	<i>M. saudiarabica</i>	S. Arabia	22.2525	41.8796	KM411206	--	--	--	--
318	NHMC80.3.69.17	<i>M. saudiarabica</i>	S. Arabia	23.5388	40.5893	KM411192	--	--	--	--
319	NHMC80.3.69.18	<i>M. saudiarabica</i>	S. Arabia	23.5038	41.3472	KM411193	--	--	--	--
320	NHMC80.3.69.19	<i>M. saudiarabica</i>	S. Arabia	24.2531	41.1539	KM411194	--	--	--	--
321	NHMC80.3.69.20	<i>M. saudiarabica</i>	S. Arabia	23.5114	41.4220	KM411195	--	--	--	--

Nº	Sample code	Species	Country	Latitude	Longitude	Cyt-b	B-fib7	OD	MC1R	PgD7
322	CN11193	<i>M. sp.</i>	S. Arabia	24.4441	46.6756	MK551725	--	--	MK551654	--
323	CN11194	<i>M. sp.</i>	S. Arabia	24.4441	46.6756	MK551732	--	--	MK551660	--
324	CN11195	<i>M. sp.</i>	S. Arabia	24.4441	46.6756	MK551726	--	--	MK551655	--
325	CN11200	<i>M. sp.</i>	S. Arabia	24.3236	46.3961	MK551731	--	--	--	--
326	J16/04	<i>M. sp.</i>	Jordan	32.1690	37.0078	MH040047	--	--	MH040087	--
327	NHMC80.3.72.36	<i>M. sp.</i>	S. Arabia	26.4278	47.3789	KM411184	--	--	--	--
328	NHMC80.3.72.37	<i>M. sp.</i>	S. Arabia	26.4066	47.7070	KM411185	--	--	--	--
329	NHMC80.3.72.38	<i>M. sp.</i>	S. Arabia	26.4153	47.4736	KM411186	--	--	--	--
330	NHMC80.3.72.39	<i>M. sp.</i>	S. Arabia	23.2786	46.3534	KM411187	--	--	--	--
331	NHMC80.3.72.40	<i>M. sp.</i>	S. Arabia	23.1930	46.4223	KM411188	--	--	--	--
332	NHMC80.3.72.41	<i>M. sp.</i>	S. Arabia	23.2417	46.4537	KM411189	--	--	--	--
333	NHMC80.3.72.52	<i>M. sp.</i>	Jordan	31.8817	36.9133	KM411179	--	--	MH040088	--
334	NHMC80.3.72.59	<i>M. sp.</i>	Kuwait	29.4624	47.6407	KM411238	--	--	MH040089	--
335	S10332	<i>M. spp.</i>	S. Arabia	25.2681	46.6237	MH040048	--	--	MH040090	--
336	IR001	<i>M. watsonana</i>	Iran	35.1109	50.8977	MK551694	--	--	MK551626	--
337	IR006	<i>M. watsonana</i>	Iran	30.2702	57.1231	MK551696	--	--	MK551628	--
338	IR013	<i>M. watsonana</i>	Iran	30.0243	57.2848	MK551697	--	--	MK551629	--
339	KUSH12	<i>M. watsonana</i>	Iran	35.1109	50.8977	MK551695	--	--	MK551627	--
340	NHMC80.3.144.1	<i>M. watsonana</i>	Iran	35.6962	51.4229	KM411217	--	--	--	--
341	NHMC80.3.144.15	<i>M. watsonana</i>	Iran	26.1592	60.1861	KM411153	--	--	--	--
342	NHMC80.3.144.16	<i>M. watsonana</i>	Iran	26.1592	60.1861	KM411154	--	--	--	--
343	NHMC80.3.144.17	<i>M. watsonana</i>	Afghanistan	34.5833	68.9500	KM411219	--	--	--	--
344	NHMC80.3.144.18	<i>M. watsonana</i>	Pakistan	26.4948	66.6677	KM411221	--	--	--	--
345	NHMC80.3.144.19	<i>M. watsonana</i>	Pakistan	26.4948	66.6677	KM411220	--	--	--	--
346	NHMC80.3.144.2	<i>M. watsonana</i>	Iran	32.5777	59.7978	KM411218	--	--	--	--
347	NHMC80.3.144.4	<i>M. watsonana</i>	Iran	32.3830	48.3982	KM411126	--	--	--	--
348	NHMC80.3.144.5	<i>M. watsonana</i>	Iran	31.6516	49.2775	KM411127	--	--	--	--
349	NHMC80.3.144.6	<i>M. watsonana</i>	Iran	31.6516	49.2775	KM411128	--	--	--	--
350	NHMC80.3.144.7	<i>M. watsonana</i>	Iran	32.3081	52.0158	KM411152	--	--	--	--

N°	Sample code	Species	Country	Latitude	Longitude	Cyt-b	B-fib7	OD	MC1R	PgD7
351	NHMC80.3.144.8	<i>M. watsonana</i>	Iran	34.4164	50.8608	KM411155	--	--	--	--
352	NHMC80.3.144.9	<i>M. watsonana</i>	Iran	31.1956	59.3201	KM411156	--	--	--	--
353	TAB11	<i>M. watsonana</i>	Iran	33.5993	56.9123	MK551698	--	--	MK551630	--
354	VAZ10	<i>M. watsonana</i>	Iran	28.9974	54.7813	MH040049	--	--	MH040091	--
		<i>Acanthodactylus erythrurus</i>				--	--	--	--	--
		<i>Gallotia atlantica</i>				AY151836	KX080696	--	KX080779	--
		<i>Psammodromus algirus</i>				AY151835	KX080700	--	KX080785	--
		<i>Podarcis lilfordi</i>				AF052639	--	--	JX126668	--
		<i>Podarcis pityusensis</i>				AF052640	--	--	JX126689	--

Table S2. Information on all datasets used in the phylogenetic, calibration, and network reconstruction analyses, including partitions, models, and parameters.

Dataset	Data	Analysis	Partition	Model	Clock Model	Tree model	Run Specification
1	mtDNA (378 sequences)	Bayesian Inference [BEAST]	<i>Cyt-b</i>	HKY+G+I	Relaxed Uncorrelated Lognormal	Speciation: Yule Process	3 runs; 100000000 generations; 10000 sampling frequency; 10% burn-in
2	nDNA (outgroups included)	Bayesian Inference [BEAST]	<i>B-fib7</i>	HKY+G	Relaxed Uncorrelated Lognormal	Speciation: Yule Process	3 runs; 100000000 generations; 10000 sampling frequency; 10% burn-in
			<i>MC1R</i>	HKY+I	Relaxed Uncorrelated Lognormal		
			<i>OD</i>	HKY	Relaxed Uncorrelated Lognormal		
			<i>PgD7</i>	K80+G	Relaxed Uncorrelated Lognormal		
3	Concatenated cytonuclear (Datasets 2+3) [BEAST]	Divergence time estimation	<i>B-fib7</i>	HKY+G	Relaxed Uncorrelated Lognormal	Speciation Yule Process	3 runs; 100000000 generations; 10000 sampling frequency; 10% burn-in
			<i>Cyt-b</i>	HKY+G+I	Relaxed Uncorrelated Lognormal		
			<i>MC1R</i>	HKY+I	Relaxed Uncorrelated Lognormal		
			<i>OD</i>	HKY	Relaxed Uncorrelated Lognormal		
			<i>PgD7</i>	K80+G	Relaxed Uncorrelated Lognormal		

Table S3. Material examined for biometric comparisons and original measurements for each specimen. Codes of morphological characters are given in section Material and Methods. M = Male; F = Female. Sample locations are given in Table S2.

Code	Species	Sex	SVL	HL	HW	HH	TE	RN	PS
BEV.10457	<i>M. adrarensis</i> sp. nov.	F	53.04	11.45	6.65	3.86	1	2	3
BEV.14800	<i>M. adrarensis</i> sp. nov.	F	44.01	9.99	6.42	4.26	1	1	3
BEV.15060	<i>M. adrarensis</i> sp. nov.	M	33.23	8.44	4.92	3.16	2	2	3
BEV.15061	<i>M. adrarensis</i> sp. nov.	F	40.80	9.38	5.57	3.79	1	2	3
BEV.15062	<i>M. adrarensis</i> sp. nov.	M	33.15	8.49	5.38	3.24	3	2	3
BEV.15063	<i>M. adrarensis</i> sp. nov.	M	38.05	9.78	6.13	3.62	3	1	3
BEV.15064	<i>M. adrarensis</i> sp. nov.	M	33.53	8.72	5.06	3.09	2	1	3
BEV.15163	<i>M. adrarensis</i> sp. nov.	F	42	9.00	6	3	2	1	3
BEV.10013	<i>M. olivieri</i>	M	40.78	10.28	5.51	4.25	3	1	2
BEV.11948	<i>M. olivieri</i>	F	44.64	9.43	6.36	4.35	1	1	2
BEV.12808	<i>M. olivieri</i>	F	47.25	10.51	6.83	5.08	1	2	1
BEV.13621	<i>M. olivieri</i>	M	49.59	12.17	8.40	5.27	2	1	2
BEV.14833	<i>M. olivieri</i>	M	44.95	10.45	6.49	4.13	2	1	2
BEV.5925	<i>M. olivieri</i>	F	41.00	10.21	6.33	3.75	1	1	1
BEV.5861	<i>M. olivieri</i>	F	46.68	9.55	6.40	4.53	1	1	1
BEV.5864	<i>M. olivieri</i>	F	38.52	8.61	5.30	3.59	1	1	1
BEV.5867	<i>M. olivieri</i>	F	40.17	8.67	5.33	3.66	1	1	1
BEV.5870	<i>M. olivieri</i>	M	41.53	10.17	6.62	4.26	3	2	2
BEV.5871	<i>M. olivieri</i>	F	42.98	9.64	5.80	4.17	1	1	2
BEV.5875	<i>M. olivieri</i>	F	42.66	9.60	6.24	4.45	1	1	2
BEV.5876	<i>M. olivieri</i>	M	44.03	10.60	6.96	5.19	2	1	1
BEV.5877	<i>M. olivieri</i>	F	44.63	8.73	5.41	4.13	1	2	1
BEV.5879	<i>M. olivieri</i>	M	45.91	11.20	6.77	5.01	3	1	1
BEV.5880	<i>M. olivieri</i>	F	47.22	9.90	6.28	4.48	1	2	1
BEV.5881	<i>M. olivieri</i>	M	42.31	10.30	6.90	4.61	3	2	1
BEV.5882	<i>M. olivieri</i>	F	42.37	9.31	5.95	4.42	1	1	1
BEV.5888	<i>M. olivieri</i>	F	36.43	9.05	6.14	3.89	2	1	2
BEV.5889	<i>M. olivieri</i>	M	43.41	10.90	7.26	4.99	2	1	1
BEV.5890	<i>M. olivieri</i>	M	41.30	10.46	6.02	3.65	3	1	3
BEV.5899	<i>M. olivieri</i>	F	39.38	9.76	5.96	4.50	2	1	2
BEV.5956	<i>M. olivieri</i>	M	37.35	9.22	5.39	3.57	2	1	3
BEV.5959	<i>M. olivieri</i>	M	36.09	9.24	5.59	3.99	2	1	2
BEV.8830	<i>M. olivieri</i>	M	43.28	10.65	7.27	5.36	3	1	1
BEV.8796	<i>M. olivieri</i>	M	45.32	11.87	7.31	5.49	3	1	3
BEV.8797	<i>M. olivieri</i>	M	44.57	11.68	7.26	5.24	3	1	2
BEV.8798	<i>M. olivieri</i>	M	44.78	11.06	7.66	5.60	3	1	1
BEV.8829	<i>M. olivieri</i>	M	44.77	11.04	7.00	5.09	3	1	3

Code	Species	Sex	SVL	HL	HW	HH	TE	RN	PS
BEV.8975	<i>M. olivieri</i>	F	43.03	9.52	6.18	4.33	2	2	1
BEV.9225	<i>M. olivieri</i>	M	42.39	10.23	7.09	5.35	3	1	1
BEV.10453	<i>M. simoni saharae ssp. nov.</i>	M	35.74	8.27	4.86	3.17	2	1	3
BEV.10849	<i>M. simoni saharae ssp. nov.</i>	M	38.07	9.24	5.56	4.39	3	2	3
BEV.10850	<i>M. simoni saharae ssp. nov.</i>	F	42.46	8.47	5.28	3.60	2	1	1
BEV.9114	<i>M. simoni saharae ssp. nov.</i>	M	40.70	9.62	5.90	4.20	2	1	2
BEV.11187	<i>M. simoni</i> ssp.	M	42.49	10.41	6.90	4.65	3	2	1
BEV.11586	<i>M. simoni</i> ssp.	M	44.74	11.08	7.44	4.95	2	1	2
BEV.11587	<i>M. simoni</i> ssp.	F	45.71	9.17	6.38	4.02	2	1	2
BEV.11588	<i>M. simoni</i> ssp.	F	46.10	9.69	6.27	4.43	1	1	2
BEV.11589	<i>M. simoni</i> ssp.	M	46.56	11.32	7.33	5.00	3	1	2
BEV.11590	<i>M. simoni</i> ssp.	M	45.23	10.45	7.11	4.70	3	1	3
BEV.11591	<i>M. simoni</i> ssp.	F	45.92	9.71	6.49	4.60	1	1	2
BEV.11594	<i>M. simoni</i> ssp.	F	47.88	10.06	6.26	3.99	1	1	2
BEV.14869	<i>M. simoni</i> ssp.	F	41.77	8.77	5.62	3.76	1	1	1
BEV.5922	<i>M. simoni</i> ssp.	M	50.79	11.08	7.00	5.43	3	1	1
BEV.5923	<i>M. simoni</i> ssp.	F	50.69	9.74	6.33	4.41	2	2	2
BEV.5924	<i>M. simoni</i> ssp.	F	48.25	10.30	6.67	4.50	1	1	2
BEV.8508	<i>M. simoni</i> ssp.	M	43.14	9.72	6.42	4.89	3	1	1
BEV.8509	<i>M. simoni</i> ssp.	F	45.75	9.45	6.26	4.36	1	2	1
BEV.9429	<i>M. simoni</i> ssp.	M	42.15	10.21	6.75	4.39	3	1	1
BEV.9430	<i>M. simoni</i> ssp.	M	43.89	10.29	6.83	4.68	3	1	2
BEV.9431	<i>M. simoni</i> ssp.	M	43.74	10.39	7.14	4.64	3	2	1
BEV.9432	<i>M. simoni</i> ssp.	M	43.34	10.71	6.61	4.52	3	1	1
BEV.10179	<i>M. pastouri</i>	M	48.32	11.83	7.44	5.63	2	1	2
BEV.10454	<i>M. pastouri</i>	M	45.41	11.04	5.98	4.10	2	1	3
BEV.10455	<i>M. pastouri</i>	M	42.17	10.42	5.57	3.90	3	1	3
BEV.14803	<i>M. pastouri</i>	M	48.31	12.01	7.74	5.44	3	2	3
BEV.14804	<i>M. pastouri</i>	F	40.38	8.94	5.59	4.16	2	1	3
BEV.14805	<i>M. pastouri</i>	M	40.61	9.95	6.44	4.05	3	1	3
BEV.5926	<i>M. pastouri</i>	M	43.75	11.17	6.27	4.07	2	1	2
BEV.5927	<i>M. pastouri</i>	F	41.81	10.09	5.56	4.25	1	1	2
BEV.9177	<i>M. pastouri</i>	M	44.70	11.23	7.50	4.64	1	1	2
BEV.9380	<i>M. pastouri</i>	F	27.77	7.19	4.54	2.99	2	1	3

Table S4. Material examined for pholidotic characters comparisons for each specimen. Codes of morphological characters are given in section Material and Methods. M = Male; F = Female.

Code	Species	Sex	V	D	DS	TR	SL(Sx)	SL(Dx)	IL(Sx)	IL(Dx)	G	Col	EL	NTS	Pf(Sx)	Pf(Dx)	Lam
BEV.10457	<i>M. adrarensis</i> sp. nov.	F	34	44	4	15	4	4	7	7	28	11	5	12	14	15	22
BEV.14800	<i>M. adrarensis</i> sp. nov.	F	32	44	3	12	4	4	7	7	24	7	5	12	14	13	20
BEV.15060	<i>M. adrarensis</i> sp. nov.	M	31	45	4	14	4	4	7	8	25	11	5	11	12	13	23
BEV.15061	<i>M. adrarensis</i> sp. nov.	F	33	52	4	14	4	4	7	8	24	10	5	11	12	14	20
BEV.15062	<i>M. adrarensis</i> sp. nov.	M	33	52	4	16	4	4	9	7	29	11	5	12	13	13	23
BEV.15063	<i>M. adrarensis</i> sp. nov.	M	30	56	4	17	4	4	7	7	29	11	5	12	17	17	23
BEV.15064	<i>M. adrarensis</i> sp. nov.	M	31	49	4	16	4	4	9	9	32	11	5	12	15	16	18
BEV.15163	<i>M. adrarensis</i> sp. nov.	F	34	48	4	15	4	4	9	8	27	11	5	10	17	15	24
BEV.10013	<i>M. olivieri</i>	M	29	44	4	15	4	4	8	8	24	7	8	9	13	14	18
BEV.11948	<i>M. olivieri</i>	F	32	50	2	19	4	4	9	8	25	11	12	10	13	13	22
BEV.12808	<i>M. olivieri</i>	F	30	46	4	17	5	4	8	7	27	8	6	10	12	12	18
BEV.13621	<i>M. olivieri</i>	M	30	64	3	16	4	4	8	9	26	9	5	9	15	16	22
BEV.14833	<i>M. olivieri</i>	M	32	44	3	17	4	4	7	8	29	12	3	10	11	12	22
BEV.5925	<i>M. olivieri</i>	F	31	46	0	14	4	4	8	8	25	12	5	10	13	12	21
BEV.5861	<i>M. olivieri</i>	F	31	43	3	17	4	4	8	8	25	9	5	9	13	14	19
BEV.5864	<i>M. olivieri</i>	F	32	43	2	12	4	4	8	7	23	9	5	8	10	10	18
BEV.5867	<i>M. olivieri</i>	F	29	41	3	17	4	5	7	8	26	9	5	8	11	10	21
BEV.5870	<i>M. olivieri</i>	M	30	45	4	16	4	4	7	6	23	11	6	11	15	13	21
BEV.5871	<i>M. olivieri</i>	F	35	48	3	16	3	4	8	9	26	8	8	10	13	13	19
BEV.5875	<i>M. olivieri</i>	F	32	42	3	14	5	5	7	8	25	9	7	10	12	10	16
BEV.5876	<i>M. olivieri</i>	M	32	44	2	16	4	4	8	8	25	12	5	9	12	12	21
BEV.5877	<i>M. olivieri</i>	F	32	40	2	16	4	5	8	8	24	11	5	11	13	12	19
BEV.5879	<i>M. olivieri</i>	M	31	40	3	16	4	4	8	9	24	9	5	10	12	13	19
BEV.5880	<i>M. olivieri</i>	F	33	46	3	15	4	4	8	7	21	9	8	9	11	10	18
BEV.5881	<i>M. olivieri</i>	M	30	47	2	18	4	4	7	8	20	9	5	10	12	11	17
BEV.5882	<i>M. olivieri</i>	F	32	42	4	16	4	4	8	8	22	8	9	10	10	12	16

Code	Species	Sex	V	D	DS	TR	SL(Sx)	SL(Dx)	IL(Sx)	IL(Dx)	G	Col	EL	NTS	Pf(Sx)	Pf(Dx)	Lam
BEV.5888	<i>M. olivieri</i>	F	27	45	4	17	4	5	9	7	26	8	8	12	12	12	18
BEV.5889	<i>M. olivieri</i>	M	30	52	1	18	4	4	9	9	28	9	3	10	13	16	21
BEV.5890	<i>M. olivieri</i>	M	33	46	2	19	4	4	7	9	31	7	7	10	16	15	29
BEV.5899	<i>M. olivieri</i>	F	33	46	2	16	4	4	8	8	22	11	7	11	12	11	19
BEV.5956	<i>M. olivieri</i>	M	30	41	3	17	5	5	9	8	30	9	7	11	14	13	21
BEV.5959	<i>M. olivieri</i>	M	30	40	4	17	4	4	7	6	29	10	5	10	11	12	21
BEV.8830	<i>M. olivieri</i>	M	30	48	1	16	5	5	8	8	28	8	6	10	14	13	26
BEV.8796	<i>M. olivieri</i>	M	30	57	1	16	6	5	9	8	27	10	6	11	13	14	24
BEV.8797	<i>M. olivieri</i>	M	30	42	2	20	5	5	9	10	26	14	9	11	13	13	25
BEV.8798	<i>M. olivieri</i>	M	30	48	2	17	4	4	9	8	20	8	6	10	16	16	25
BEV.8829	<i>M. olivieri</i>	M	28	42	2	16	5	6	8	7	23	12	10	10	11	12	22
BEV.8975	<i>M. olivieri</i>	F	30	45	2	17	4	5	8	9	23	9	6	8	12	12	21
BEV.9225	<i>M. olivieri</i>	M	27	40	4	15	4	4	9	8	24	7	6	10	11	12	21
BEV.10453	<i>M. simoni saharae</i> ssp. nov.	M	30	39	2	15	5	4	8	7	26	8	5	8	12	11	22
BEV.10849	<i>M. simoni saharae</i> ssp. nov.	M	34	42	1	15	4	4	9	8	24	8	8	9	12	12	22
BEV.10850	<i>M. simoni saharae</i> ssp. nov.	F	34	42	1	15	4	4	8	7	26	8	8	10	12	12	21
BEV.9114	<i>M. simoni saharae</i> ssp. nov.	M	28	34	4	15	4	5	7	9	25	6	5	8	10	13	24
BEV.11187	<i>M. simoni</i> ssp.	M	30	47	2	15	4	4	8	8	22	10	9	9	12	12	19
BEV.11586	<i>M. simoni</i> ssp.	M	30	45	2	16	4	4	7	8	27	12	7	13	14	12	21
BEV.11587	<i>M. simoni</i> ssp.	F	31	42	2	15	4	3	7	8	24	8	8	8	11	10	18
BEV.11588	<i>M. simoni</i> ssp.	F	33	36	2	13	4	4	7	8	24	9	8	9	13	13	18
BEV.11589	<i>M. simoni</i> ssp.	M	30	49	2	18	4	4	8	8	21	12	10	11	12	12	18
BEV.11590	<i>M. simoni</i> ssp.	M	29	44	3	15	5	5	8	8	26	11	9	11	10	10	18
BEV.11591	<i>M. simoni</i> ssp.	F	31	45	4	14	4	4	7	7	24	9	7	12	12	12	20
BEV.11594	<i>M. simoni</i> ssp.	F	34	50	2	14	4	4	7	6	23	11	5	9	10	10	18
BEV.14869	<i>M. simoni</i> ssp.	F	35	36	4	16	4	4	7	7	20	9	12	10	12	12	19
BEV.5922	<i>M. simoni</i> ssp.	M	33	42	4	15	4	4	7	9	23	10	7	9	13	13	21
BEV.5923	<i>M. simoni</i> ssp.	F	34	42	4	14	4	4	8	7	24	10	6	9	12	12	19

Code	Species	Sex	V	D	DS	TR	SL(Sx)	SL(Dx)	IL(Sx)	IL(Dx)	G	Col	EL	NTS	Pf(Sx)	Pf(Dx)	Lam
BEV.5924	<i>M. simoni</i> ssp.	F	33	43	2	14	4	4	7	8	21	12	10	8	12	13	22
BEV.8508	<i>M. simoni</i> ssp.	M	31	46	4	15	4	4	8	7	28	9	6	9	12	12	23
BEV.8509	<i>M. simoni</i> ssp.	F	34	46	4	15	4	4	7	7	28	9	5	11	11	11	25
BEV.9429	<i>M. simoni</i> ssp.	M	30	54	4	16	4	4	7	8	24	12	8	9	12	13	20
BEV.9430	<i>M. simoni</i> ssp.	M	30	46	0	16	4	4	8	8	22	11	6	15	14	5	20
BEV.9431	<i>M. simoni</i> ssp.	M	32	46	1	16	4	4	8	8	23	9	6	11	12	12	19
BEV.9432	<i>M. simoni</i> ssp.	M	31	46	2	16	4	4	9	9	22	9	6	11	13	13	21
BEV.10179	<i>M. pasteurii</i>	M	31	39	1	15	5	5	7	6	30	9	1	7	12	15	22
BEV.10454	<i>M. pasteurii</i>	M	28	40	4	15	5	5	7	8	29	9	4	10	13	12	22
BEV.10455	<i>M. pasteurii</i>	M	33	40	0	15	6	6	8	7	27	10	4	11	17	15	21
BEV.14803	<i>M. pasteurii</i>	M	29	39	1	17	5	5	9	9	28	10	4	7	12	12	26
BEV.14804	<i>M. pasteurii</i>	F	34	38	3	16	4	6	8	8	24	10	4	7	13	12	22
BEV.14805	<i>M. pasteurii</i>	M	31	40	3	16	7	5	7	8	26	10	3	10	13	12	22
BEV.5926	<i>M. pasteurii</i>	M	32	43	0	18	5	5	6	8	31	9	5	9	16	13	21
BEV.5927	<i>M. pasteurii</i>	F	31	39	4	14	4	5	8	9	27	7	4	10	10	8	20
BEV.9177	<i>M. pasteurii</i>	M	29	42	0	16	5	5	9	8	27	8	5	9	14	13	25
BEV.9380	<i>M. pasteurii</i>	F	34	42	0	14	5	6	8	8	29	7	5	8	12	13	23

Table S5. Material examined for colouration characters comparisons for each specimen. Codes of morphological characters are given in section Material and Methods. M = Male; F = Female.

Code	Species	Sex	EBL	DBF	PSDBF	PDLL	SPDLL	DDSLL	SDDLB	PSDDSL	DSO	TC
BEV.10457	<i>M. adrarensis sp. nov.</i>	F	0	2	1	2	5	1	2	0	1	1
BEV.14800	<i>M. adrarensis sp. nov.</i>	F	1	3	1	1	2	2	6	1	1	1
BEV.15060	<i>M. adrarensis sp. nov.</i>	M	1	2	1	2	2	1	3	0	2	1
BEV.15061	<i>M. adrarensis sp. nov.</i>	F	1	2	2	1	2	1	4	1	0	1
BEV.15062	<i>M. adrarensis sp. nov.</i>	M	1	2	2	1	2	1	4	2	0	1
BEV.15063	<i>M. adrarensis sp. nov.</i>	M	1	2	0	1	1	2	4	0	1	1
BEV.15064	<i>M. adrarensis sp. nov.</i>	M	1	2	2	1	2	1	4	2	0	1
BEV.15163	<i>M. adrarensis sp. nov.</i>	F	0	0	0	3	2	1	4	1	1	0
BEV.10013	<i>M. olivieri</i>	M	0	4	2	1	2	1	4	2	2	0
BEV.11948	<i>M. olivieri</i>	F	0	4	2	3	3	2	5	2	0	2
BEV.12808	<i>M. olivieri</i>	F	0	0	2	2	2	0	0	2	0	2
BEV.13621	<i>M. olivieri</i>	M	0	2	2	2	3	1	4	0	2	2
BEV.14833	<i>M. olivieri</i>	M	0	3	2	2	2	1	4	2	0	0
BEV.5925	<i>M. olivieri</i>	F	0	2	2	2	2	1	1	0	1	0
BEV.5861	<i>M. olivieri</i>	F	1	2	2	0	3	1	4	2	0	0
BEV.5864	<i>M. olivieri</i>	F	0	2	2	2	3	1	5	2	0	0
BEV.5867	<i>M. olivieri</i>	F	0	2	2	2	2	1	4	0	2	0
BEV.5870	<i>M. olivieri</i>	M	0	2	2	2	2	1	4	2	0	0
BEV.5871	<i>M. olivieri</i>	F	0	2	2	2	2	1	1	0	2	0
BEV.5875	<i>M. olivieri</i>	F	0	2	2	1	2	1	4	2	1	0
BEV.5876	<i>M. olivieri</i>	M	0	2	2	2	2	1	4	2	0	0
BEV.5877	<i>M. olivieri</i>	F	0	2	2	2	2	1	3	0	0	0
BEV.5879	<i>M. olivieri</i>	M	0	2	2	2	2	1	1	2	0	0
BEV.5880	<i>M. olivieri</i>	F	0	2	2	2	3	1	3	0	2	0
BEV.5881	<i>M. olivieri</i>	M	0	2	2	1	2	1	4	2	2	1
BEV.5882	<i>M. olivieri</i>	F	0	2	2	2	2	1	2	0	2	2

Code	Species	Sex	EBL	DBF	PSDBF	PDLL	SPDLL	DDSLL	SDDL _B	PSDDSL _L	DSO	TC
BEV.5888	<i>M. olivieri</i>	F	0	4	1	3	4	2	2	1	1	0
BEV.5889	<i>M. olivieri</i>	M	0	0	2	2	2	1	3	2	2	0
BEV.5890	<i>M. olivieri</i>	M	0	2	2	2	3	1	4	2	0	0
BEV.5899	<i>M. olivieri</i>	F	0	2	2	2	1	2	5	2	2	0
BEV.5956	<i>M. olivieri</i>	M	0	2	2	2	3	1	4	2	1	0
BEV.5959	<i>M. olivieri</i>	M	0	4	1	1	1	2	4	0	0	0
BEV.8830	<i>M. olivieri</i>	M	1	2	2	1	4	1	7	1	2	1
BEV.8796	<i>M. olivieri</i>	M	1	3	2	1	3	1	4	0	2	0
BEV.8797	<i>M. olivieri</i>	M	1	3	2	2	4	2	5	1	2	0
BEV.8798	<i>M. olivieri</i>	M	1	2	2	2	7	2	6	0	2	0
BEV.8829	<i>M. olivieri</i>	M	0	2	2	1	6	1	7	0	2	2
BEV.8975	<i>M. olivieri</i>	F	0	2	2	2	2	2	3	0	2	2
BEV.9225	<i>M. olivieri</i>	M	0	2	2	2	2	2	3	0	1	2
BEV.10453	<i>M. simoni saharae ssp. nov.</i>	M	0	3	2	2	3	0	2	2	2	0
BEV.10849	<i>M. simoni saharae ssp. nov.</i>	M	0	3	2	2	2	1	1	0	0	0
BEV.10850	<i>M. simoni saharae ssp. nov.</i>	F	0	0	0	2	2	1	3	0	0	0
BEV.9114	<i>M. simoni saharae ssp. nov.</i>	M	0	2	2	0	2	0	1	2	1	1
BEV.11187	<i>M. simoni</i> ssp.	M	1	0	2	2	2	1	4	2	0	0
BEV.11586	<i>M. simoni</i> ssp.	M	1	0	2	2	2	1	4	2	1	0
BEV.11587	<i>M. simoni</i> ssp.	F	0	0	2	2	3	2	4	1	2	1
BEV.11588	<i>M. simoni</i> ssp.	F	0	3	2	0	0	2	4	0	0	0
BEV.11589	<i>M. simoni</i> ssp.	M	0	2	2	2	2	1	5	2	1	0
BEV.11590	<i>M. simoni</i> ssp.	M	1	0	2	2	3	1	5	2	0	0
BEV.11591	<i>M. simoni</i> ssp.	F	0	0	2	2	2	2	4	1	2	1
BEV.11594	<i>M. simoni</i> ssp.	F	0	2	2	2	2	1	5	2	2	2
BEV.14869	<i>M. simoni</i> ssp.	F	1	2	2	3	4	1	3	2	0	0
BEV.5922	<i>M. simoni</i> ssp.	M	0	0	2	2	2	1	2	2	2	0
BEV.5923	<i>M. simoni</i> ssp.	F	0	2	0	1	1	2	4	2	2	0

Code	Species	Sex	EBL	DBF	PSDBF	PDLL	SPDLL	DDSLL	SDDL _B	PSDDSL _L	DSO	TC
BEV.5924	<i>M. simoni</i> ssp.	F	1	2	2	0	0	1	2	2	2	0
BEV.8508	<i>M. simoni</i> ssp.	M	0	2	2	2	3	1	8	0	2	0
BEV.8509	<i>M. simoni</i> ssp.	F	0	3	1	2	4	1	4	0	2	0
BEV.9429	<i>M. simoni</i> ssp.	M	0	3	2	2	3	1	6	1	2	0
BEV.9430	<i>M. simoni</i> ssp.	M	1	3	2	2	3	2	6	2	1	0
BEV.9431	<i>M. simoni</i> ssp.	M	1	2	2	2	3	2	6	2	0	1
BEV.9432	<i>M. simoni</i> ssp.	M	1	3	2	1	2	2	5	2	0	2
BEV.10179	<i>M. pasteurii</i>	M	0	0	1	3	2	0	1	0	2	0
BEV.10454	<i>M. pasteurii</i>	M	0	0	2	3	3	2	1	0	2	0
BEV.10455	<i>M. pasteurii</i>	M	0	0	0	3	3	3	1	0	0	0
BEV.14803	<i>M. pasteurii</i>	M	0	0	1	3	2	1	3	1	2	0
BEV.14804	<i>M. pasteurii</i>	F	0	0	2	3	2	2	3	0	0	0
BEV.14805	<i>M. pasteurii</i>	M	0	0	0	3	2	3	1	0	0	0
BEV.5926	<i>M. pasteurii</i>	M	0	0	0	3	2	3	2	0	1	0
BEV.5927	<i>M. pasteurii</i>	F	0	0	0	3	3	3	1	0	0	0
BEV.9177	<i>M. pasteurii</i>	M	0	0	2	3	2	0	5	0	2	0
BEV.9380	<i>M. pasteurii</i>	F	0	0	0	3	2	3	3	0	0	0

Table S6. Categories of the variable Land Cover used in the ecological models. Variable derived from Campos and Brito (2018).

Code	Category	Definition
LC_01	Yellow dunes	Frequently fixed dunes composed by yellow sand. Sparse shrubs with isolated <i>Acacia</i> sp. or no vegetation cover
LC_02	White dunes	Mobile dunes composed by white sand (e.g. barchan dunes). No vegetation cover
LC_03	Orange dunes	Frequently fixed dunes composed by orange sand. Sparse shrubs with isolated <i>Acacia</i> sp. or sometimes no vegetation cover
LC_04	Compact sand	Flat areas composed by consolidated sandy soils. Shrubs and sparse trees (e.g. <i>Acacia</i> sp.)
LC_05	Gravel + Sand floodplains	Soil composed by similar amounts of gravel and sand. Sparse vegetation or no vegetation cover
LC_06	Gravel floodplains	Large floodplains covered by gravel (locally known as <i>Reg</i>). Usually without vegetation cover
LC_07	Compact soil	Soils frequently composed by silt and/or clay. Sparse vegetation or no vegetation cover
LC_08	Rocky soil	Non-flat areas with soils composed by stones, silt and/or clay. Sparse vegetation or no vegetation cover
LC_09	Rocky plateaux	Flat areas totally covered by stones (locally known as <i>Hammada</i>). Isolated <i>Acacia</i> sp. or no vegetation cover
LC_10	Bare rock	Large rock outcrops
LC_11	Grasslands	Flat flooding areas covered by grasses (e.g. <i>Cenchrus biflorus</i>)
LC_12	Savannah	High vegetation cover (grasses, shrubs, and trees)
LC_13	Croplands	Areas of crop cultivation (e.g. rice and sorghum)
LC_14	Permanent water	Permanent water features (rivers, lakes, and mountain lagoons)
LC_15	Salt pans	Flat areas covered by salt (locally known as <i>Sebkha</i>). No vegetation cover
LC_16	Railroads	Railroads and linear infra-structures
LC_17	Roads	Paved roads
LC_18	Urban	Major cities and villages

Reference

Campos, J.C., Brito, J.C. (2018) Mapping underrepresented land cover heterogeneity in arid regions: The Sahara-Sahel example. ISPRS J. Photogram. Rem. Sens. 146, 211-220.

Table S7. Descriptive statistics, including minimum-maximum value, mean and standard deviation (n=sample size) for selected characters in the *Mesalina olivieri* species complex.

	<i>M. adrarensis</i> sp. nov.			<i>M. simoni saharae</i> ssp. nov.			<i>M. simoni</i> ssp.			<i>M. olivieri</i>			<i>M. pastouri</i>		
	M	F	J	M	F	J	M	F	M	F	J	M	F	J	
SV L	min-max	33-38	41-53	25-25	36-43	42.46-45.75	-	43-51	43-51	33-50	36-47	20-42	48-48	40-42	28-28
	mean ± SD	34±2.3	42±5.5	25±0	42±3.03	44.10±2.32	-	45±2.81	45±2.6	41±4.3	42±3.3	34±7.0	45±2.9	41±1.0	28±0
	N	(4)	(3)	(1)	(4)	(45.75)	-	(4)	(6)	(24)	(21)	(8)	(7)	(2)	(1)
HL	min-max	9-11	9-10	7-7	8-10	8.47-9.45	-	10.29-11.32	8.77-10.3	8.07-12.17	8.27-11.04	5.86-10.42	9.95-12.01	8.94-10.09	7.19-7.19
	mean ± SD	10±1.0	9±0.62	7±0	9±0.7	9±0.69	-	11±0.39	10±0.4	10±1.0	9±0.64	8±1.22	11±0.7	10±0.8	7.19±0
	N	(4)	(3)	(1)	(4)	(9.45)	-	(8)	(8)	(25)	(21)	(15)	(7)	(2)	(1)
HW	min-max	5.57-6.65	4.92-6.13	4.41-4.41	5.28-6.26	4.86-6.75	-	6.61-7.44	5.62-6.67	4.45-8.84	4.78-6.92	3.29-6.69	5.57-7.74	5.56-5.59	4.54-4.54
	mean ± SD	6±0.47	5±0.54	4.41±0	5.77±0.69	5.9±0.73	-	7.05±0.26	6.28±0.3	6.28±1.09	5.98±0.53	4.88±0.96	6.71±0.84	5.58±0.02	4.54±0
	N	(4)	(4)	(1)	(2)	(5)	-	(8)	(8)	(25)	(21)	(15)	(7)	(2)	(1)
HH	min-max	3.09-3.62	3-4.26	3.9-3.9	3.17-4.89	3.6-4.36	-	3.76-4.6	4.52-5.43	2.88-5.49	3.31-5.08	2.21-4.29	3.9-5.63	4.16-4.25	2.99-2.99
	mean ± SD	3.28±0.23	3.73±0.57	3.9±0	4.21±0.63	3.98±0.53	-	4.28±0.3	4.82±0.29	4.13±0.85	4.16±0.45	3.65±0.55	4.55±0.71	4.21±0.06	2.99±0
	N	(4)	(4)	(1)	(5)	(2)	-	(8)	(8)	(20)	(21)	(15)	(7)	(2)	(1)
TE	min-max	2-3	1-2	-	1-3	1-2	1-2	2-3	1-2	1-3	1-2	1-2	1-3	1-2	2-2
	mean ± SD	3±1	1±1	-	2.28±0.75	2.28±0.70	1.5±0.70	3±0.48	1±0.46	2±0.55	1±0.47	2±0.51	2±0.55	1±0.51	2±0
	N	(4)	(4)	-	(5)	(2)	(2)	(10)	(8)	(32)	(22)	(15)	(17)	(8)	(3)
RN	min-max	1-2	1-2	1-2	1-2	1-2	1-3	1-2	1-2	1-2	1-2	1-1	1-2	1-2	1-2
	mean ± SD	2±0.5	2±0.54	2±0.57	1±0.53	2±0.57	2±1	1±0.51	1±0.48	2±0.43	1±0.4	1±0	1±0.51	2±0.5	2±0.57
	N	(11)	(5)	(3)	(7)	(3)	(3)	(10)	(10)	(34)	(25)	(3)	(21)	(9)	(3)
PS	min-max	1-3	3-3	1-3	1-3	1-1	2-3	1-3	1-3	1-3	1-3	1-3	1-3	1-3	2-3
	mean ± SD	3±0	3±0	2±1.15	2±0.81	1±0	3±0.57	2±0.7	1±0.58	2±0.7	1±0.58	2±0.67	2±0.65	3±0.72	2±0.53

	<i>M. adrarensis</i> sp. nov.			<i>M. simoni saharae</i> ssp. nov.			<i>M. simoni</i> ssp.		<i>M. olivieri</i>			<i>M. pasteurii</i>			
	M	F	J	M	F	J	M	F	M	F	J	M	F	J	
	N	(10)	(5)	(3)	(7)	(2)	(3)	(10)	(25)	(35)	(25)	(15)	(21)	(9)	(3)
V	min-max	27-33	32-34	31-32	28-34	34-34	31-32	29-33	33-35	27-35	27-35	25-35	28-33	30-34	26-34
	mean ±	30.14 ±	33.25 ±	31.67 ±	30.6 ± 2.	34 ± 0	31.5 ± 0	30.56 ± 1	34 ± 1.4	30.22 ±	31.55 ±	30 ± 2.5	30.17 ±	31.13 ±	30.33 ±
	SD	2.03	0.95	0.57	19		.7	.23	1	1.78	1.73	6	1.68	1.6	4.04
D	N	(7)	(4)	(3)	(5)	(2)	(2)	(8)	(5)	(22)	(21)	(16)	(18)	(6)	(3)
	min-max	45-56	44-52	52-52	34-54	39-46	-	42-49	36-50	40-64	37-60	36-50	39-43	38-39	42-42
	mean ±	50.5 ± 4.	47 ± 3.8	52 ± 0	44.57 ± 1	42.33 ± 3	-	45.63 ± 2	42.5 ± 4.	45.54 ±	45.38 ±	42.79 ±	40.43 ±	38.5 ± 0.	42 ± 0
TR	SD	65	2		0.06	.51		.06	78	5.64	5.16	4.19	1.51	7	
	N	(4)	(4)	(1)	(3)	(3)	-	(8)	(8)	(24)	(21)	(13)	(7)	(2)	(1)
	min-max	14-17	12-15	16-16	15-1	15-15	-	15-18	13-16	14-20	12-18	14-18	15-18	14-16	14-14
SL (Sx)	mean ±	15.75 ±	14 ± 1.4	16 ± 0	15.2 ± 0.	15 ± 0	-	15.88 ± 0	14.38 ±	16.63 ±	16.22 ±	15.31 ±	16 ± 1.1	15 ± 1.4	14 ± 0
	SD	1.25	1		44			.99	0.91	1.66	1.84	1.6	5	1	
	N	(4)	(4)	(1)	(5)	(2)	-	(8)	(8)	(21)	(15)	(13)	(7)	(2)	(1)
SL (Dx)	min-max	4-5	4-4	-	4-5	4-4	-	4-5	4-4	4-6	3-5	4-5	5-7	4-4	5-5
	mean ±	4.2 ± 0.4	4 ± 0	±	4.29 ± 0.	4 ± 0	-	4.09 ± 0.	4 ± 0	4.35 ± 0.	4.09 ± 0.	4.24 ± 0.	5.33 ± 0.	4 ± 0	5 ± 0
	SD	4			48			3	56	42	43	7			
IL(Sx)	N	(5)	(4)	()	(7)	(2)	-	(11)	(11)	(24)	(22)	(17)	(9)	(2)	(1)
	min-max	4-5	4-4	4-5	4-5	4-4	4-4	4-5	3-4	4-6	4-5	3-6	4-6	4-6	5-6
	mean ±	4.27 ± 0.	4 ± 0	4.33 ± 0.	4.25 ± 0.	4 ± 0	4 ± 0	4.13 ± 0.	3.88 ± 0.	4.31 ± 0.	4.29 ± 0.	4.06 ± 0.	4.91 ± 0.	5 ± 0.5	5.33 ± 0.
IL(Dx)	SD	46		57	5			35	35	53	46	55	42		57
	N	(11)	(5)	(3)	(4)	(2)	(2)	(8)	(8)	(32)	(24)	(17)	(22)	(9)	(3)
	min-max	7-9	7-9	7-8	7-9	7-8	8-8	7-9	7-8	7-9	7-9	6-10	6-11	8-9	6-8
IL(Dx)	mean ±	7.8 ± 1.0	7.5 ± 1.4	7.5 ± 0.7	7.83 ± 0.	7.5 ± 0.7	8 ± 0	7.7 ± 0.6	7.2 ± 0.4	7.93 ± 0.	7.86 ± 0.	7.41 ± 0.	7.73 ± 1.	8.33 ± 0.	7 ± 1.41
	SD	9	1		75			7	2	79	57	93	48	57	
	N	(5)	(4)	(2)	(6)	(2)	(1)	(10)	(10)	(29)	(21)	(17)	(11)	(3)	(2)
	min-max	6-9	7-8	7-8	7-9	7-7	7-7	8-9	6-8	6-10	6-9	5-9	6-10	6-9	6-8
	mean ±	7.11 ± 0.	7.6 ± 0.5	7.33 ± 0.	7.8 ± 0.8	7 ± 0	7 ± 0	8.25 ± 0.	7.38 ± 0.	7.91 ± 1.	7.68 ± 0.	7.41 ± 0.	7.32 ± 0.	7.22 ± 0.	7 ± 1
	SD	92	4	57	3			46	74	05	69	93	99	97	
	N	(9)	(5)	(3)	(5)	(2)	(2)	(8)	(8)	(32)	(24)	(17)	(22)	(9)	(3)

	<i>M. adrarensis</i> sp. nov.			<i>M. simoni saharae</i> ssp. nov.			<i>M. simoni</i> ssp.		<i>M. olivieri</i>			<i>M. pasteurii</i>			
	M	F	J	M	F	J	M	F	M	F	J	M	F	J	
G	min-max	21-32	24-28	24-27	24-28	26-28	22-30	21-27	20-24	20-34	21-33	17-29	22-31	24-28	25-30
	mean ± SD	27.63±2.82	25.75±2.06	25.33±1.52	25.4±1.67	27±1.41	26±5.65	23.43±2.12	22.86±1.6	25.73±3.29	24.77±2.8	23.41±2.98	26.46±2.56	26.5±1.73	29±2.64
	N	(8)	(4)	(3)	(5)	(2)	(2)	(8)	(8)	(30)	(22)	(17)	(15)	(4)	(3)
	min-max	10-11	7-11	11-12	6-12	8-9	11-11	9-12	8-12	6-14	7-12	8-14	8-12	7-11	7-12
Col	mean ± SD	10.88±0.35	9.33±0.08	11.33±0.57	8.6±2.19	8.5±0.7	11±0	10.5±1.19	9.75±1.28	9.72±1.98	9.36±1.29	9.75±1.43	10.13±1.12	9.8±1.64	9.5±3.53
	N	(8)	(3)	(3)	(5)	(2)	(2)	(8)	(8)	(29)	(22)	(16)	(15)	(5)	(2)
	min-max	5-6	5-5	5-6	6-10	8-5	-	9-12	5-12	3-10	5-12	4-8	1-7	5-6	5-5
EL	mean ± SD	5.11±0.33	5±0	5.33±0.577	7.5±1.6	6.5±2.12	-	10.5±1.19	8.38±2.44	6±1.78	6.86±2.03	5.83±1.32	4.83±1.64	5.25±0.5	5±0
	N	(9)	(5)	(3)	(8)	(2)	-	(8)	(8)	(17)	(14)	(6)	(12)	(4)	(1)
	min-max	11-13	10-13	10-13	8-10	10-11	8-11	9-15	8-12	7-13	8-12	7-10	6-11	7-10	8-9
NTS	mean ± SD	12.36±0.67	11.6±1.14	12±1.73	8.71±0.75	10.5±0.7	9.33±1.52	10.9±1.91	9.7±1.41	10±1.06	9.68±1.03	9.17±0.92	8.57±1.43	8.89±1.26	8.67±0.57
	N	(11)	(5)	(3)	(7)	(2)	(3)	(10)	(10)	(36)	(25)	(18)	(21)	(9)	(3)
	min-max	12-18	12-17	14-15	10-12	11-12	12-13	10-14	10-14	11-18	10-16	9-14	11-17	10-13	9-12
Pf (Sx)	mean ± SD	14.6±1.83	14.25±2.06	14.33±0.57	11.6±0.89	11.5±0.7	12.5±0.7	12.44±1.23	12±1.19	13.19±1.75	12.45±1.77	12.2±1.69	13.44±1.65	11.67±1.03	11±1.73
	N	(10)	(4)	(3)	(5)	(2)	(2)	(9)	(8)	(27)	(19)	(15)	(18)	(6)	(3)
	min-max	12-17	14-15	14-14	12-13	11-12	12-13	5-13	10-14	11-18	4-15	10-15	11-17	8-13	9-13
Pf (Dx)	mean ± SD	14.6±1.83	14.25±0.95	14±0	12.2±0.83	11.5±0.7	12.5±0.7	11.33±2.55	12±1.41	13.29±1.75	11.5±2.41	12.38±1.41	13.44±1.65	11.33±1.75	11.33±2.08
	N	(10)	(4)	(3)	(5)	(2)	(2)	(9)	(8)	(28)	(20)	(16)	(18)	(6)	(3)
	min-max	18-23	20-24	23-23	22-24	21-25	23-23	18-23	19-22	17-29	16-24	10-15	11-17	8-13	16-24
Lam	mean ± SD	22.14±1.86	21.5±1.91	23±0	22.75±0.95	23±2.82	23±0	20±1.65	20.25±1.5	21.44±3.05	19.5±2.3	12.38±1.41	13.44±1.65	11.33±1.75	19.93±2.63
	N	(7)	(4)	(1)	(4)	(2)	(1)	(9)	(4)	(25)	(20)	(16)	(18)	(6)	(15)

Table S8. Details and metrics of the 20 model replicates developed for *Mesalina adrarensis* sp. nov., including average (standard deviation) training and tests Area under curve (AUC), average (standard deviation) percentage contribution of each variable to the model replicates.

	Maximum temperature of warmest month	Minimum temperature of coldest month	Temperature annual range	Annual total precipitation	Land-cover	Terrain ruggedness index
% contribution	3.136 (2.180)	10.022 (3.766)	0.000 (0.003)	8.800 (4.505)	35.416 (11.808)	42.625 (13.414)
Permutation importance	6.098 (6.733)	15.762 (12.539)	0.037 (0.161)	21.808 (16.403)	24.962 (13.477)	31.332 (22.383)
Training gain without	3.069 (0.387)	2.931 (0.400)	3.096 (0.387)	2.892 (0.345)	2.458 (0.342)	2.404 (0.446)
Training gain with only	0.323 (0.110)	0.215 (0.095)	0.314 (0.101)	0.760 (0.226)	1.300 (0.370)	1.642 (0.307)
Test gain without	3.289 (1.029)	3.004 (1.192)	3.274 (1.077)	3.109 (1.092)	2.634 (1.041)	2.662 (1.086)
Test gain with only	0.350 (0.521)	0.351 (0.223)	0.348 (0.561)	0.837 (0.404)	1.528 (0.913)	1.694 (0.870)
AUC without	0.979 (0.019)	0.970 (0.036)	0.978 (0.022)	0.974 (0.025)	0.960 (0.039)	0.955 (0.051)
AUC with only	0.741 (0.145)	0.752 (0.090)	0.756 (0.145)	0.848 (0.079)	0.891 (0.107)	0.913 (0.080)

Table S9. Percentage of pixels with presence of each species of the *olivieri* species complex in each land cover unit, number of observations (N), and Standardised Levin's B (Bs) measure of niche breadth.

Land cover types	<i>M. adrarensis</i> sp. nov.	<i>M. olivieri</i>	<i>M. pastouri</i>	<i>M. simoni</i> ssp.
Sandy areas	15.0	43.7	42.1	18.1
Compact soil	0.0	0.0	2.6	0.0
Rocky plateaus	5.0	25.0	26.3	54.5
Bare rock	70.0	12.5	7.9	18.2
Gravel + Sand floodplains	5.0	0.0	5.3	0.0
Grasslands	0.0	12.5	5.3	9.1
Savannah	0.0	0.0	2.6	0.0
Croplands	5.0	6.3	7.9	0.0
N	20	16	38	11
Bs	0.132	0.351	0.394	0.241

Table S10. Known localities of *M. adrarensis* sp. nov.. The designation “BEV” indicates samples or records from the collection of the Biogeography and Ecology of Vertebrates in the CEFE lab in Montpellier. The designation “CIBIO” indicates samples from the CIBIO / InBIO, Research Centre in Vairão, Portugal.

Code	Record Type	Date	Latitude	Longitude	Province	Locality	Country
BEV.10457	Specimen	24/03/2009	21.015	-11.718	Adrar	Foum N. Mouei, guelta	Mauritania
BEV.10823	Specimen	16/04/2009	17.398228	-12.03051	Tagant	Gleitet el Khâdem	Mauritania
BEV.14800	Specimen	07/04/2017	22.608563	-12.556853	Tiris Zemmour	Oumm el Habâl, guelta	Mauritania
BEV.15060	Specimen	12/09/2015	20.553695	-12.691632	Adrar	Chinguetti, 44km from Atar	Mauritania
BEV.15061	Specimen	13/09/2015	21.159582	-11.93623	Adrar	Oumm Lekhterat	Mauritania
BEV.15062	Specimen	13/09/2015	21.159582	-11.93623	Adrar	Oumm Lekhterat	Mauritania
BEV.15063	Specimen	13/09/2015	21.159582	-11.93623	Adrar	Oumm Lekhterat	Mauritania
BEV.15064	Specimen	13/09/2015	21.159582	-11.93623	Adrar	Oumm Lekhterat	Mauritania
BEV.15163	Specimen	29/10/2011	20.553695	-12.691632	Adrar	Chinguetti, 44km from Atar	Mauritania
BEV.T661	Tissue	08/11/2007	20.74854	-13.12755	Adrar	Atar, 39km after towards Choûm	Mauritania
BEVO_170	Observation	07/04/2017	21.52119	-12.86248	Tiris Zemmour	Châr oasis (Choûm, 32.5km NE of)	Mauritania
BEVO_397	Observation	13/04/2017	21.1217	-13.0881	Adrar	Choûm, 19.7km SSSSW of (reg)	Mauritania
BEVO_469	Observation	19/09/2006	20.580946	-13.136361	Adrar	Oumm Lemhâr (=Molomhar), guelta	Mauritania
CIBIO11440	Tissue	01/12/2014	22.15568	-15.34678	Atlantic Sahara	Koudiet Laghnem	Morocco
CIBIO11973	Tissue	09/09/2015	19.826485	-14.255477	Inchiri	Araguib ej Jahfa	Mauritania
CIBIO12011	Tissue	13/09/2015	21.159582	-11.93623	Adrar	Oumm Lekhterat	Mauritania
CIBIO12018	Observation	14/09/2015	21.150235	-11.962342	Adrar	Oumm Lekhterat	Mauritania
CIBIO13640	Tissue	07/04/2017	22.608563	-12.556853	Tiris Zemmour	Oumm el Habâl, guelta	Mauritania
CIBIO13758	Observation	13/04/2017	23.80014	-10.632	Tiris Zemmour	Zednes	Mauritania
CIBIO13814	Tissue	19/04/2017	19.628933	-12.534387	Adrar	Es Sbâ'iya, guelta	Mauritania
CIBIO1861	Tissue	03/10/2008	19.79718	-12.998011	Adrar	Ouagchodda, 3km SW of	Mauritania
CIBIO1862	Tissue	04/10/2008	19.863228	-12.990913	Adrar	Ouagchodda, 8km N of	Mauritania
CIBIO206	Observation	07/01/2002	20.553717	-12.601817	Adrar	Chinguetti, after Amogjar pass	Mauritania
CIBIO2902	Tissue	23/03/2009	21.428225	-11.313882	Tiris Zemmour	Guelb er Richât, Plateaux	Mauritania
CIBIO2952	Tissue	28/03/2009	18.984935	-13.06473	Adrar	Tâmkart	Mauritania

Code	Record Type	Date	Latitude	Longitude	Province	Locality	Country
CIBIO5865	Tissue	29/10/2011	20.553695	-12.691632	Adrar	Chinguetti, 44km from Atar	Mauritania
CIBIO5905	Tissue	31/10/2011	21.152082	-11.94698	Adrar	Arhmakou, SW of (on plateaux)	Mauritania